

SEDIMENTOLOGY AND MICROPALAEONTOLOGY OF
GRAVITY CORES FROM THE N.E. ATLANTIC CONTINENTAL SLOPE
SOUTH WEST OF IRELAND.

by

P J Buck

Thesis submitted in fulfilment of the
requirements for the Degree of Master of
Science in the Department of Geology,
University of Cape Town, under the
supervision of Doctor John Rogers.

December 1988.

The University of Cape Town has been given
the right to reproduce this thesis in whole
or in part. Copyright is held by the author.

The copyright of this thesis vests in the author. No quotation from it or information derived from it is to be published without full acknowledgement of the source. The thesis is to be used for private study or non-commercial research purposes only.

Published by the University of Cape Town (UCT) in terms of the non-exclusive license granted to UCT by the author.

ABSTRACT

Eleven gravity cores from the continental margin off Eire and Land's End (SW England) were examined and found to document the major trends of the Late Pleistocene climate.

Several stratigraphic indicators; - carbonate content, sediment texture, grain size, composition, nature of terrigenous components, ice-rafted debris and foraminiferal diversity were examined and show that the glacial history of the study area can be closely correlated with the palaeoclimatic evolution of the adjacent European shelf.

Sediments deposited during Late Pleistocene glacial conditions show the following characteristics when compared to the surface sediments deposited under Holocene interglacial conditions: an increase in the quantity of ice-rafted debris and percentage of mica, and a notable increase in the degree of frosting and pitting of the quartz grains. Overall grain size was finer resulting in a silty sediment package. Sedimentologically the cores fall into two groups (1 and 2). The major difference being that Group 1 (located on the Pendragon Escarpment) received increased quantities of fine silts from a 'shelf spill-over' mechanism operating on the Fastnet and Western Approaches Basins, during glacial regressions. All sediment samples displayed polymodal characteristics reflecting the interaction of several different physical processes e.g. ice-rafting, contour currents etc.

Striking variations in the populations of planktonic foraminifera were noted, alternating between Arctic and Sub-Arctic assemblages, reflecting the waxing and waning of glacial activity. The coccolith-carbonate minima correlate with the Arctic-fauna maxima and the $^{18}\text{O}/^{16}\text{O}$ maxima of the oxygen-isotope curves. Foraminiferal-test analysis (ratio of whole foraminifera : fragmented foraminifera) revealed that no correlation existed with any of the other parameters analysed. However, the cores were severely affected by the presence of bottom currents which were strong enough to remove the fragmented tests. Parallel-laminated contourites and evidence of erosion were noted in all cores.

Ten cores penetrated sediments deposited during the last glacial maximum of 20,000 B.P - 18,000 B.P. near the 75cm depth mark (Core 1865 was too short to reach such sediments). However sediments reflecting the 11,000 B.P glacial readvance, detected at around the 25cm mark, were not as clearly represented. Bioturbation has smoothed the climatic record throughout the lengths of these cores and has also suppressed the high-frequency oscillations ($<10^3$ B.P).

ACKNOWLEDGEMENTS

Special thanks are due to Professor R V Dingle who provided the inspiration and guidance for this project.

Dr John Rogers is thanked for taking over supervision during the final phase of this project. Dr Amos Winter and Mr Malcolm Europa assisted me in obtaining reliable oxygen-isotope data. Mrs Sue Sayers and Ms Kathy Kruger's drafting expertise and advice were invaluable. Mrs Sharon van Greuning is thanked for typing the bones of the manuscript.

Further thanks are given Dr Keith Martin and Dr Steve Goodlad who provided fruitful discussion and good humour when needed most. Mr Matthew Smith who helped with the sedimentological analyses.

The cores were collected by Professor R V Dingle and Dr R A Scrutton on two cruises in the area on the R V "Shackleton" during 1978 and 1979. These were sponsored by the National Environmental Research Council of Great Britain.

Finally my thanks to Ms Dorothy Coffey and Mr Ki Chin who provided the moral support and ignored the paper holocaust in my study.

<u>CONTENTS</u>		<u>PAGE</u>
ABSTRACT		i
ACKNOWLEDGEMENTS		iii
CONTENTS		iv
LIST OF FIGURES		vi
LIST OF TABLES		viii
1	INTRODUCTION	1
1.1	Physiography and Geology of the Study Area	2
1.2	Structural History of the Study Area	4
1.3	Previous Work	5
2	MATERIALS AND METHODS	8
2.1	Laboratory Analysis	9
2.1.1	Core Description and Sampling	9
2.1.2	Chemical Analysis	10
2.1.3	Foraminiferal Analysis	11
2.1.4	Grain-Size Analysis	12
2.1.5	Component Analysis (Sedimentological [sand])	13
2.1.6	Oxygen-Isotope Analysis	13
3	RESULTS	15
3.1	X-Ray Examination of Split Cores	15
3.2	Core Descriptions	16

3.3	Micropalaeontology	18
3.3.1	Introduction	18
3.3.2	Ratio-of-Species Analysis	18
3.3.3	Morphological Changes	21
3.3.4	Planktonic-Foraminiferal Fragment Analysis	21
3.3.5	Calcium-Carbonate Analysis	23
3.3.6	Oxygen-Isotope Analysis	25
3.3.7	Relationship between Oxygen-Isotope Data and Calcium-Carbonate Data from DSDP Borehole 552A	27
3.4	Sedimentology	28
3.4.1	Grain-Size Analysis	28
3.4.2	Silt in the Sand Fraction	34
3.4.3	Ice-Rafted Debris Analysis	34
3.4.4	Mica Analysis	38
4	CONCLUSIONS	40
5	REFERENCES	45
6	APPENDICES	
6.1	Appendix A	56
6.2	Appendix B	57
6.3	Appendix C	58

LISTS OF FIGURES

- FIG. 1 Bathymetry of the Goban Spur and Porcupine Bank including Core location sites
- FIG. 2 Generalized Bathymetry of the Goban Spur and Vicinity
- FIG. 3a Detailed Bathymetry of the Goban Spur and Porcupine Bank
- FIG. 3b Fault pattern in the basement of the Goban Spur
- FIG. 3 Bathymetric Map of the Goban Spur and Vicinity
- FIG. 5 Seismic-Stratigraphy of the Goban Spur
- FIG. 6 Deglacial Polar Front Movements
- FIG. 7 Methodological Flow Charts
- FIG. 8 A-K. Upcore Percentage Display of Sub-Arctic/Arctic/Arctic(Total) Planktonic Foraminifera
- FIG. 9 Upcore Display of Percentage of Globigerina quinqueloba and Globigerina pachyderma (dex)
- FIG. 10 Upcore Display of Percentage C_aCO_3 , Sand and Mud

- FIG. 11 Oxygen-Isotope Result for Globigerina bulloides
- FIG. 12 Frequency Curves for core 1862
- FIG. 13a Semi Quantitive Bar Graph display of upcore Ice Rafted Debris results for Borehole 1869
- FIG. 13b Semi-Quantitive Bar Graph display of upcore Mica Results for Borehole 1869
- FIG. 14 Location Map for DSDP 552A
- FIG. 15 Percentage C_aCO_3 Display vs Depth for DSDP 552A
- FIG. 16 Percentage C_aCO_3 Display vs Depth for Borehole 1869
- FIG. 17 Oxygen-Isotope Ratio Display for DSDP 552A
- FIG. 18 Upcore Percentage total Terrigenous Curves
- FIG. 19 Location of Fastnet and Western Approaches Basins
- FIG. 20 Distribution of Quartz and Mica in Core 12328-5 (West Africa) in % of Total Coarse Fraction $>0,149mm$

LIST OF TABLES

Table 1. Table displays water depths at each Core site plus the Core lengths.

INTRODUCTION

This study is an examination of the effects of the last glacial warming on sedimentation in the vicinity of the Goban Spur and Porcupine Bank on the continental margin south west of Eire (FIG.1). The area falls within the Sub-Polar Gyre, a region where many authors consider the largest Quaternary temperature changes in the World Ocean occurred [Molina-Cruz and Thiede (1977), Ruddiman and McIntyre (1981a, b), Duplessy et al (1981), Mix and Fairbanks (1985)]. The study area is of additional interest to marine geologists and geophysicists because of its relatively thin sediment cover, thereby allowing the detailed study of the morphology and structure of acoustic basement along the continent-ocean boundary of a passive (tensionally rifted) continental margin [Dingle and Scrutton (1979)].

Eleven gravity cores were available for study (7 from the Goban Spur, 2 from the Pendragon Terrace, 1 from the mouth of the Porcupine Sea Bight and 1 from the Porcupine Bank) and they are used here to document major trends of the late Pleistocene climate (FIG.1).

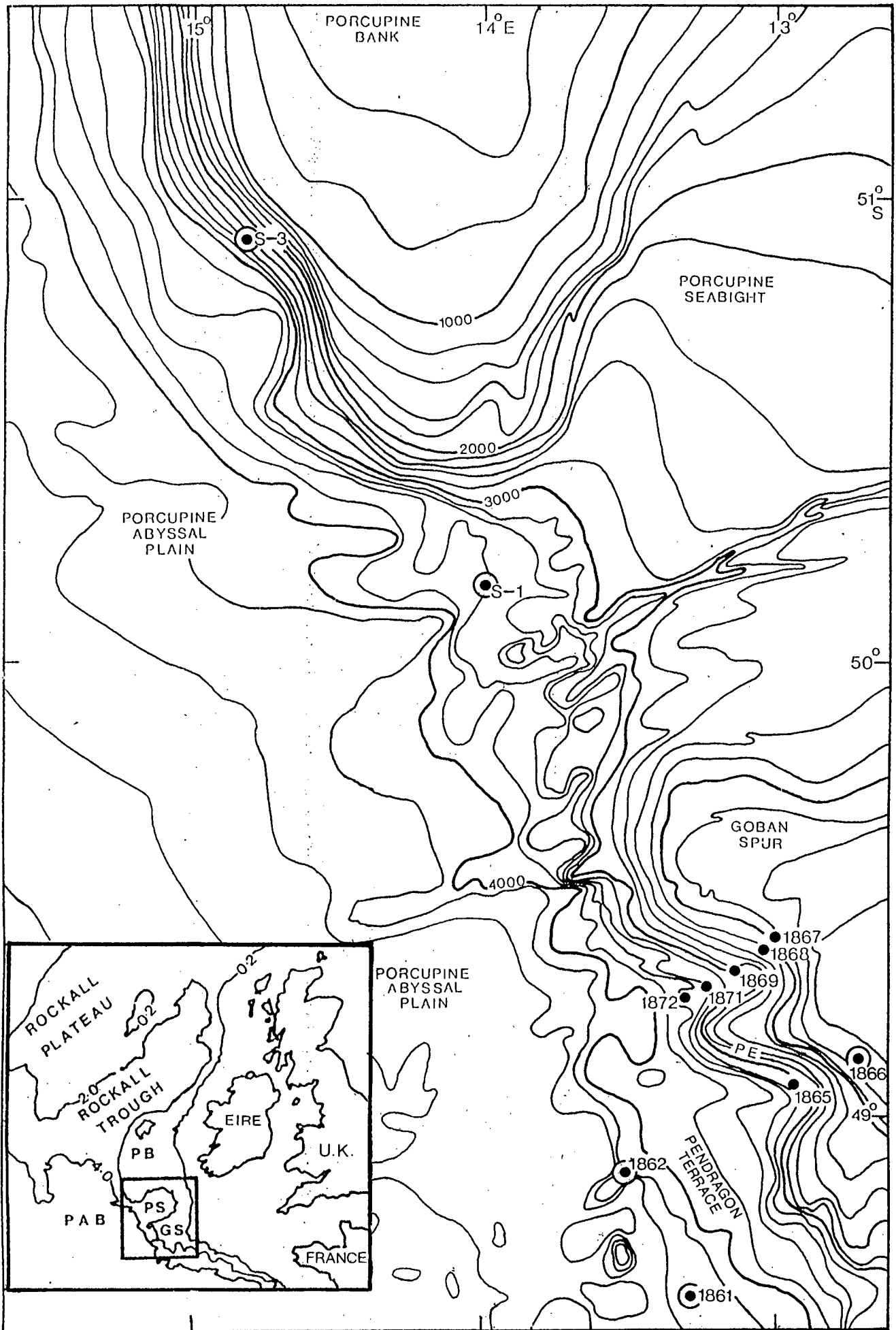


FIG. 1: BATHYMETRY OF THE GOBAN SPUR AND PORCUPINE BANK (DEPTHS IN METRES)
 ABBREVIATIONS: PE PENDRAGON ESCARPMENT
 INSET SHOWS LOCATION OF THE STUDY AREA ON THE OUTER MARGIN (SW OF EIRE)
 GROUP 1 CORE LOCATIONS ● GROUP 2 CORE LOCATIONS ⊙

1.1 Physiography and Geology of the Study Area

The Goban Spur and Porcupine Bank lie on the West European outer continental margin to the south west of Ireland (FIG. 1). The 2700m deep Rockall Trough separates the continental shelf of Great Britain from the Rockall Plateau to the west. [Cooper (1967), Emery and Uchupi (1978), Duplessy et al (1980) and Roberts et al (1981)]. The Goban Spur separates the northwest-trending Celtic Margin from the north-trending Porcupine Seabight (FIG.2).

The Goban Spur is a submarine plateau 250km south west of the Irish Mainland (FIG.3A), which is demarcated by three faults (FIG.3B) which also control its elevation: the western edge is the Outer Boundary Fault, which probably marks the continent-ocean discontinuity; the northern boundary is marked by the Porcupine Fault, separating it from the Porcupine Sea Bight and Porcupine Bank; and the southern boundary is marked by the Southern Boundary Fault [Dingle and Scrutton (1979), Montadert et al (1977)]. The Spur descends gently southwest to a depth of 2500m where it is sharply truncated at the Pendragon Escarpment (FIG.4). West of the Pendragon Escarpment, low hills occupy depths between 3500m and 4000m.

The north and south flanks of the Goban Spur are asymmetrical. The southern flank is marked by the long and steep Jean Charcot

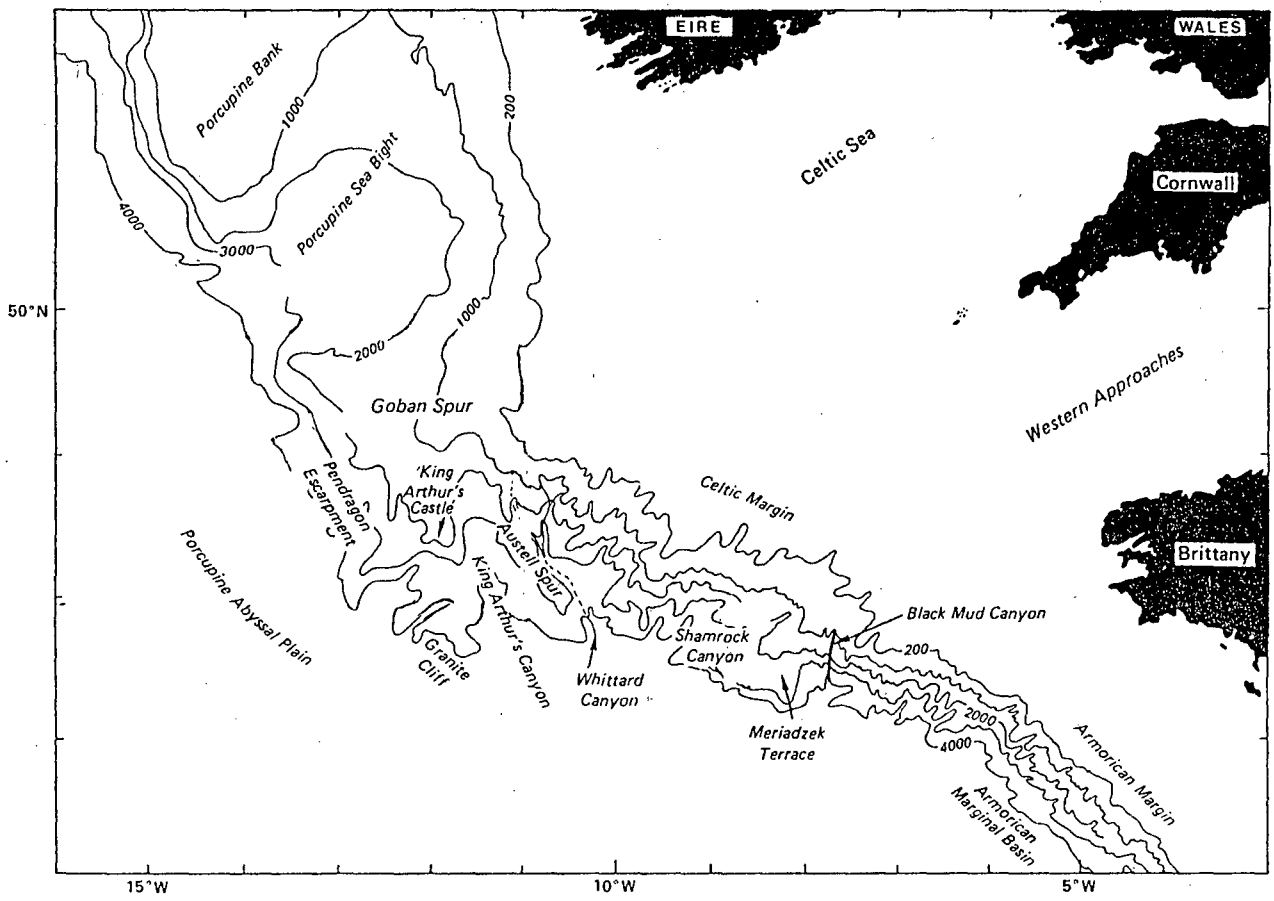


FIG 2. Generalized Bathymetry of the Goban Spur and vicinity.
(Depth in metres)

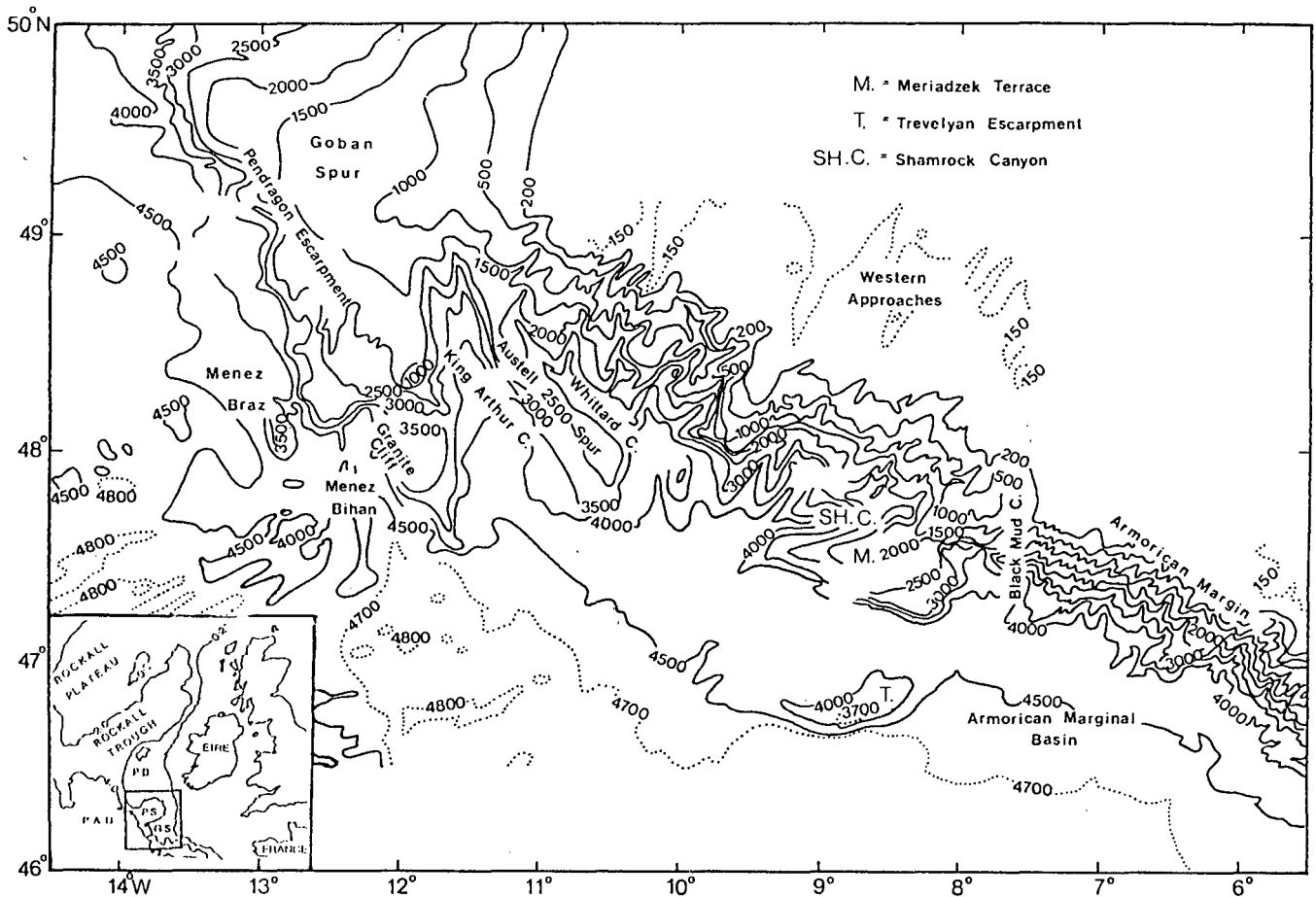


FIG. 3a

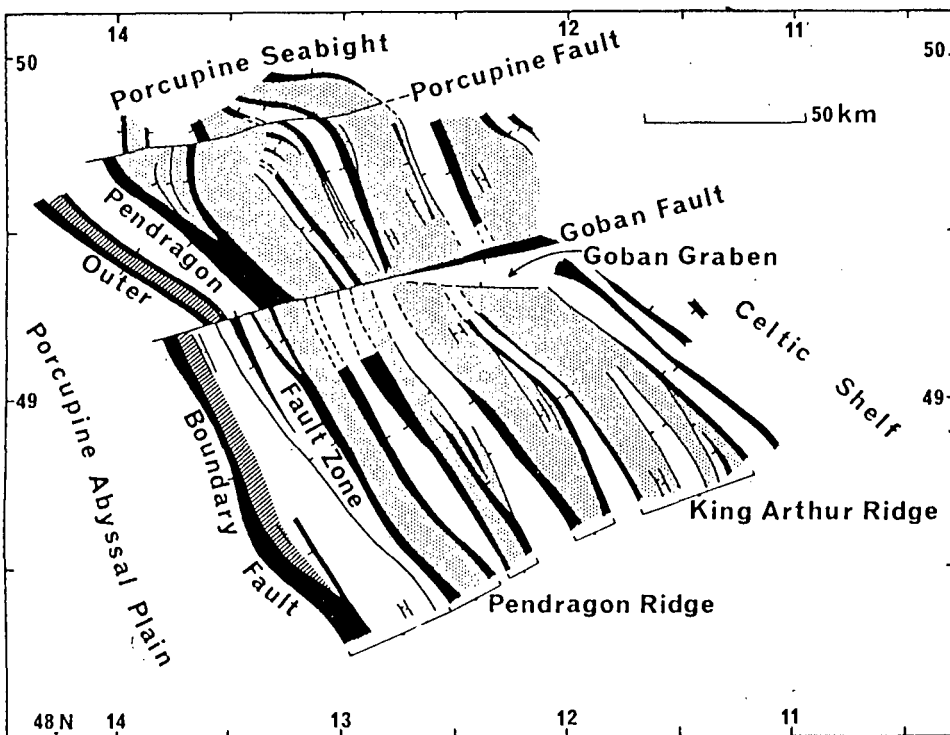


Fig 3b. Fault pattern in the basement of Goban Spur. Dotted areas are "basement highs", the shaded area constitutes the Outer Ridge. Fault zones are shown solid. (After Dingle and Scrutton (1979))

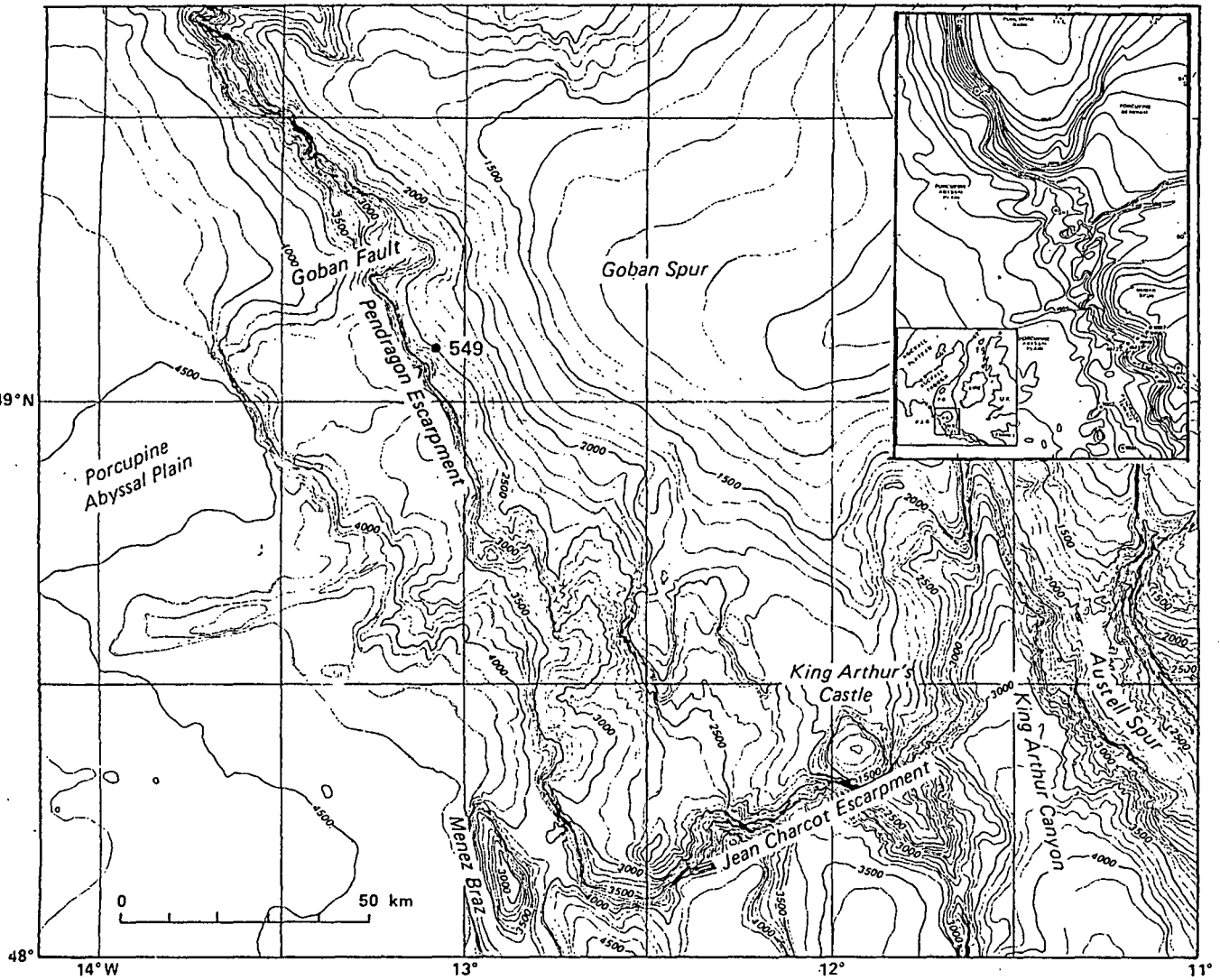


FIG 4. Bathymetric Map of the Goban Spur and Vicinity [Sibuet et al (1981)]
 (Depth in metres)

Escarpment (FIG.4), which is incised by the King Arthur and Whittard Canyons either side of Austell Spur.

The northern flank of the Goban Spur is a smooth gentle slope leading down into the Porcupine Seabight. The Porcupine Seabight is bounded to the east and to the west by north-trending faults. It is connected to the Porcupine Abyssal Plain by a narrow and deep depression (3000m - 4000m water depth), which is bounded to the north by the Porcupine Bank and to the south by the Goban Spur (FIG.2). The general physiography of the continental slope defines several provinces that correspond roughly to underlying geological structures [Roberts et al (1981)]. The narrow steep Armorican Margin is bounded to the southwest by the deep Mesozoic-Cenozoic Armorican Marginal Basin (FIG.2). The Western Approaches Basin intersects the basin of the northern Bay of Biscay near Black Mud Canyon (FIG.2). The continental slope is cut by several submarine canyons that trend obliquely downslope (FIG.3A). The regularity of the slope here is also interrupted by features such as the Meriadzek Terrace (FIG.2).

To the north, the Rockall Trough separates the Rockall Plateau from the continental margin of western Eire and the Porcupine Bank. At its southern end, it passes into the Porcupine Abyssal Plain (FIG.1).

Four distinct sedimentary layers were recognised by Dingle and

Scrutton (1979) in their seismostratigraphic study (FIG.5). These layers are separated by prominent reflecting horizons and dated by correlation with strata in the Meriadzek Terrace 270 km to the south east. Layer 1 (Upper Jurassic-Albian) lies on basement, but probably never covered the main basement ridge crests and upper parts of the western boundary fault scarps. Overlying this, Layer 2 is thought to be Upper Cretaceous to Lower Eocene. Layer 3 (Middle and Upper Eocene) is interpreted by Dingle and Scrutton to be the result of pelagic sedimentation in a low-energy environment, though in the Porcupine Seabight there is strong evidence for current moulding causing southerly or south westerly dips. Layer 4 (Oligocene to Recent) was deposited under varying conditions, with pelagic sediments over the main crest of the Goban Spur, slumps along the Western Escarpment, and possible contourites to the north. The upper surface of Layer 4 locally shows evidence of recent erosion.

1.2 Structural History of the Study Area

The continental margin of northwest Europe has been involved in several phases of rifting, drifting and convergence between Europe and North America. The structure of the Goban Spur has resulted chiefly from the rifting of Europe from North America. The Goban Spur was not involved in the more complex tectonic history of the Iberian region, but it was involved in compressional tectonism during the Eocene (Pyrenean

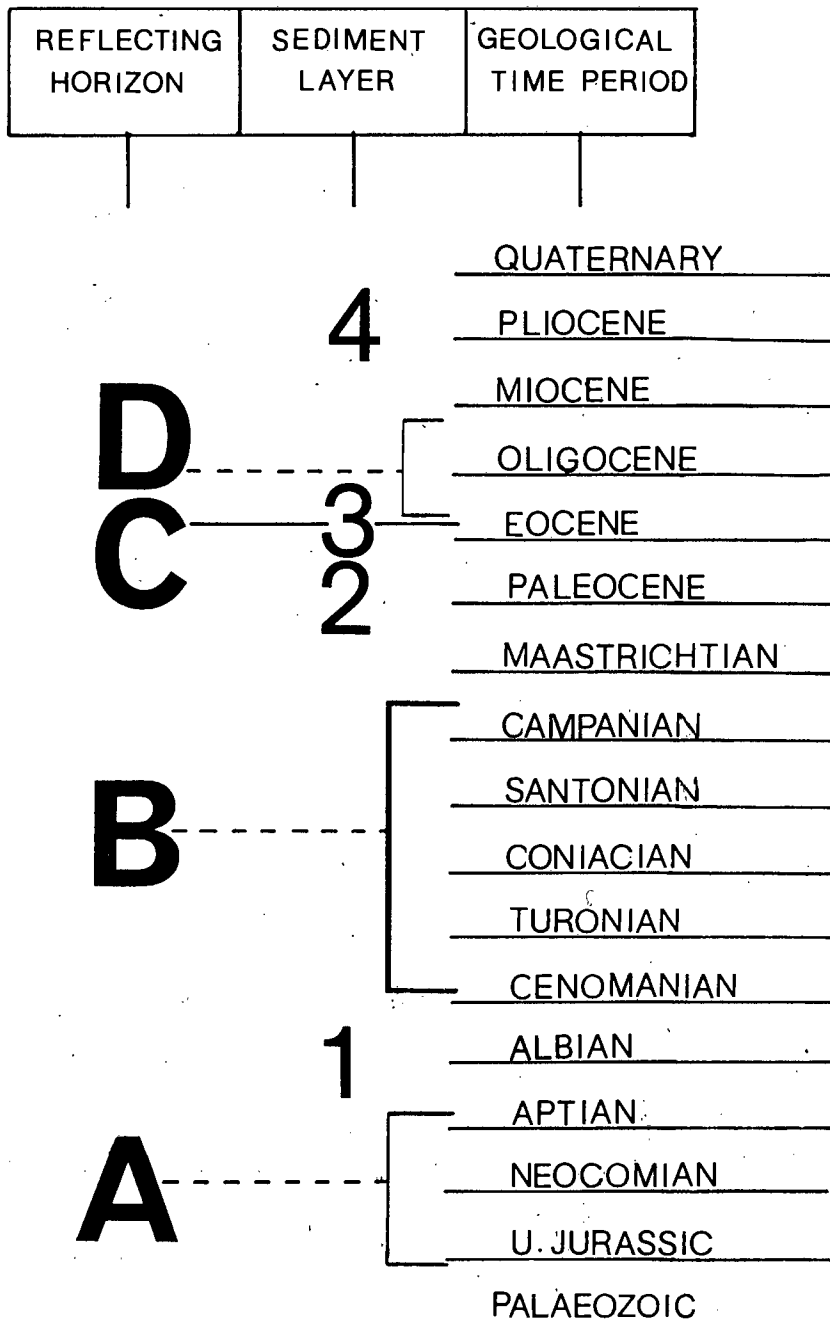


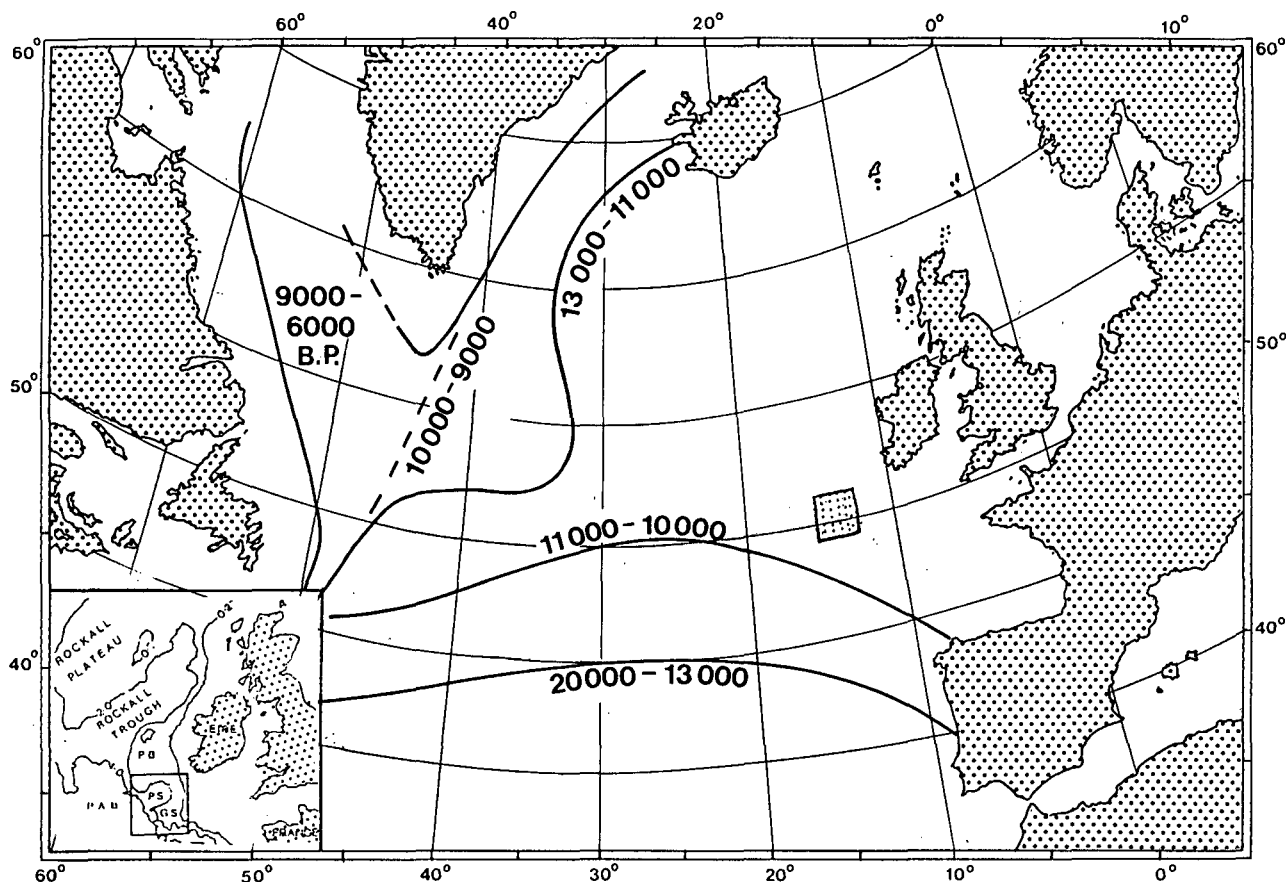
FIG.5 SEISMIC STRATIGRAPHY OF THE GOBAN SPUR
AFTER DINGLE AND SCRUTTON (1979)

tectonism). The structural features of the northwest European continental margin are chiefly controlled by two distinctive, nearly perpendicular fault systems that have created a complex series of horsts and grabens within the continental crust. Over the positive horsts blocks sediment cover is thin and contains numerous unconformities, whilst grabens (and half grabens) are filled with thick layers of Mesozoic and Cenozoic sediments.

1.3 Previous Work

The last glacial period ended abruptly in what Broecker and Van Donk (1970) referred to as Termination 1. Following the last glacial maximum of 20,000 - 18,000 B.P [Ruddiman and McIntyre (1981a), Delmas et al (1980), Grosswald (1980) and Pastouret et al (1978)] deglaciation of the Atlantic in the northern hemisphere occurred in three phases with major warmings in the northeastern and central regions, the northern sections and the Labrador Sea occurring at 13,000 B.P, 10,000 B.P and 9,000 B.P to 6,000 B.P respectively.

The Polar Front was located NW of Portugal at 43°N (FIG.6) between 20,000 to 13,000 B.P [Ruddiman and McIntyre (1981a, b), Jansen and Erlenkeuser (1985)]. At about 13,000 B.P it retreated to the northwest, allowing temperate waters to invade the eastern part of the sub-polar Gyre. 11,000 B.P saw the readvance of a major glacial to a position off NW Spain (FIG.6)



DEGLACIAL POLAR FRONT MOVEMENTS

Fig.6 Retreat positions of the North Atlantic polar front from the glacial maximum position 18000 B.P. to the modern interglacial location after 6000 B.P.

After Ruddiman and McIntyre 1981b

near the glacial maximum of 18,000 B.P. Ruddiman and McIntyre (1981a), suggest that ocean temperatures were only slightly less cold than the full glacial ocean in the earlier Würm III interval. This cooling ended abruptly at 10,000 B.P. allowing the polar front to retreat to a position along the eastern edge of the Labrador Sea (FIG.6) [McIntyre et al (1976), CLIMAP project members (1976), Ruddiman and McIntyre (1981a, b, c), Duplessy et al (1981), De Graciansky and Bourbon (1985), De Graciansky and Poag (1985)].

The termination of the most recent (Würm = Wisconsin) glaciation occurred approximately 11,000 B.P. - 10,000 B.P. [Berggren (1972), McIntyre et al (1972), Boltovskoy (1973), Bjerkli and Holtedahl (1975), Ruddiman and McIntyre (1981a, b)]. Using an average sedimentation rate of 3 to 5 cms/1000 years [Berger (1976), McIntyre et al (1972)] and assuming that the cores are complete, the influx of polar water detected in the cores at 50cm would lie at 10000 B.P. to 16,000 B.P. close to the Pleistocene/Holocene boundary [Broecker et al (1960)]. Ericson et al (1967) found sediments corresponding to the last glaciation at depths of 30cm to 40cm in the North Atlantic.

This deglaciation process is now complete except for high-altitude and high-latitude glaciers. However the disintegration of the Northern Hemisphere ice sheets did not proceed at equal rates and thus the final melting at different localities was not synchronous [Duplessy et al (1981), Belderson et al (1981)].

It appears that the deglacial retreat of the polar waters from the North Atlantic Ocean was a complicated time-transgressive process. The irregular path of deglaciation included reversals of trend as indicated by evidence of glacial readvance 8,800 B.P - 8,200 B.P in England and Denmark and about 11,000 B.P - 10,000 B.P (younger Dryas) North America (Lake Superior) [Frakes (1979)]. Ruddiman and McIntyre (1981c) note that between 13,000 B.P and 6,000 B.P that the retreat of the polar waters was not unidirectional and that a polar water readvance occurred at around 10,000 B.P. Similarly, between 11,000 B.P and 10,000 B.P tundra vegetation returned to Western Norway [Lamb (1977)] and glaciers become re-established in Ireland and Scotland [Duplessy et al (1981)]. The 11,000 B.P readvance brought the dominant Arctic fauna all the way south to the Bay of Biscay (45°N) [Ruddiman and McIntyre (1981a)]. Ruddiman et al (1980) noted that in North Atlantic cores with high deposition rates, three very abrupt climatic changes occurred.

- (i) An initial warming at an estimated 13,500 B.P;
- (ii) A subsequent cooling beginning 11,500 B.P and;
- (iii) a final warming centred just before 9,300 B.P;

Furthermore they concluded that if bioturbational mixing effects could have been removed that the observed abrupt transitions would have been even faster.

2 MATERIALS AND METHODS

Eleven gravity cores (7 from the Goban Spur, 2 from the Pendragon Terrace, 1 from the mouth of the Porcupine Seabight and 1 from the Porcupine Bank) were recovered by Drs R V Dingle and R A Scrutton aboard S.S. "Shackleton" during cruises in 1977 and 1979. The distribution of the coring stations are depicted in Figure 1. Water depths range from 1361m to 4493m and core lengths vary between 40cm (core 1865) and 160cm (core 1862).

Table 1

Display of water depths and core lengths at core sites

<u>Core Number</u>	<u>Water Depths (m)</u>	<u>Core Lengths (cm)</u>
1861	4165	110
1862	2088	164
1865	2198	40
1866	1361	121
1867	1720	121
1868	4493	120
1869	2187	155
1871	3238	143
1872	4200	120
S-1	3500	130
S-3	2650	112

2.1 Laboratory Analysis

This section provides a condensed review of the analytical techniques on which this sedimentological and biological study is based. The complementary flow-charts (FIGS.7A to 7E) depict the laboratory analysis in diagrammatic form.

2.1.1 Core Description and Sampling

The cores were split and the split sections X-rayed and photographed (Appendix A). Samples one centimetre deep were taken at five-centimetre intervals and extra samples were taken at significant lithological or structural interfaces.

Core-description procedures adopted in this investigation are based on methods employed by Høltedahl et al (1974). Core descriptions are presented in Appendix B. These include graphic log illustrations, lithology, structures and intraclasts. In addition each core log contains detailed upcore analyses of the grain-size distributions ($>63 \mu\text{m}$), statistical analyses and percentage calcium carbonate content (coarse and fine fractions). Furthermore the logs display a detailed foraminiferal-diversity analysis (Globigerina bulloides, Globigerina pachyderma(sin) and Globorotalia inflata). Colours were recorded utilizing the Geological Society of America Colour Chart (1951).

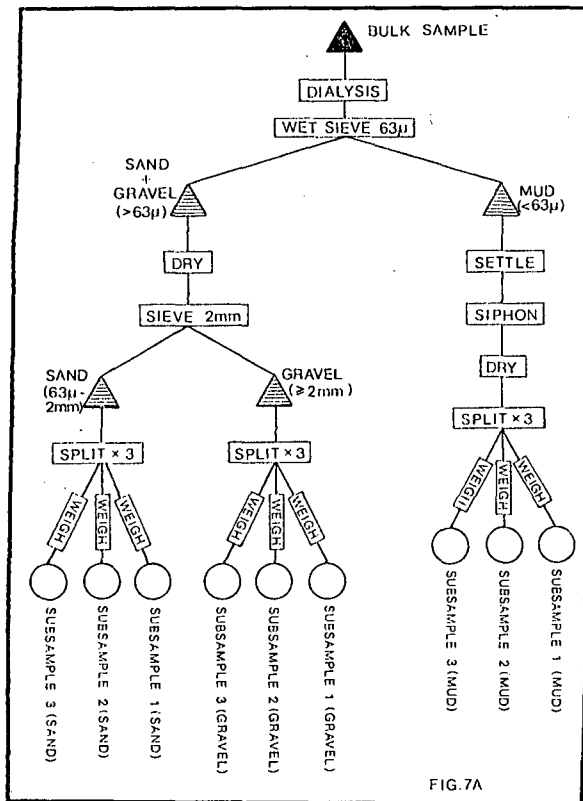


FIG. 7A

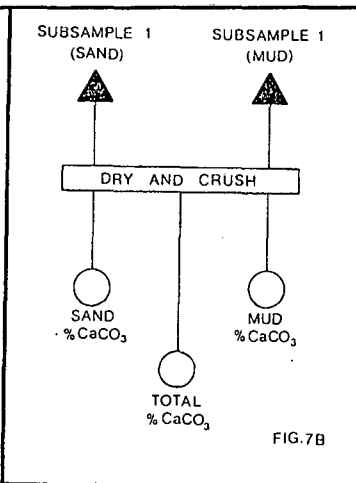


FIG. 7B

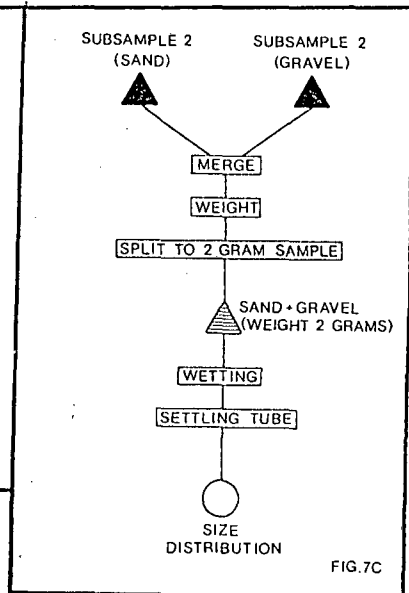


FIG. 7C

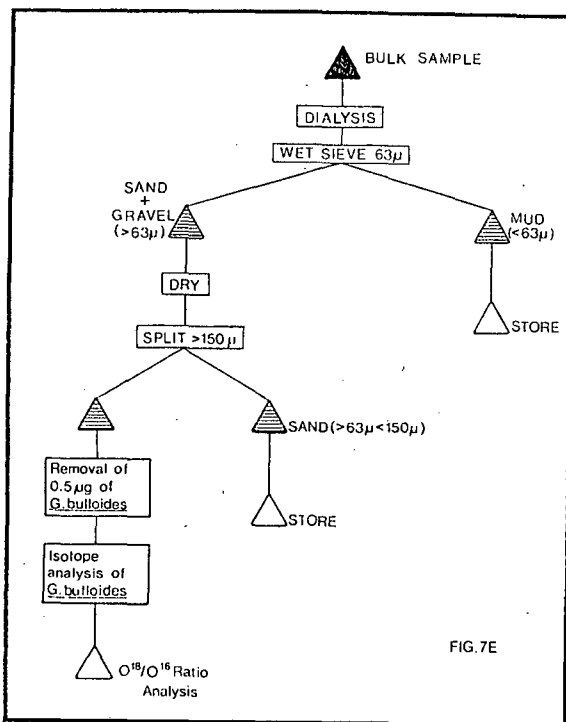


FIG. 7E

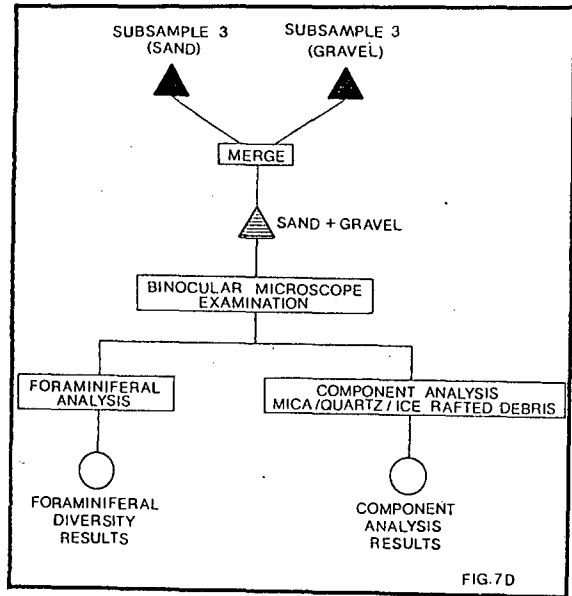


FIG. 7D

FIG. 7

METHODOLOGICAL FLOW CHARTS

Dialysis was performed on all bulk samples to remove soluble interstitial salts. Samples were dialysed in semi-permeable membranes while placed in slowly running tap water from 24-36 hours.

Thereafter the entire mud fraction (<63 microns size fraction) was separated by wet sieving. The suspended mud fraction was then allowed to settle before the water was decanted and/or siphoned off. The samples were then oven dried and weighed.

Material greater than 63 microns was oven dried and sieved through a 2mm sieve to separate gravel and sand. However most samples contained no gravel except for an occasional rock fragment. Both fractions were nevertheless weighed and the sand fraction was further split into three subsamples.

2.1.2 Chemical Analysis

Calcimetry was performed using the 'Karbonat-Bombe' technique [Birch (1981)]. In analysis, one gram of crushed sample is reacted with 5ml conc. HCl in a sealed perspex vessel. The pressure of evolved CO₂, proportional to the CaCO₃ content, is registered on a graduated manometer. On calibration using Analar grade Calcium Carbonate, the manometer reading provides a direct measure of the CaCO₃ content. Standards were run every 5 to 10 samples.

The accuracy and precision of this method has been rigorously tested by Birch (1981) and the Bombe results compared well with those of other, more complicated procedures. An error of only 2% was reported by Birch (1981) for samples containing more than 10% carbonate material. An amount of 4 grams of sample was used when low abundances of carbonate were detected (Birch, 1981).

Routine calcimetry was performed on subsample 1 (sand) and subsample 1 (mud) in order to provide an extensive CaCO_3 data base. All calcimetry results are tabulated in Appendix C.

2.1.3 Foraminiferal Analysis

Samples were examined under a binocular microscope to provide planktonic and benthic foraminiferal diversity data up core in subsample 3 (sand and gravel) ($>63 \mu\text{m}$) (FIG.7D). Each dried sample, which consisted of all material $>63 \mu\text{m}$, was sprinkled onto a gridded tray and examined under reflected light. Utilising the works of Kennett and Srinivasan (1983) and Saito, Thompson and Breger (1981) twenty one species of planktonic foraminifera were identified and their respective abundances counted in each sample. On average the first 300 specimens were counted per sample in order to obtain a statistically acceptable database.

2.1.4 Grain-Size Analysis

Routine grain size analysis was performed on subsample 2. The sand and gravel fractions were combined as the gravel fraction constituted, in the majority of samples analysed, only a small percentage. The combined subsample was weighed and split using a microsplitter to obtain a 2 gram sample. The sample was then processed in a settling tube [Flemming and Thum (1978)] to furnish hydraulic grain-size parameters Doeglas (1968), Gibbs (1972), Brenchley and Williams (1978), Allen (1985), Coates and Hulse (1985).

The preference for the use of the settling-tube technique over routine sieve analysis was twofold. Firstly sieving is time consuming and often inaccurately reflects the true size distribution of the sediment as particles are sorted by shape rather than size Fleming and Thum (1977). Secondly as most natural sediments are deposited during hydraulic transport [Bagnold (1968)] settling analysis may be a more meaningful technique in the study of subaqueous depositional processes. Computerised data reduction of these velocities provide the 'settling diameter' as a resultant grain-size parameter.

The samples were not leached prior to settling, albeit this would have been desirable, as the inorganic sediment (>63 μm) would, in the majority of cases have been too small to settle successfully.

2.1.5 Component Analysis (Sedimentological [sand])

A detailed component analysis was conducted in conjunction with the foraminiferal study (subsample 3 - sand/gravel) using reflected light. The areas covered were: i) occurrence of planktonic-foraminiferal fragments, ii) occurrence of ice-rafted debris, iii) occurrence of mica, iv) quartz-grain characteristics.

2.1.6 Oxygen-Isotope Analysis

All cores were resampled at 5cm intervals taking 0,5cm deep samples. The bulk samples were dialysed for 48 hours. Thereafter the entire mud content (<63 μ m) was separated by wet sieving. All material greater than 63 μ m was oven dried. The coarse fraction was then sieved and the 212-300 micron fraction obtained. From this about 0,5 milligrams of well preserved Globigerina bulloides were picked (equivalent to about 50 specimens) and stored temporarily in labelled gelatin capsules. G. bulloides specimens were chosen for isotopic determination because they were abundant in most samples examined and had been used in core CH73139C from the Rockall Trough (FIGS. 1 and 12) [Duplessy et al (1981)]. Specimens were crushed in ethanol and dried for 30 minutes at 50°C. The calcium carbonate was dissolved in approximately 100% H₃PO₄ under vacuum at 50°C according to the method of Shackleton (1974), except that the samples were dropped into acid and kept at constant temperature with a water jacket.

(Dr A Winter supervised a parallel study of piston cores from the Natal Valley by Ficham (1987), who has described the standardised oxygen-isotope procedures employed).

At present, no facilities are available at the University of Cape Town to connect the extraction line in the Marine Geoscience Unit directly to the Micromass VG602D mass spectrometer in the Archaeology Department. Samples had first to be isolated in 6mm internal diameter glass tubing (break-seals) and sealed with a butane flame. Instrumental corrections of the results were calculated according to Craig (1957). The results are reported in per mil deviations relative to PDB and calibrated with standard NBS-20 according to the equation:

$$S^{180} = \frac{(^{180}/^{160}) \text{ SAMPLE}}{(^{180}/^{160}) \text{ STANDARD}} - 1 * 1000$$

As a result of mechanical errors in both the Micromass VG602D Mass Spectrometer and the Extraction Line, several samples had to be discarded as a result of atmospheric contamination. The major problem appears to have been poor 'O Ring' rubber quality which resulted in leaky seals.

3 RESULTS

3.1 X-Ray Examination of Split Cores

Examination of the cores by X-ray photography (Appendix A) yielded three major results. Firstly it determined that very little disturbance had taken place during the coring. Apart from minor drag effects, only core 1865 showed any badly distorted areas. Secondly it showed that all cores contained pebbly horizons, though in cores 1862, 1865, 1868 and S-1, these were not extensive. Several cores are pebbly throughout their entire lengths, but there is a general decrease in size, number and angularity of pebbles upcore. In addition, several large clasts were located. Of these a few were isolated and thin sectioned. Among these were a basalt, an amphibolite and a granite. The former two are of unknown origin but the latter may have come from the Goban Spur itself [Pautot et al (1976)]. Thirdly distinctive fine laminae, not visually apparent, were found in all cores. These have been compared with structures noted by Stowe (1979) and by Stowe and Lovell (1979) who interpreted them as contourites [Stowe and Holbrook (1985)].

In addition to these structures, distinctive bands approximately 1cm thick appear in cores 1861 (95cm) 1862 (160cms and 100cm), 1868 (110cms), 1872 (30cm), S-3 (50cms). Only in core 1869 is any corresponding band visually apparent.

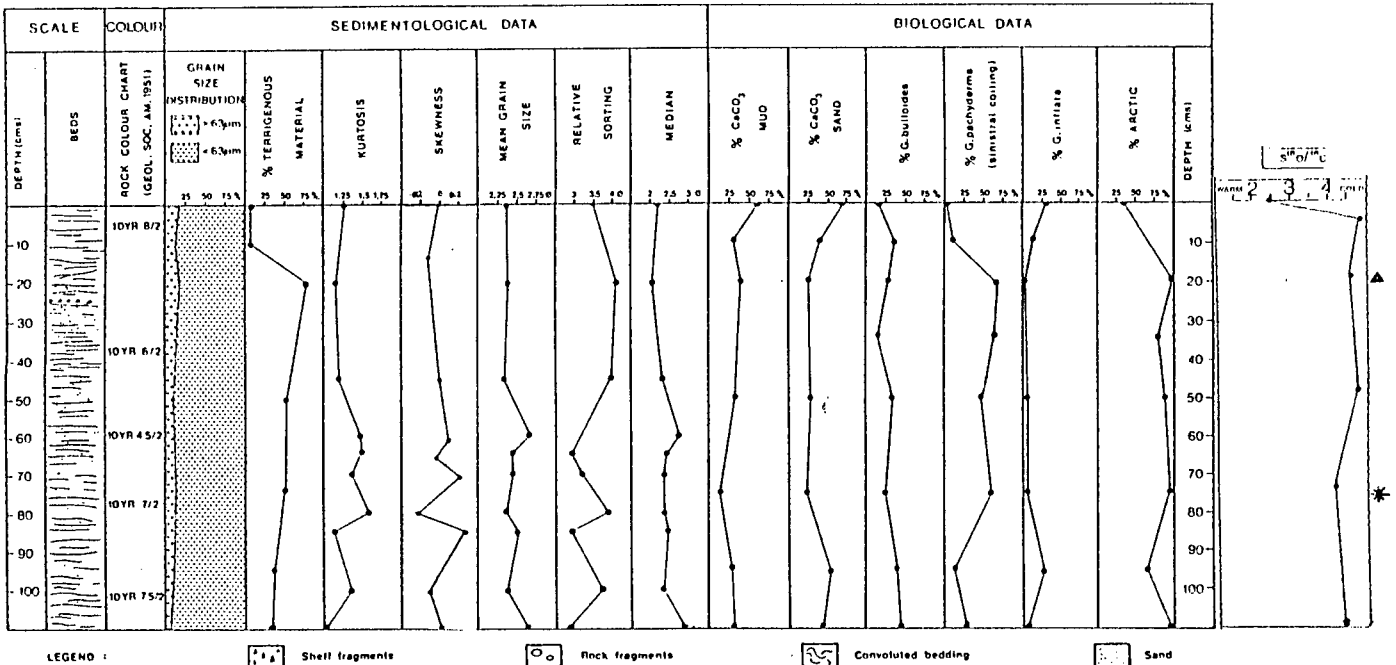
and this is poorly defined. The sample taken from this horizon in core 1869 contains a rich cold-water fauna with a high proportion of Globorotalia inflata, Globorotalia hirsuta, Globorotalia truncatulinoides and Orbulina universa.

The character of the sediments undergoes striking change upcore in all cores. The amount of terrigenous material decreases markedly upcore from a maximum of nearly 80% of the sediment in two samples: 1861 sample 6 (25-26 cms), and 1869 sample 14 (70-71cms), and from 64-65% in several others: 1869 sample 18 (90-91 cms) and 1872 sample 14 (65-66cms). The terrigenous material consists largely of subangular to subrounded quartz grains, but rock fragments are also fairly common. The top samples of all cores are Globigerina oozes with few, if any, terrigenous grains (Appendix B). (Inserted following page 16 on instructions of external examiner, with addition of oxygen isotope curves from Figure 11).

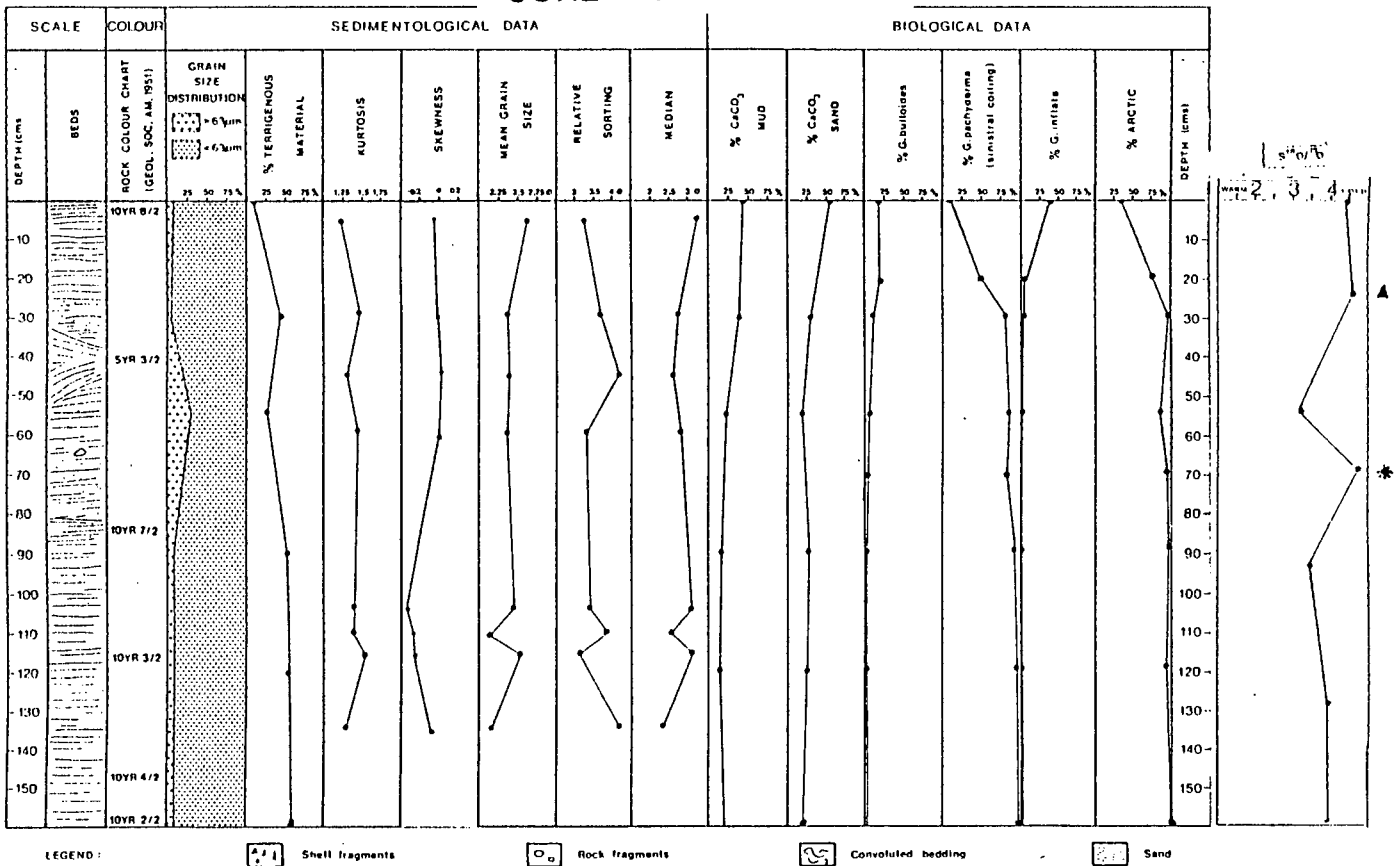
3.2 Core Descriptions

Visual inspection of the entire cores showed a number of lithologic changes, and horizons of coarser grained or even pebbly sediment. Some small scale colour changes within the individual cores were often striking (Appendix B). Core 1872 at 79cm changed from very pale orange (10 YR 8/2) to dark brown (10 YR 4/2) upcore.

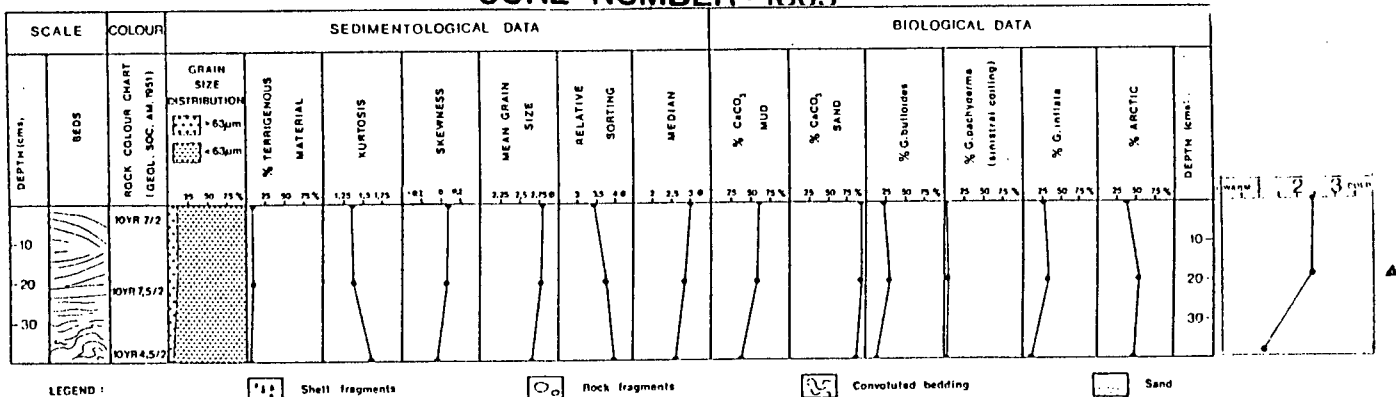
CORE NUMBER : 1861



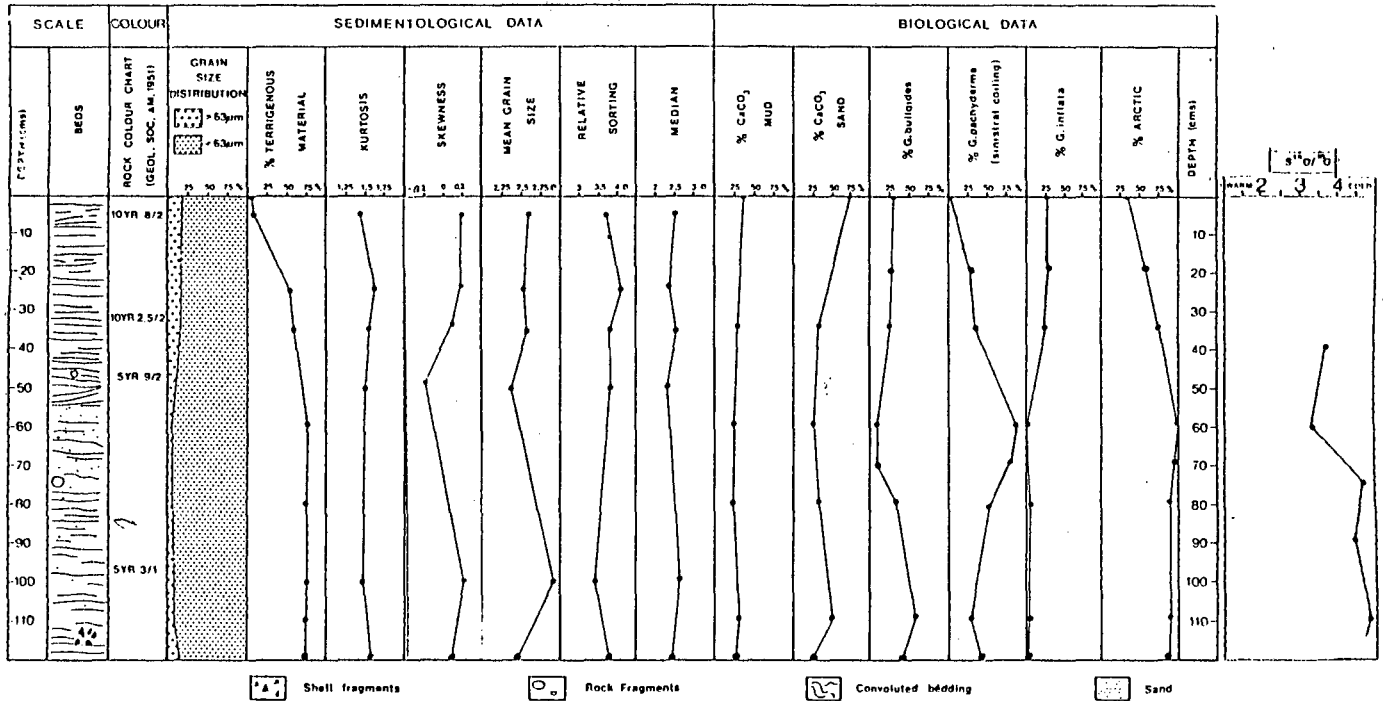
CORE NUMBER : 1862



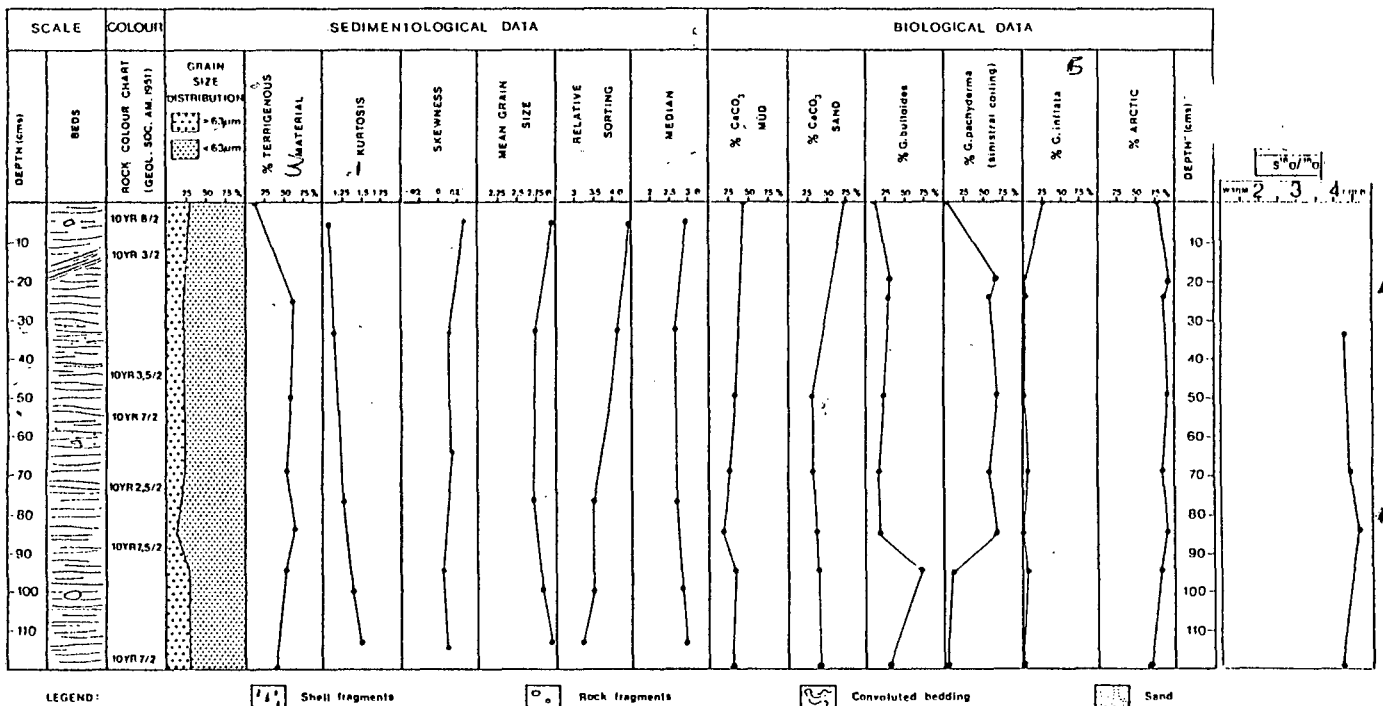
CORE NUMBER : 1865



CORE NUMBER : 1866



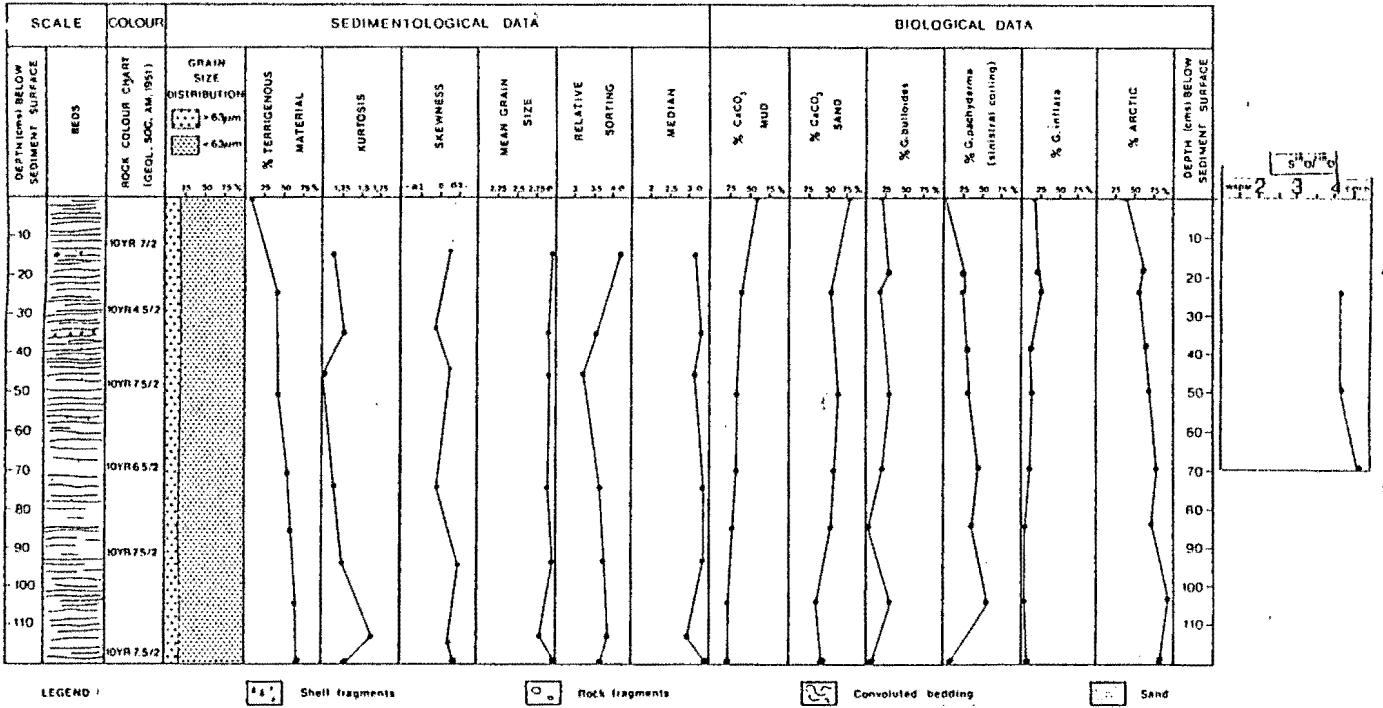
CORE NUMBER : 1867



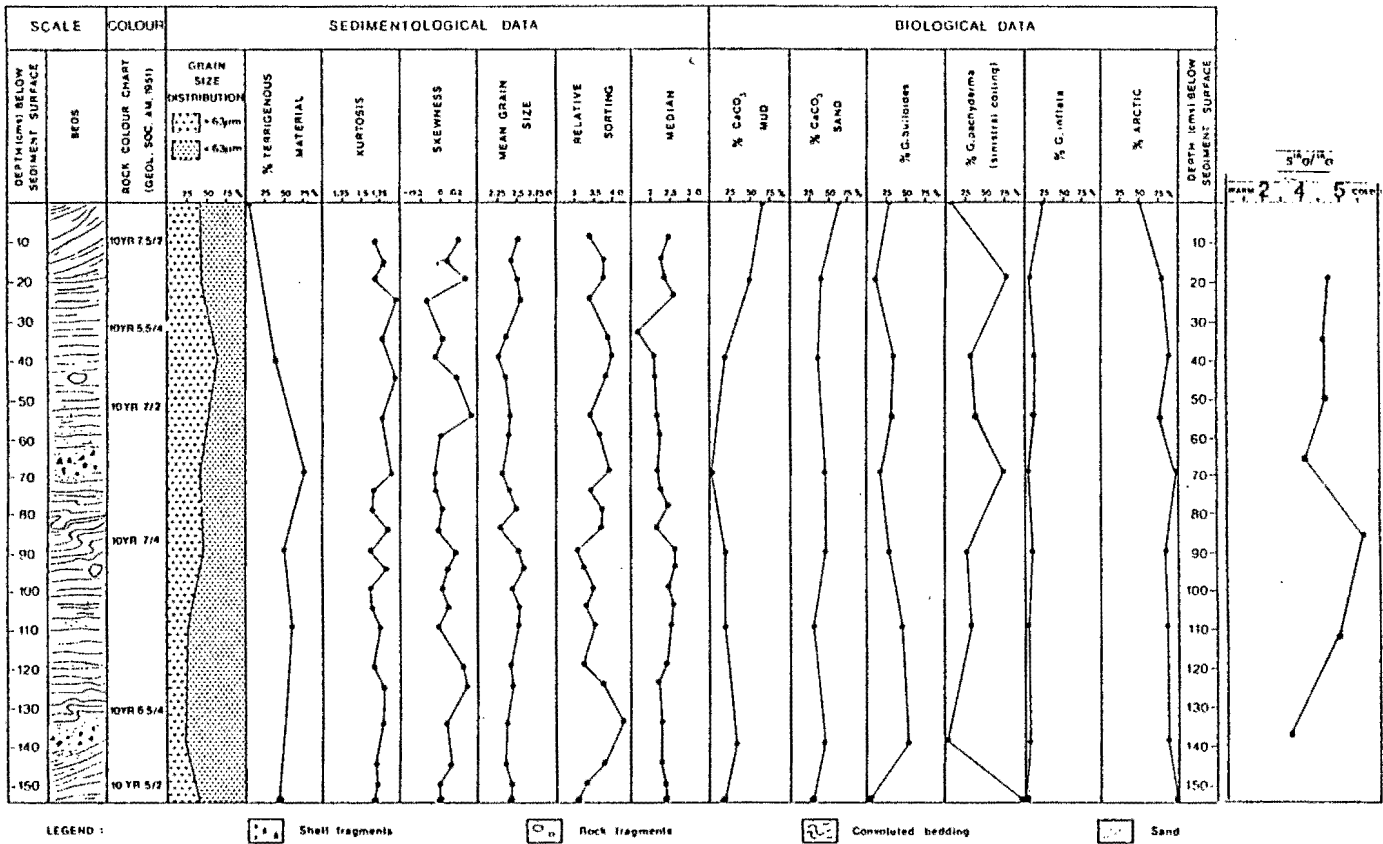
* Estimated 18000 B.P.

▲ Estimated 11000 B.P.

CORE NUMBER : 1868

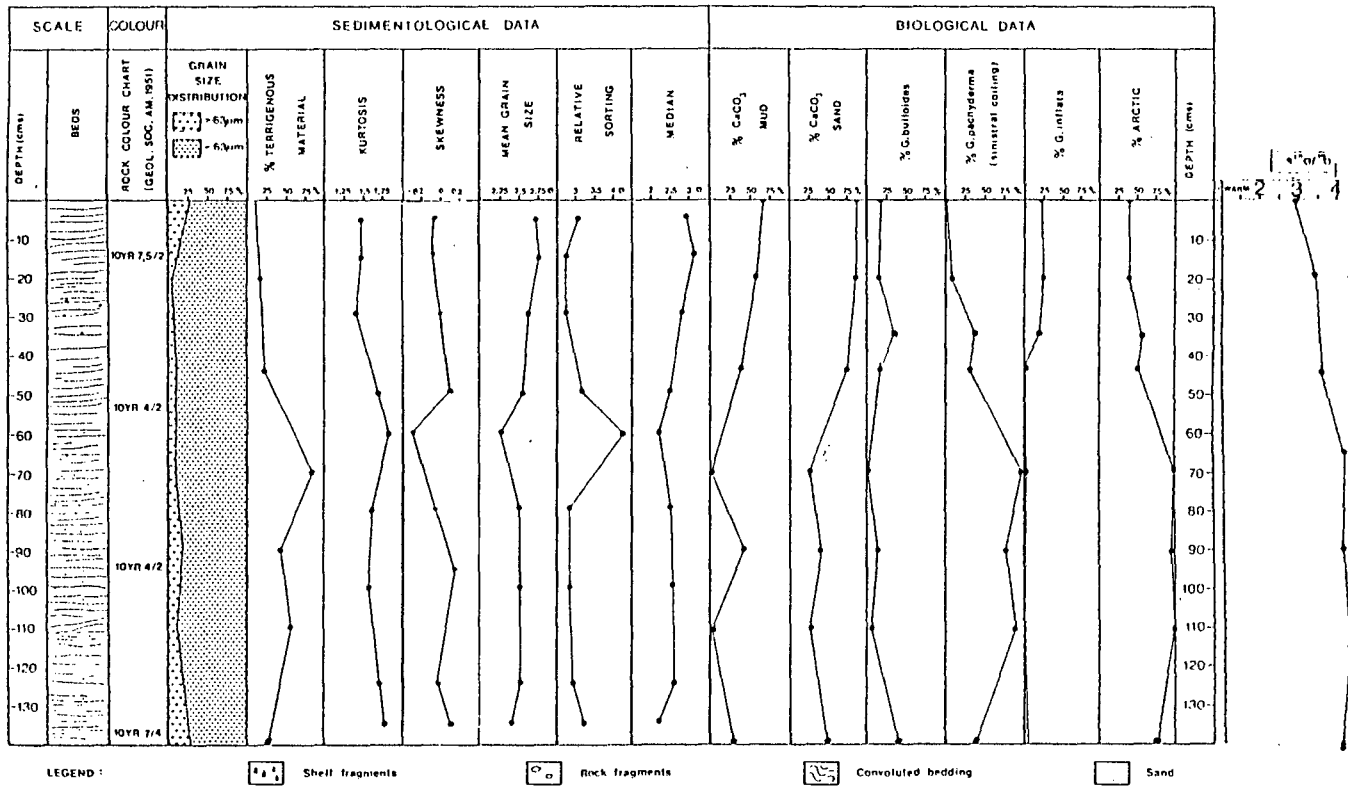


CORE NUMBER : 1869

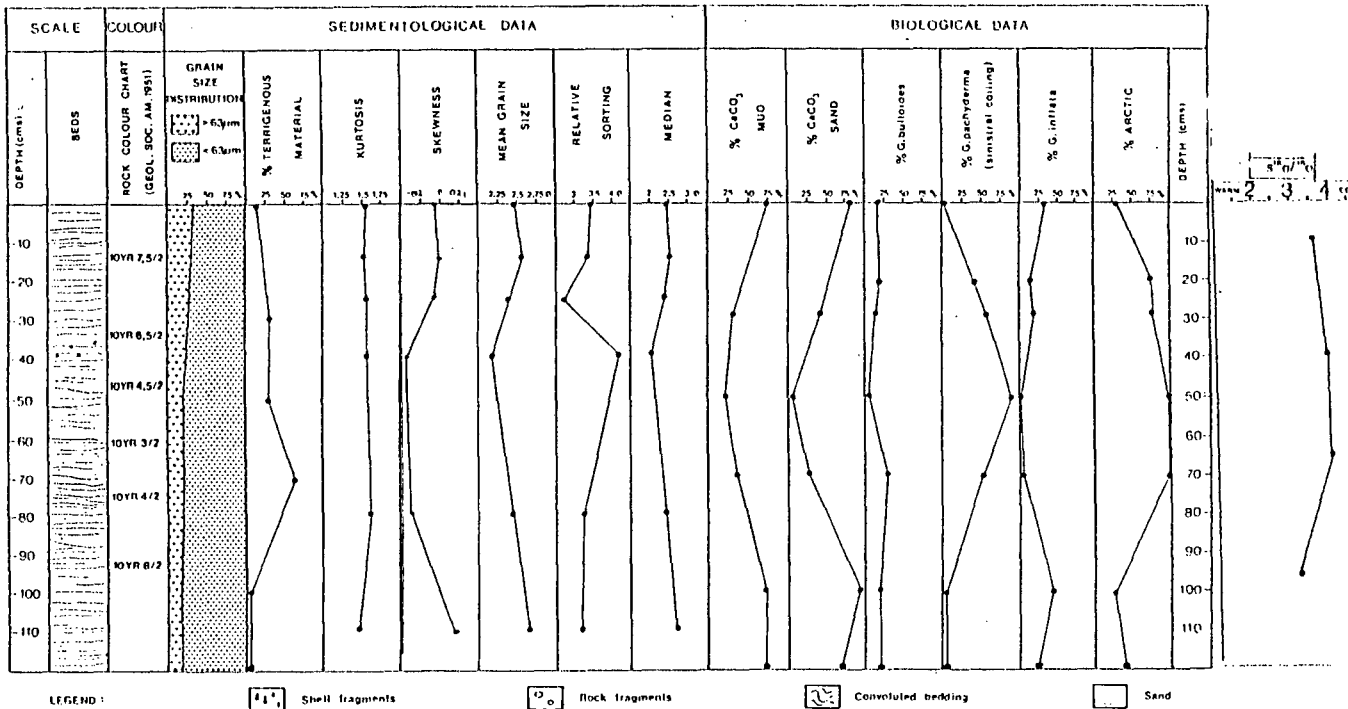


* Estimated 18 000 B.P.
 ▲ Estimated 11 000 B.P.

CORE NUMBER : 1871



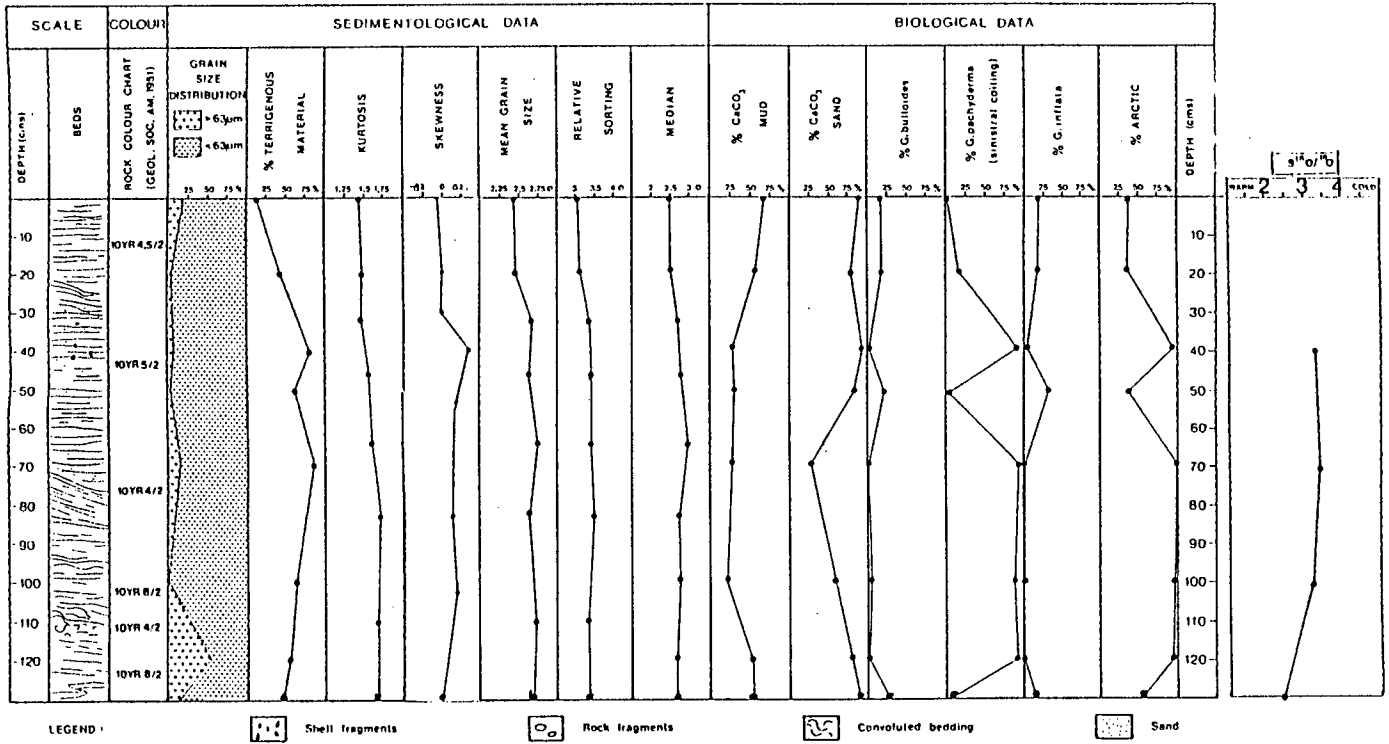
CORE NUMBER : 1872



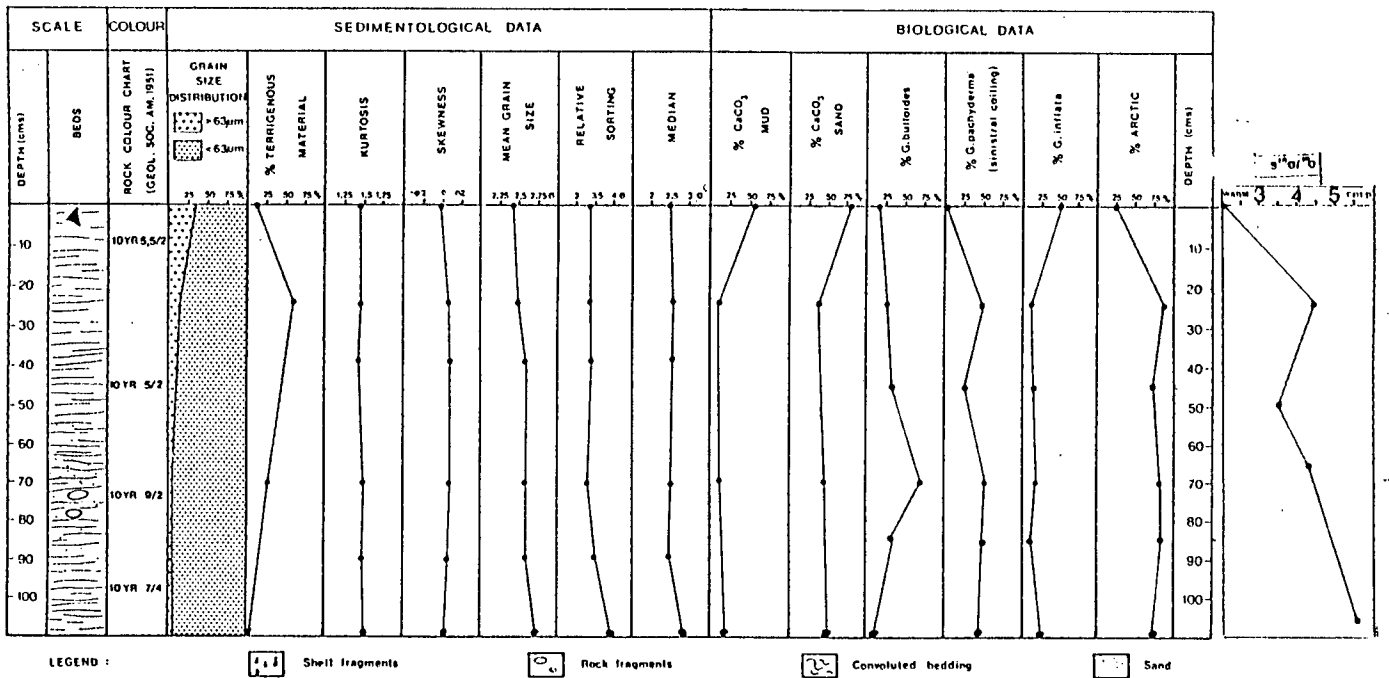
* Estimated 18 000 B.P.

▲ Estimated 11 000 B.P.

CORE NUMBER : S-1



CORE NUMBER : S-3



* Estimated 18 000 B.P.

▲ Estimated 11 000 B.P.

Similar trends were noted in cores 1869 at 86cm (10 YR 7/4 to 10 YR 6/2), 1865 at 40cm (10 YR 7,5/2 to 10 YR 4,5/2), 1861 at 18cm (10 YR 8/2 to 10 YR 4/2) and 46cm (10 YR 4,5/2 to 10 YR 7,5/2), 1868 at 22cm (10 YR 7/2 to 10 YR 4/2), 1862 at 6cm (10 YR 8/4 to 5 YR 3/1). However, overall colour is somewhat monotonous in all cores, usually an olive-grey (10 YR 7/2) or yellow grey (10 YR 5/2), but much of this monotony may be due to post-coring changes, as colour alterations moving from the outside to the centre were noted in several places. Areas of distorted laminae, possibly due to coring disturbances were noted in cores S-1, 1862, 1865, 1867, 1869, however these were not widespread and confined within 1-3 centimetres-wide zones, except for 1865 where larger disturbances were noted. Spotting or mottling indicative of bioturbation, was found in numerous places, most noticeably in cores 1861 (throughout), 1862 (several parts, most prominent lower down) and 1866 (90-105cms, 15-35cms, S-3 (105cms, 10-15cms).

3.3 Micropalaeontology

3.3.1 Introduction

Twenty one species of planktonic foraminifera were identified in these cores, with the total assemblage indicating a largely sub-Arctic to Arctic regime. The two dominant species were Globigerina bulloides and Globigerina pachyderma (sinistrally coiled). Both of these occur in every sample and in many constitute greater than 90% of the total fauna. The most important secondary species were Globorotalia inflata, Globorotalia scitula, with persistent occurrence of Globigerina rubescens, Globoquadrina aequilateralis, G. dutertrei, Globorotalia truncatulinoides and Orbulina universa: The species distribution is given in Appendix C.

3.3.2 Ratio-of-Species Analysis

Using Boltovskoy and Wright (1978) as a guide, Globigerina pachyderma (dextrally coiled) Globigerina bulloides and Globigerina quinqueloba were picked to represent the sub-Arctic population while Globigerina pachyderma (sinistrally coiled) represented the Arctic species.

The tops of all cores contain (FIGS.8A to 8K) a fauna typical of areas transitional between sub-Arctic and sub-tropical waters. In all but Core 1869 the surface samples contain less than 50% cold-water species and in two cores (1867 and S-3) the cold-water foraminifera constitute 25% or less. A relatively

large number of species are present, with higher proportions among the warmer-water species. Most prominent are *G. inflata*, *G. truncatulinoides* and *G. hirsuta*, but the colder-water species are also present in significant numbers. The number of species present increases upcore. All samples at depth are strongly dominated by cold-water fauna (often 100%). (Core 1862 Sample 6 (94,1%), Core 1862 sample 24 (99,9%) Core 1866 sample 13 (99,9%), Core 1866 sample 23 (91,1%), Core 1869 1 sample 31 (98,9%), Core 1871 sample 15 (99,6%), Core 1871 sample 24 (98,5%), Core S-1 sample 21 (99,7%). The tops of the cores contain 25-50 % cold-water planktonic foraminifera. The cold-water species in Core S-3 (FIG.8K) constituted 63,9% at 105-106cms, rising to 73.6% at 70-71cms, 83% at 25-26cms and decreasing abruptly to 25% at the top of the core. The cold-water species contained in Core 1867 (FIG.8E) constituted 60.8% at 120-121cms rising to 84,3% at 85-86cms, 93.3% at 20-21cms and decreasing abruptly to 21,5% at the top. Core 1869 (FIG.8G) displayed 98.9% at 155-156cms, 83,7% at 90-91cms, 94% at 70-71cms and decreasing gradually to 55,5% at the top. Finally Core 1872 (FIG.8I) displayed 96,7% at 50-51cms decreasing sharply to 28,4% cold-water species at the core top. In the other cores, the fluctuations in total numbers of cold-water species does not alter as markedly, however the proportion of *Globigerina pachyderma* (sin) does change significantly.

CORE NUMBER: 1861

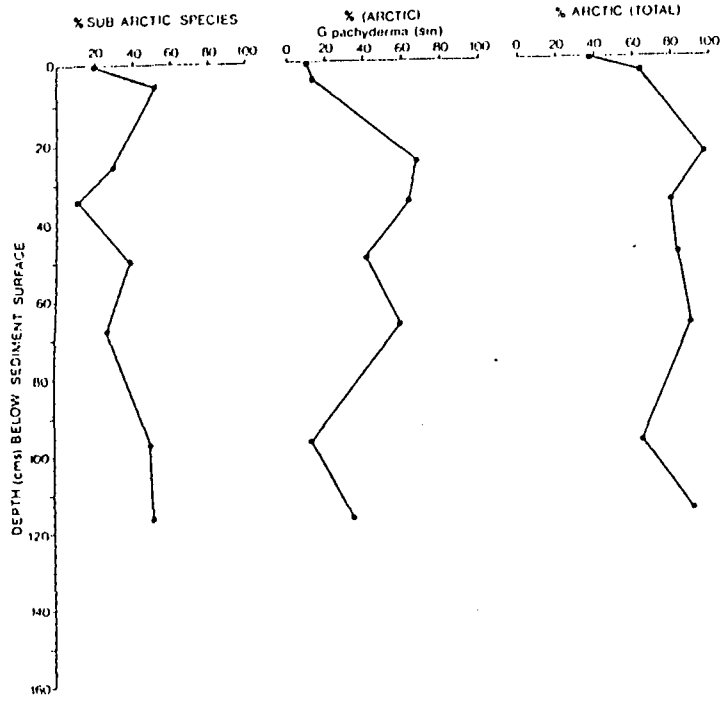


FIG. 8A (Graphs display % of forams per group vs depth)

CORE NUMBER: 1862

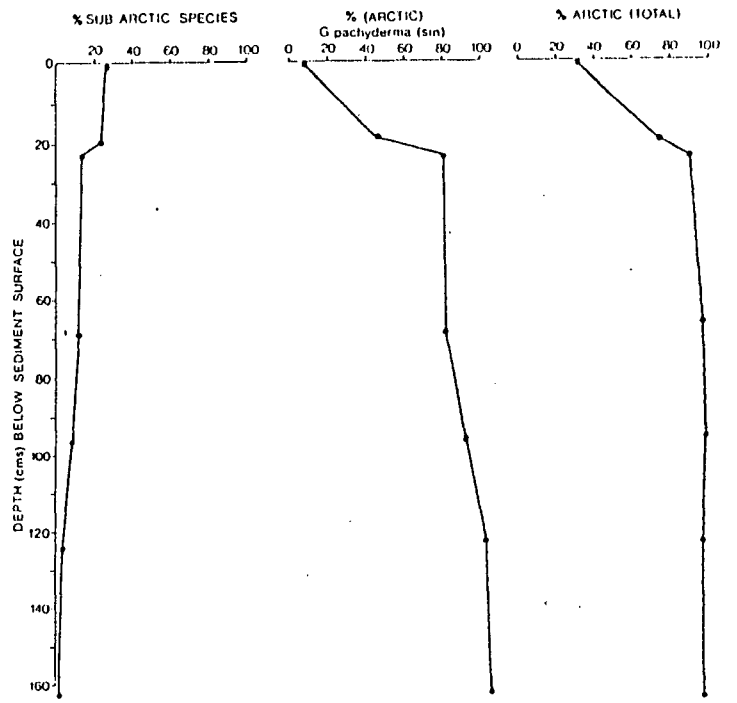


FIG. 8B (Graphs display % of forams per group vs depth)

CORE NUMBER: 1865

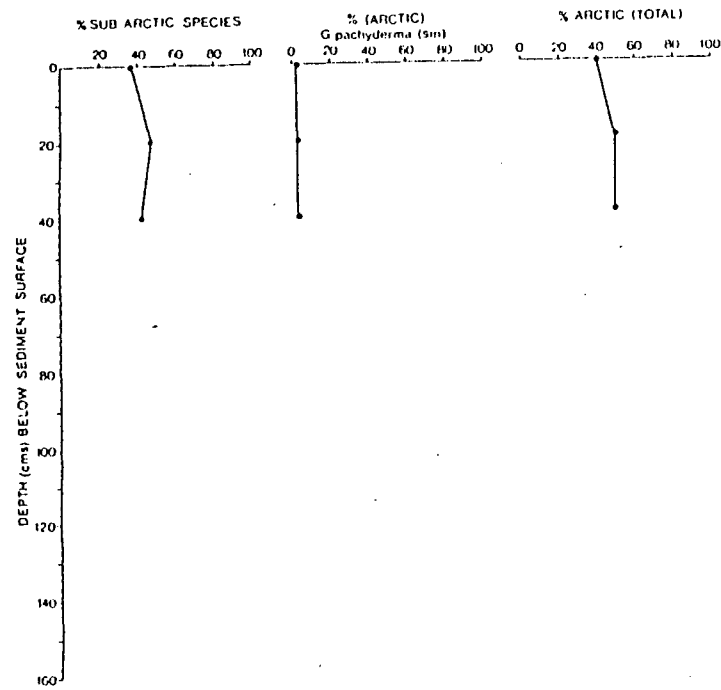


FIG. 8C (Graphs display % of forams per group vs depth)

CORE NUMBER: 1866

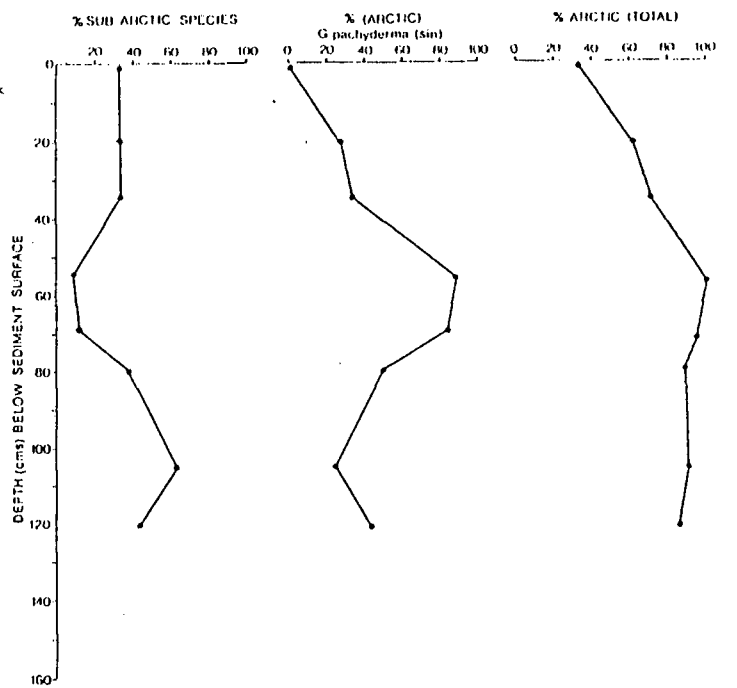


FIG. 8D (Graphs display % of forams per group vs depth)

CORE NUMBER: 1867

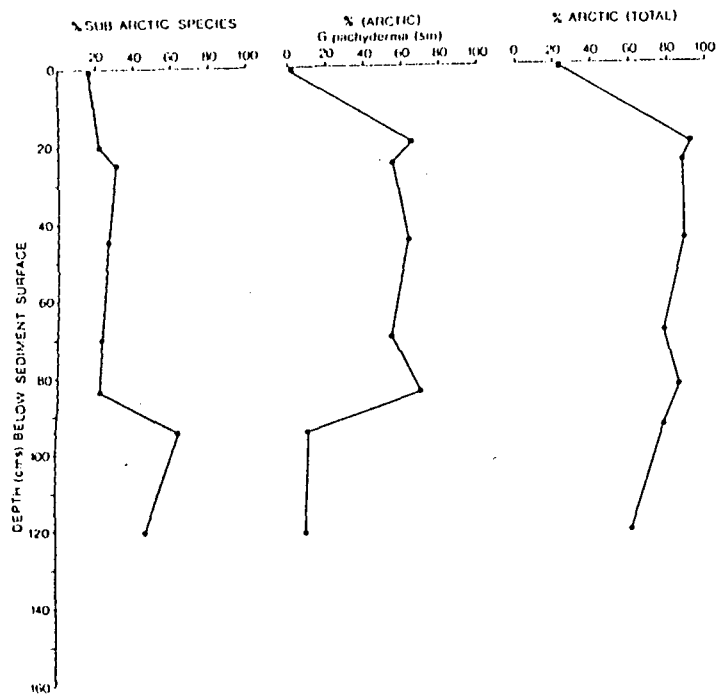


FIG. 8E (Graphs display % of forams per group vs depth)

CORE NUMBER: 1868

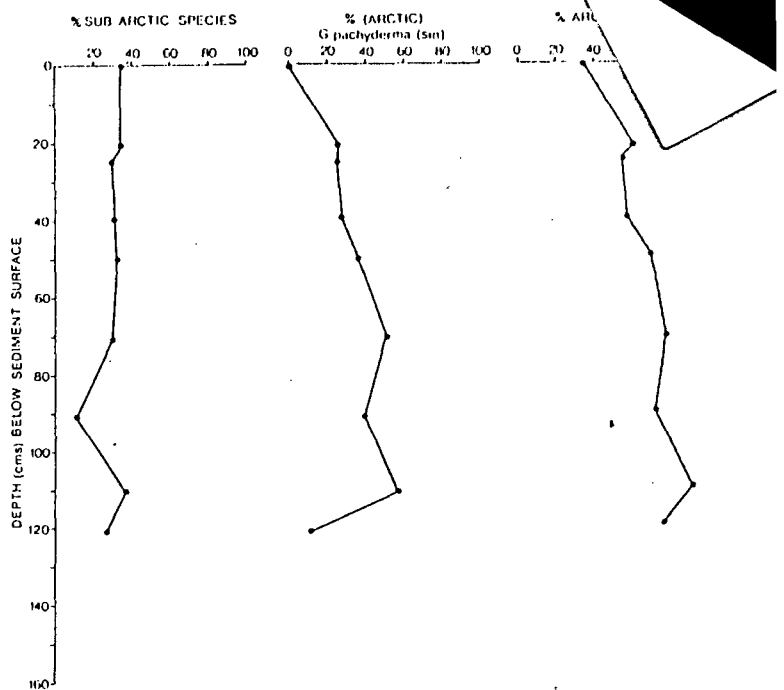


FIG. 8F (Graphs display % of forams per group vs depth)

CORE NUMBER: 1869

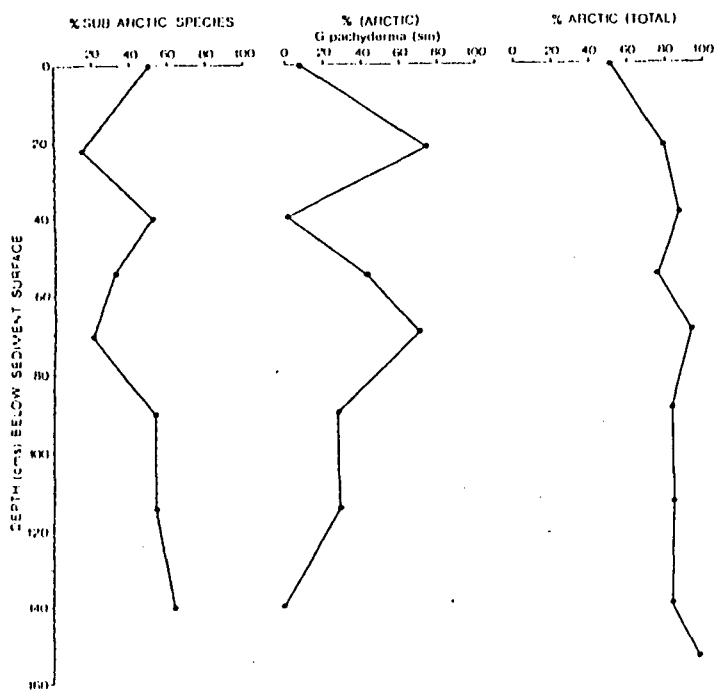


FIG. 8G (Graphs display % of forams per group vs depth)

CORE NUMBER: 1871

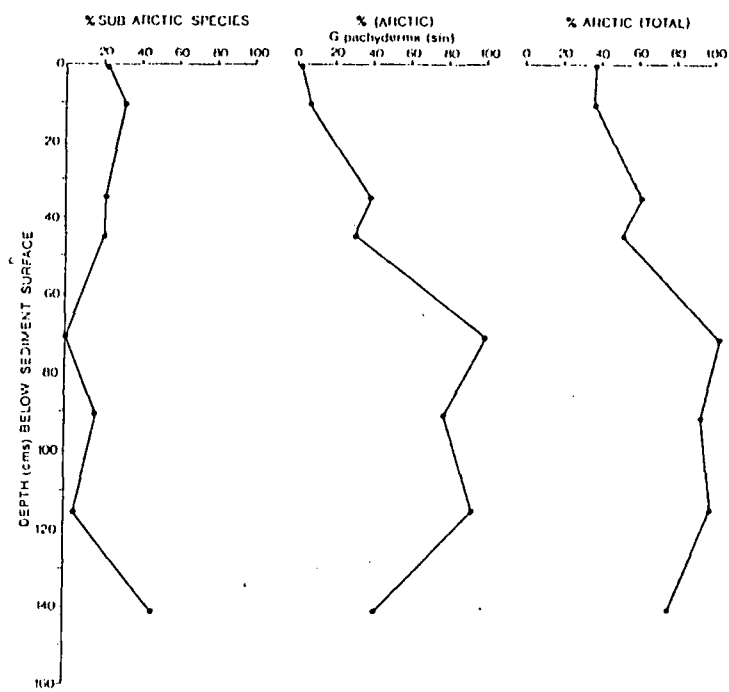


FIG. 8H (Graphs display % of forams per group vs depth)

CORE NUMBER: 1872

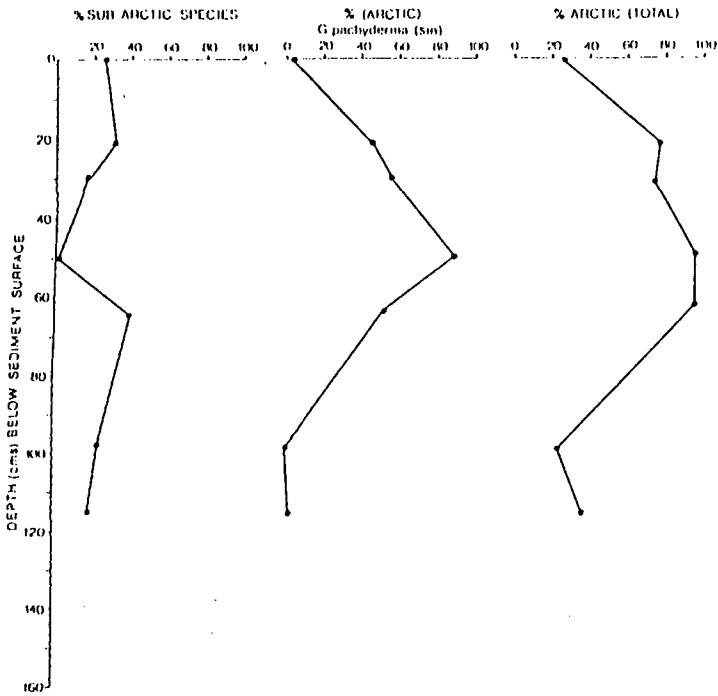


FIG. 0 I (Graphs display % of forams per group vs depth)

CORE NUMBER: S-1

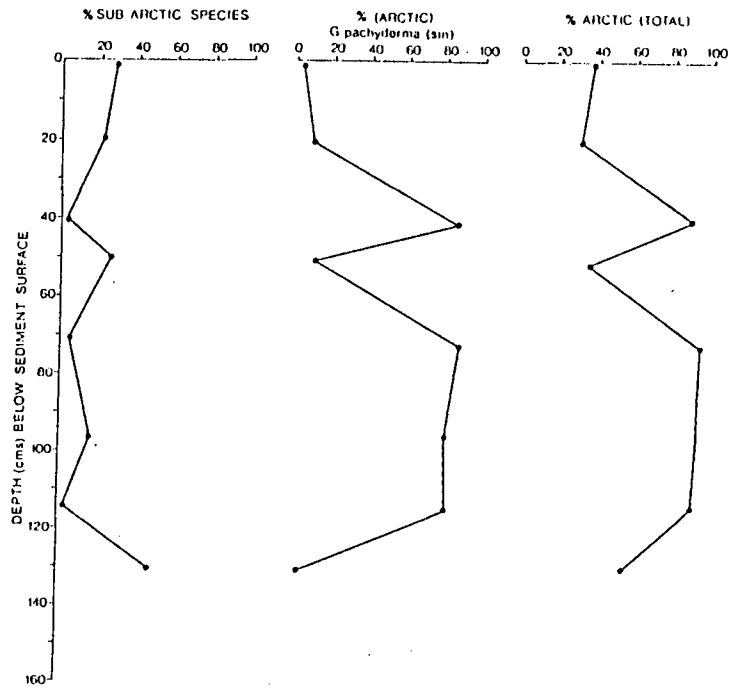


FIG. B J (Graphs display % of forams per group vs depth)

CORE NUMBER: S-3

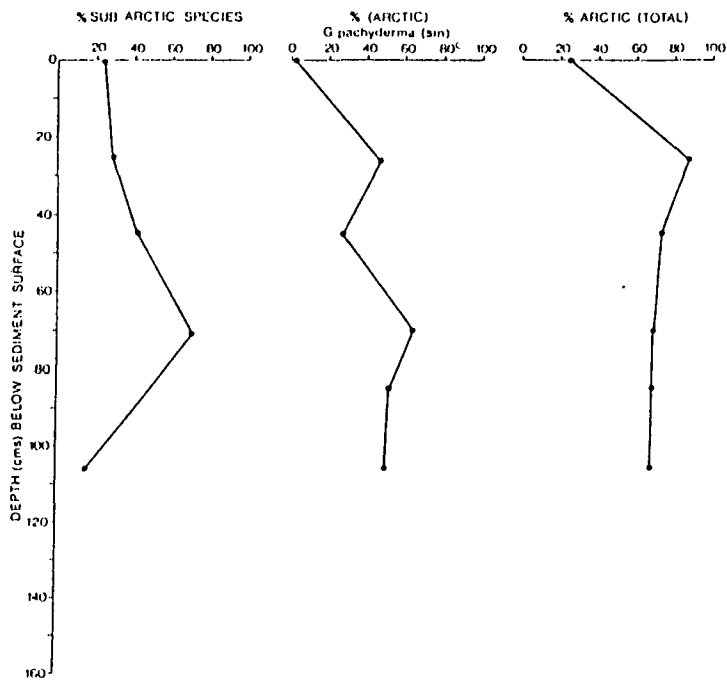


FIG.8K (Graphs display % of forams per group vs depth)

Globigerina pachyderma (dex) and Globigerina quinqueloba display greatly reduced numbers between 80-60 cms as exhibited by Cores 1868 and 1869 (FIG.9). Similarly Globorotalia inflata follows this trend (Appendix.B).

3.3.3 Morphological Changes

In addition to the change noted in the overall populations, several individual species show morphologic changes.

G. pachyderma displays considerable variation in the size of its aperture and slight variation in the amount of inflation of the final chambers. The size of the aperture appears to decrease during the colder periods.

G. bulloides also shows considerable variation in the size and shape of its aperture and there appears to be a definite tendency for the aperture to be smaller and the test more compact in those samples containing a high proportion of cold-water fauna.

3.3.4 Planktonic-Foraminiferal Fragment Analysis

Fragments of foraminifera (mainly planktonic) (any incomplete test) constituted only about 0-10% of any of the samples throughout the cores. Some foram tests may have been broken during wet sieving, although this was done with care.

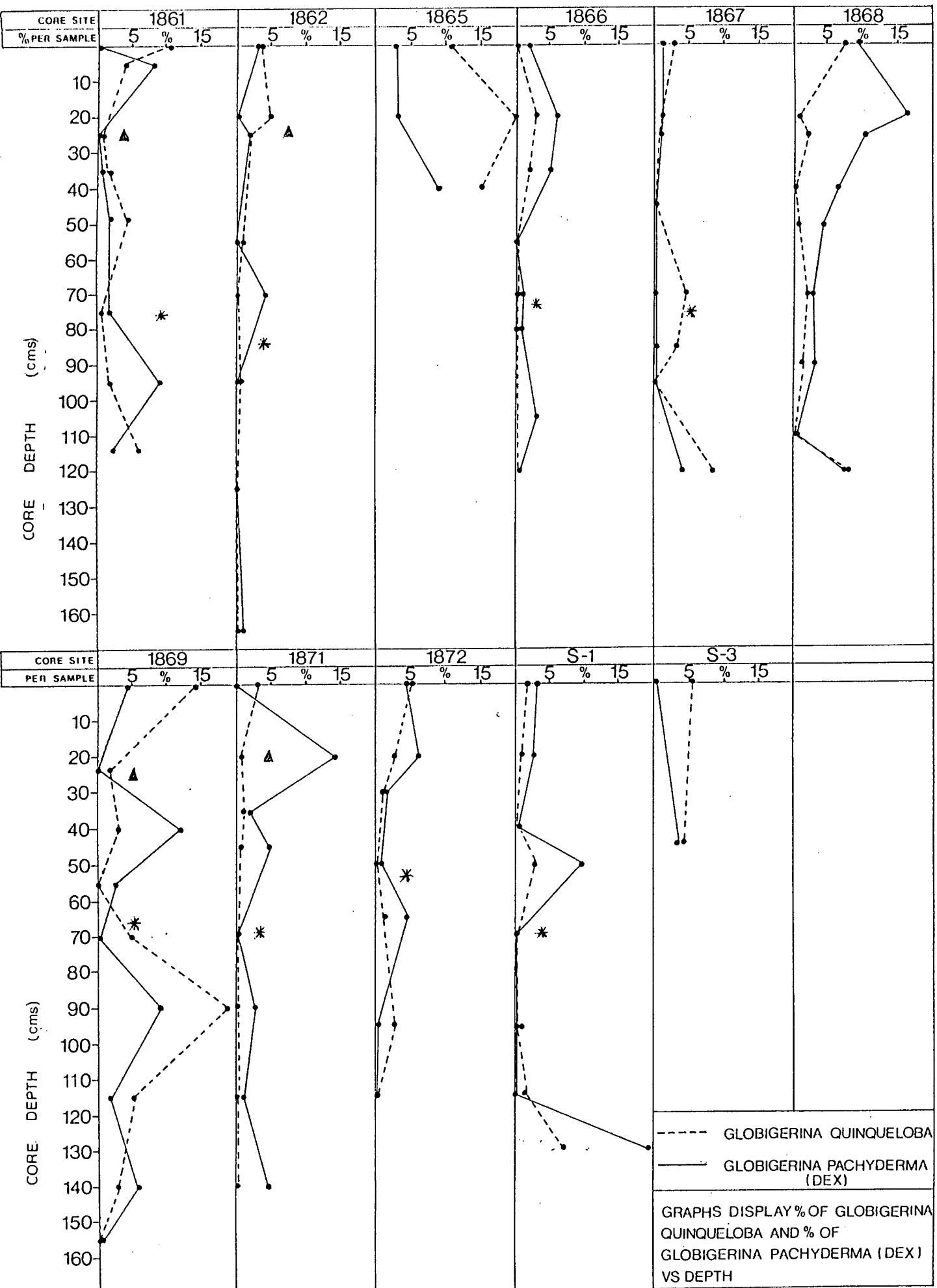


FIG. 9

* Estimated 18 000 B.P.

▲ Estimated 11 000 B.P.

Similarly some planktonic test fragments smaller than 63 microns would have been lost. Test-wall thickness varied from sample to sample and from species to species. All stations are above the Carbonate Compensation Level so dissolution of the test can be disregarded.

3.3.5 Calcium-Carbonate Analysis

Surface samples contain relatively large percentages of CaCO_3 (Core S-1, 92% in the coarse fraction; 70% in the fine fraction) (Core S-3, 80% in the coarse fraction, 55% in the fine fraction), (Core 1865, 95% in the coarse fraction, 65% in the fine fraction), (Core 1868, 79% in the coarse fraction, 62% in the fine fraction), (Core 1871, 89,5% in the coarse fraction, 67% in the fine fraction), (Core 1872, 84% in the coarse fraction, 73% in the fine fraction). The remaining six cores all contained at least 50% CaCO_3 in the coarse fraction and 42% CaCO_3 in the fine fraction. (Appendix C) (FIG.10).

The upcore carbonate records for the eleven cores display various significant similarities and differences (FIG.10). Cores 1861, 1868, 1869, 1872 and S-1 display relatively low carbonate percentages at the 20cm -30cm interval while Cores 1865, 1866, 1867 and 1871 do not exhibit this trend. However all cores display low carbonate percentages at around the 70cm interval.

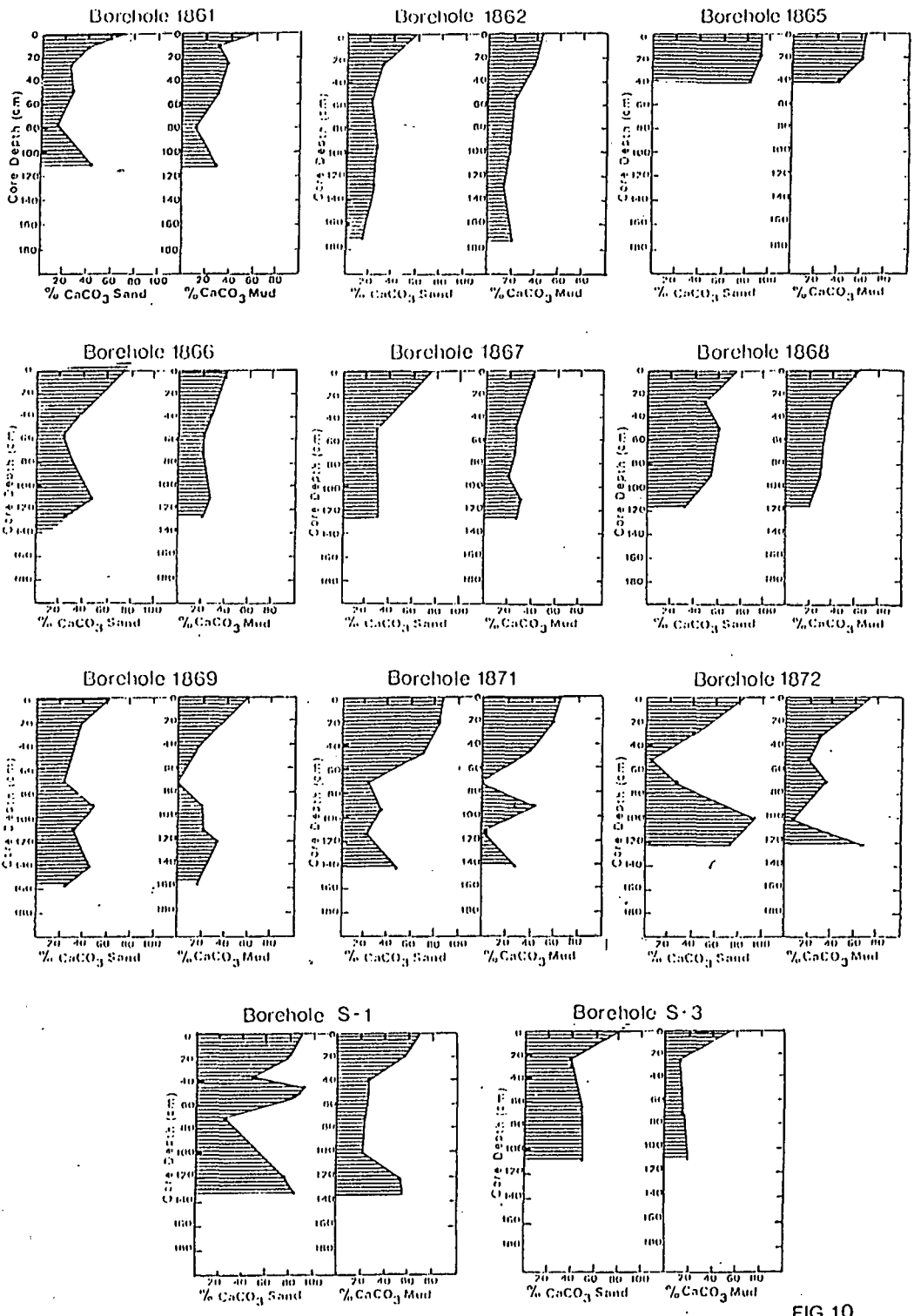


FIG.10

3.3.6 Oxygen-Isotope Analysis

Oxygen-isotope analysis of the cores revealed several interesting trends:(data in Appendix C) (FIG.11).

- a) There is often an increase in the $^{18}\text{O}/^{16}\text{O}$ ratio between 60-110cm in all cores with a tendency for the ratio to be peaked around the 70cm mark.
- b) The majority of cores exhibit an upcore $^{18}\text{O}/^{16}\text{O}$ ratio decrease from 70cm although Cores 1862,1869 and S-3 display increases in this ratio at 25cm.

3.4 Sedimentology

3.4.1 Grain-Size Analysis

The settling diameters of the grains are calculated according to the settling velocities of equivalent quartz spheres, irrespective of grain density and shape. The sand fraction is treated as an ideal hydraulic population and the mud ($< 63\ \mu\text{m}$) component has been excluded from computation of statistical grain-size parameters. The populations are therefore truncated artificially at $63\ \mu\text{m}$.

The spatial distribution patterns for various grain-size parameters of the sand fraction are listed within this

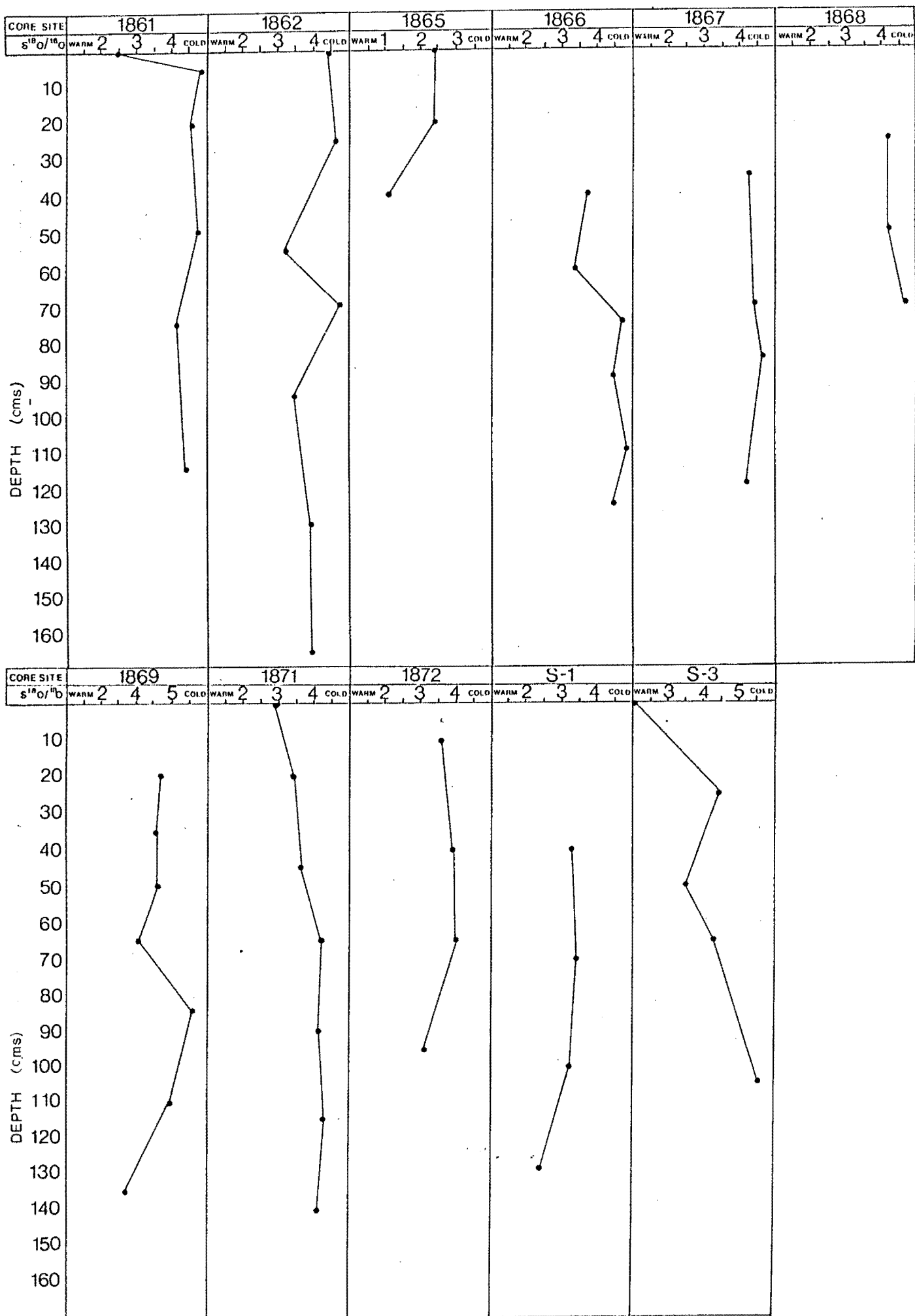


FIG.11 STABLE ISOTOPE RESULTS (PDP%) FOR GLOBIGERINA BULLOIDES

section. Distribution patterns therefore reflect a combination of mechanisms controlling the deposition of biogenic and terrigenous sand-size components. Grain diameters and statistical parameters have been computed in phi(ϕ) notation.

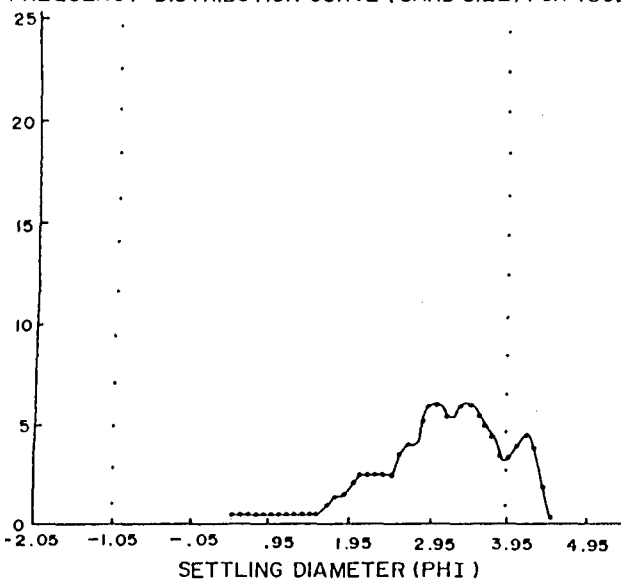
The granulometry of the coarse fraction ($>63 \mu\text{m}$) has been determined for all cores in the study area. The statistical coefficients calculated for this granulometric analysis are: central tendency (mean, median); kurtosis, (degree of peakedness); skewness and relative sorting. (The data are plotted in Appendix B and listed in Appendix C).

All cores display polymodality throughout their lengths (FIG.12).

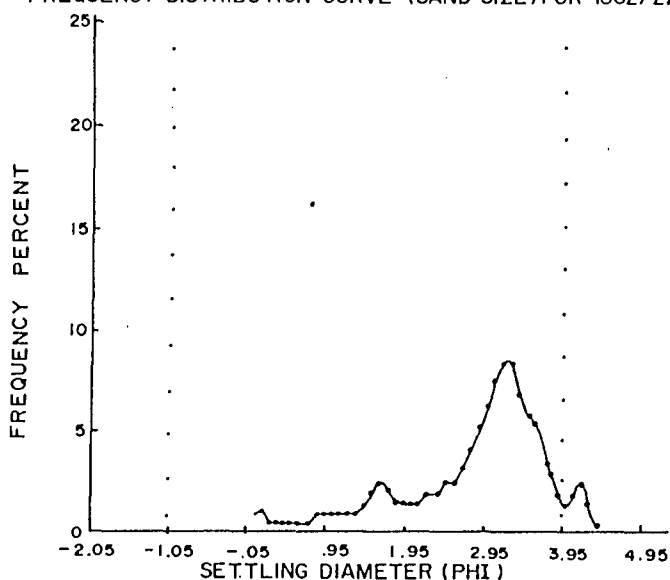
Cores 1867, 1868, 1869, 1871 and 1872 (FIG.1) display decreasing mud content from about the 80cm-60cm interval upcore. Similarly mean and median grain size decreases upcore. Samples are poorly sorted throughout their lengths however this improves upcore from the 100cm-60cm mark. Samples within this interval were found to be negatively skewed.

Cores 1861, 1862, 1866, S-1 and S-3 (FIG.1) display less dramatic statistical fluctuations upcore than the above cores. Mud content decreases markedly upcore. All samples are poorly sorted although this does improve upcore. Samples between 100cm-60cm were found to be positively skewed.

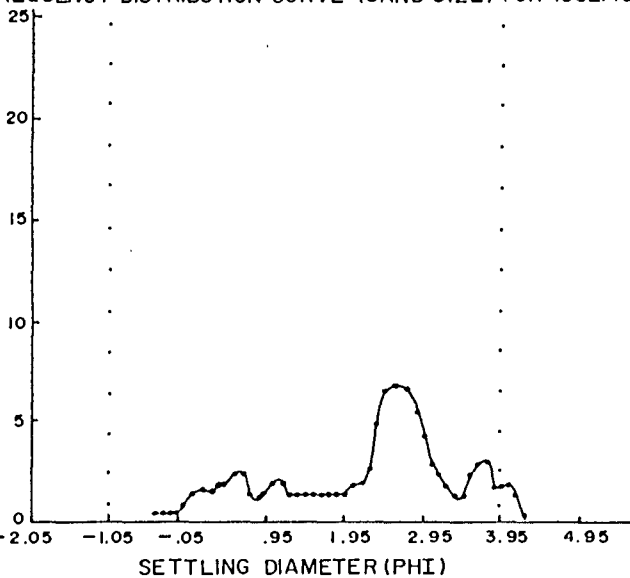
FREQUENCY DISTRIBUTION CURVE (SAND SIZE) FOR 1862/2



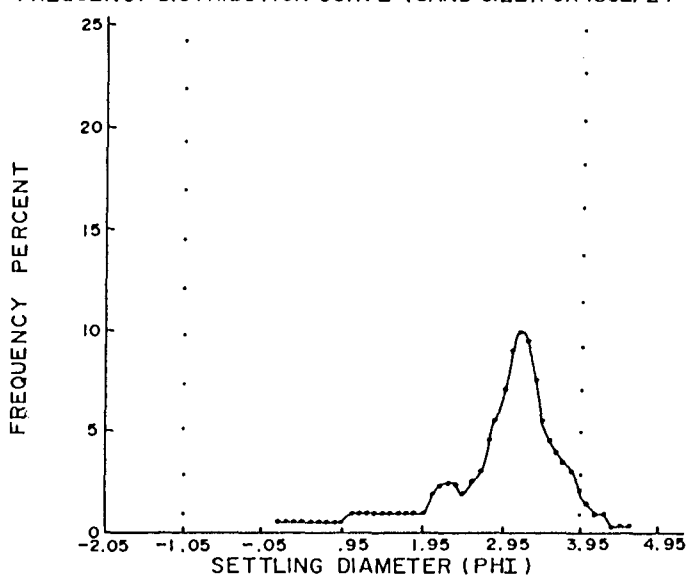
FREQUENCY DISTRIBUTION CURVE (SAND SIZE) FOR 1862/22



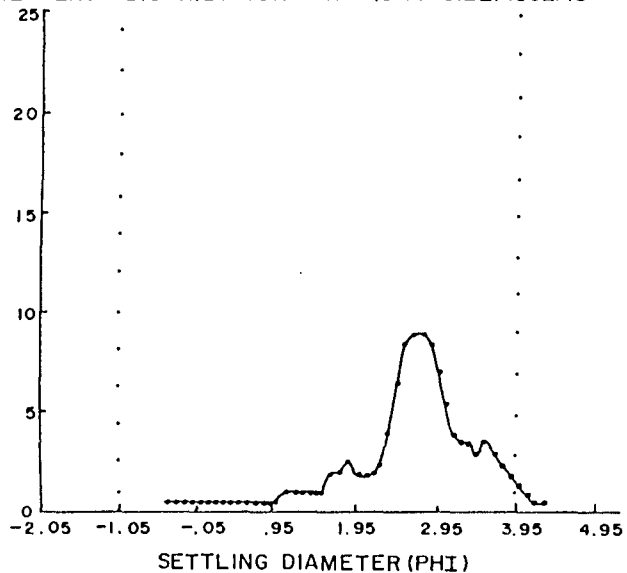
FREQUENCY DISTRIBUTION CURVE (SAND SIZE) FOR 1862/10



FREQUENCY DISTRIBUTION CURVE (SAND SIZE) FOR 1862/24



FREQUENCY DISTRIBUTION CURVE (SAND SIZE) 1862/13



FREQUENCY DISTRIBUTION CURVE (SAND SIZE) FOR 1862/28

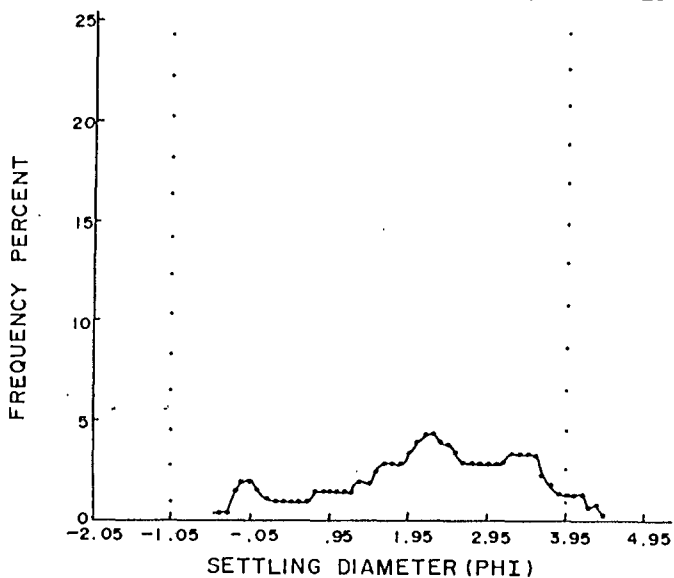


FIG. 12 Displays frequency distribution curves for borehole 1862; Sample No. 2, 10, 13, 22, 24, 28

3.4.2 Ice-Rafted Debris Analysis

Ice-rafted debris is easily identifiable, as it characteristically consists of a mixture of angular, poorly sorted mineral (e.g. mica, quartz, zircon) and rock fragments. The sand fraction invariably displays polymodality in its size distribution (FIG.12). The size, poor sorting, general angularity and wide lithological range of this detritus, found in pelagic sediments far from land, indicate that it has been dropped from melting ice. [Connolly and Ewing (1965), Smythe et al (1984)].

All cores in this study exhibit zones composed of ice-rafted debris which contain large quantities of angular quartz grains (both frosted and on occasions pitted) and an assortment of poorly sorted rock and mineral fragments.

All cores contain glacial detritus up to about 15cm. (Core 1861 up to 24cm) (Core 1862 up to 16cm) (Core 1865 up to 7cm) (Core 1866 up to 20cm) (Core 1868 up to 18cm) (Core 1871 up to 20cm) (Core 1872 up to 25cm) (Core S-1 up to 30cm) (Core S-3 up to 15cm) (Core 1869 up to 15cm) (Core 1867 up to 25cm). Visual examination of several characteristics displayed by the ice-rafted debris (angularity, frosting, pitting and colour) revealed some small scale changes upcore especially with regard to frosting and pitting.

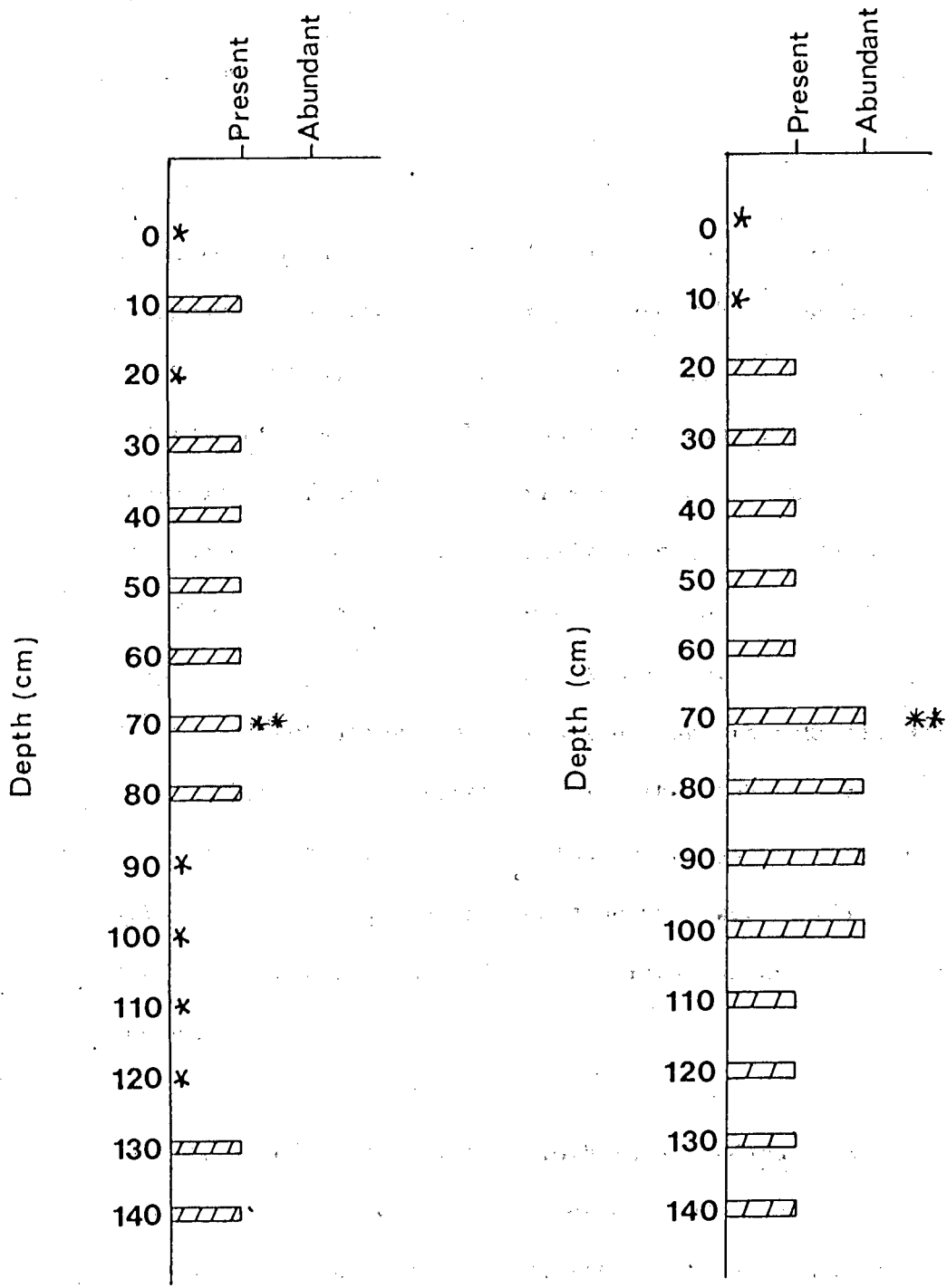
Abundant ice-rafted debris was noted at 75cm and 48cm in Core 1861 at 90cm and 55cm in core 1862, at 55cm and 35cm in Core 1866, at 55cm in Core 1868, at 80cm and 30cm in Core 1869, at 115cm, 70cm, 45cm in Core 1871, at 50cm in Core 1872 and at 70cm and 40cm in Core S-1.

Semi-quantitative values for Core 1869 are plotted in figure 13B.

3.3.3 Mica Analysis

Increased quantities of mica are present in samples associated with cold periods within these cores, (Core 1867 at 70cm and 46cm), (Core 1869 at 41cm), (Core 1866 at 80cm and 35cm), (Core S-1 at 40cm), (core 1861 at 75cm). Many sample sites however display no visible mica.

Semi-quantitative mica values for Core 1869 are plotted in figure 13A.



(a) Mica

(b) Ice-rafted debris

FIG 13. Bar graphs display semi-quantitative analysis of mica and ice-rafted debris for borehole 1869.

* Denotes no mica/ice-rafted debris present.

** Estimated 18000 B.P.

although the 40-24 cms peak is not as well pronounced. Examination of both the foraminiferal and sedimentological data indicate that the 80-60 cms interval most likely represents the 18000-20000 BP last glacial maximum, while the 40-25 cms interval the 11000 BP readvance.

An analysis conducted into the relationship between *Globigerina pachyderma* (dex) and *Globigerina quinqueloba* indicated that both fluctuate in concert with climatic change (FIG.9). Decreasing temperatures result in decreasing numbers as exhibited by cores 1868 and 1869 at between 80-60 cms. Similarly *Globorotalia inflata* follows this trend (Appendix. B).

Examination of the calcium carbonate data revealed that the CaCO_3 content of the fine fraction ($<63 \mu\text{m}$) is inversely proportional to the percentage of the Arctic fauna, and a maximum Arctic fauna was always accompanied by a minimum CaCO_3 content (FIGS.8A to K and 10). The trend in the coarse fraction was similar, though not as pronounced or consistent. McIntyre et al (1973) noted a similar trend in the North Atlantic cores, and examination of their fine fraction revealed a minimum or total absence of coccoliths during the polar influxes. They concluded that the coccolith minima (= fine-fraction-carbonate minima) are indicative of glacial conditions. Several samples from the Goban Spur and Porcupine Bank cores were examined qualitatively under a microscope and were found to exhibit a severe reduction of coccoliths during the colder periods.

Obviously there can be other causes of low carbonate content, notably dissolution and dilution by terrigenous material. The former seems unlikely in this area since the foraminiferal content remains high and very few specimens show signs of solution [Huddlestrun (1985)]. In addition all stations are above the carbonate compensation level (5000-6000m) [Friedman and Sanders (1968)]. Dilution with terrigenous material has undoubtedly occurred in the sand fraction; large amounts of terrigenous material occur in the cores, the amount tending to increase with the content of Arctic fauna. Dilution by terrigenous material has no doubt affected the fine fraction as well, but may serve merely to exaggerate the established trend in the coccolith carbonate.

As bioturbation smooths the climatic record, and has been identified in these cores, [Ruddiman and McIntyre (1981a, c)] it is not surprising that the 20cm-30cm spike (probably representing the 11,000 B.P glacial readvance), is not resolved in all cores because the degree of bioturbation differs from site to site. Nevertheless Cores 1868 and S-1 do exhibit the 11000 BP readvance at a level of 20-40 cms. All cores display their minimum CaCO_3 values at the glacial maximum (20,000 B.P - 18,000 B.P) situated at the level of approximately 70cm because this period persisted for a sufficient length of time and was less affected by bioturbation.

The low carbonate-low productivity segments of the carbonate curves therefore reflect the widespread effects of sea ice and downwelling within the broadly cyclonic circulation of surface water in the Goban Spur-Greenland sector of the glacial North Atlantic. Under interglacial conditions the return of the warm North Atlantic Drift stimulated an increase in biologic productivity. The spikes of low carbonate content suggest, therefore intensely cold periods during which sea ice cover was extensive. Ruddiman and McIntyre (1981a) note that the carbonate content is controlled by glacial-interglacial depositional regimes. Similarly Zimmerman (1985) notes that coccoliths and foraminifera are deposited two to three times more rapidly during interglacials, because of greater surface water productivity.

The increase in the oxygen isotope ratio at around the 70 cm interval in the majority of cores indicates the 18,000 B.P. glacial maximum. This was an intensely cold period of long duration, as deduced from foraminiferal evidence. The spread of the peak I suggest can be directly attributed to two factors. Firstly, sediment mixing has no doubt occurred as contourites, identified from the X-ray photographs, are present throughout the lengths of all cores (Appendix A). This would tend to smudge the isotope record decreasing amplitude and increasing the width of the peak. However there is a tendency for the oxygen isotope ratio to be peaked at around the 70cm mark indicating maximum glacial conditions.

This is in keeping with the foraminiferal (section 3.3), sedimentological (section 3.4) and calcimetric (section 3.3.5), results which similarly indicate a major glacial at approximately the 70cm level.

The majority of cores fail to exhibit an oxygen isotope ratio peak at or around the 25cm mark (FIG.11), a level at which I consider, from the foraminiferal evidence represents the 11,000 B.P. glacial readvance for this area. Nevertheless Cores 1862, 1869 and S-3 do display an increase in this ratio at 25cm. Bioturbation is most likely responsible for this dilution or suppression of the oxygen-isotope record as it smooths short-term events [Ruddiman and McIntyre (1981a, b)]. Bioturbation, deduced from the presence of mottling throughout the core lengths, was noted in all cores and throughout their lengths. However this is not easily visible from the X-ray photographs in Appendix A and was identified predominantly on close examination of the split-core surface. It appears from this evidence and from the work of Shackleton and Opdyke (1975), Berger et al (1985), Shackleton et al (1984) and Zahn et al (1985) that the oxygen-isotope record is very susceptible to minor influences such as small-scale bioturbation and sediment mixing. The sedimentological and foraminiferal data presented here have apparently fared better in retaining the geological record of the last major glacial maximum than the oxygen isotope record.

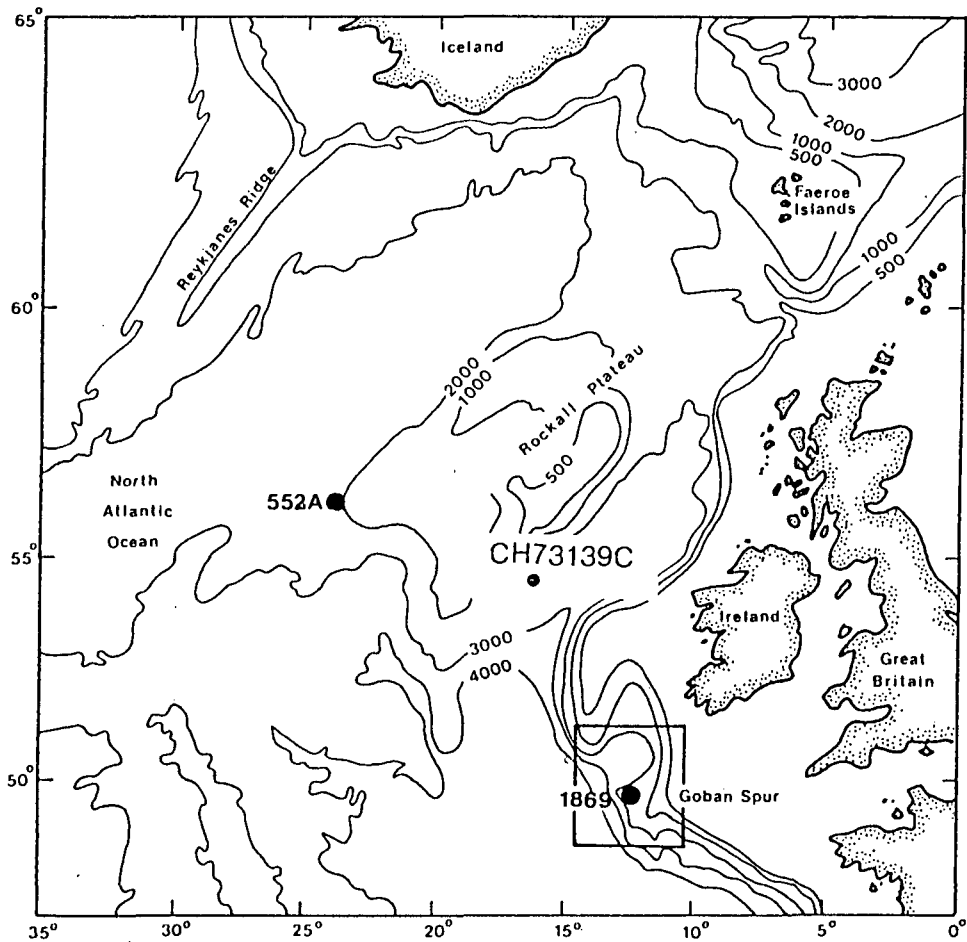
An analysis was conducted into the relationship between the oxygen-isotope data and calcium-carbonate data from DSDP 552A (FIG.14) and this studies cores in an attempt to observe a possible correlation.

DSDP borehole 552A is located at a water depth of 2311m on the Hatton sediment drift at the base of the Western Flank of the Rockall Plateau (FIG.14).

O^{18}/O^{16} variations examined by Duplessy et al (1981), Ruddiman and McIntyre (1981a, b), Zimmerman et al (1985) and others are found to be inversely proportional to variations of carbonate exhibited by these and other North Atlantic cores.

In Figures 15 and 16 plots of $CaCO_3\%$ vs depth for boreholes DSDP 552A Zimmerman et al (1985) and Core 1869 are presented. Core 1869 was chosen and compared to the DSDP 552A core data because it is relatively long and because it is representative of the cores in this study. The two plots display similar profiles. Figure 17, an oxygen-isotope ratio plot from DSDP 552A, presents an inverse relationship to that of the $CaCO_3$ plots, ie. a rise in the $^{18}O/^{16}O$ ratio being accompanied by a decrease in the $CaCO_3$ present. An excellent correlation therefore exists between the Zimmerman et al (1985) data and the data obtained from Core 1869 (FIG.11).

Similarly the oxygen-isotope ratio plots in cores of this study correlate with the isotope plots from DSDP borehole 552A.



Location map for Hole 552A (56°02', 56°N, 23°13', 39'W, water depth 2311m). (After Hall, 1985)

FIG.14

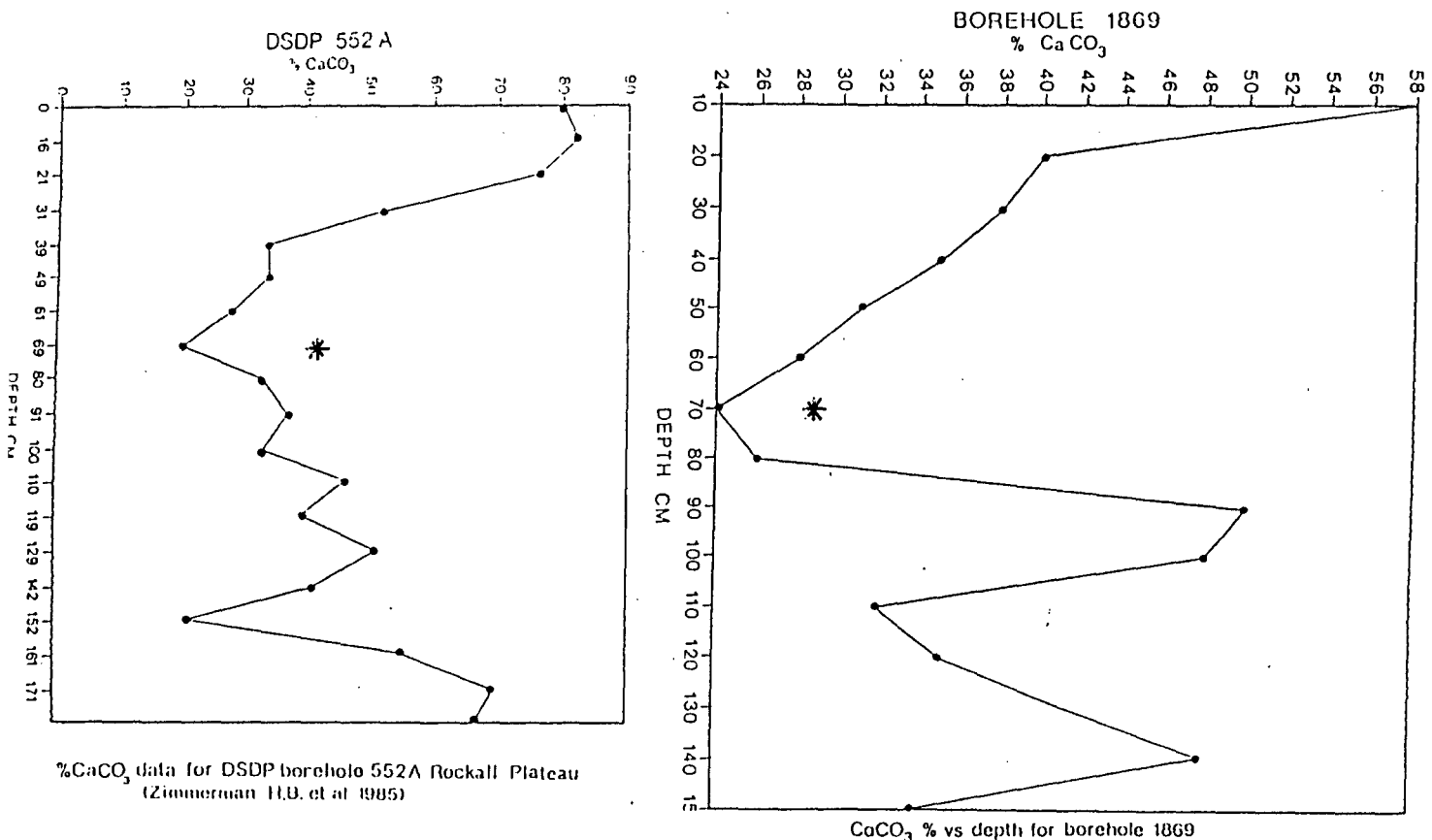


FIG. 16

15

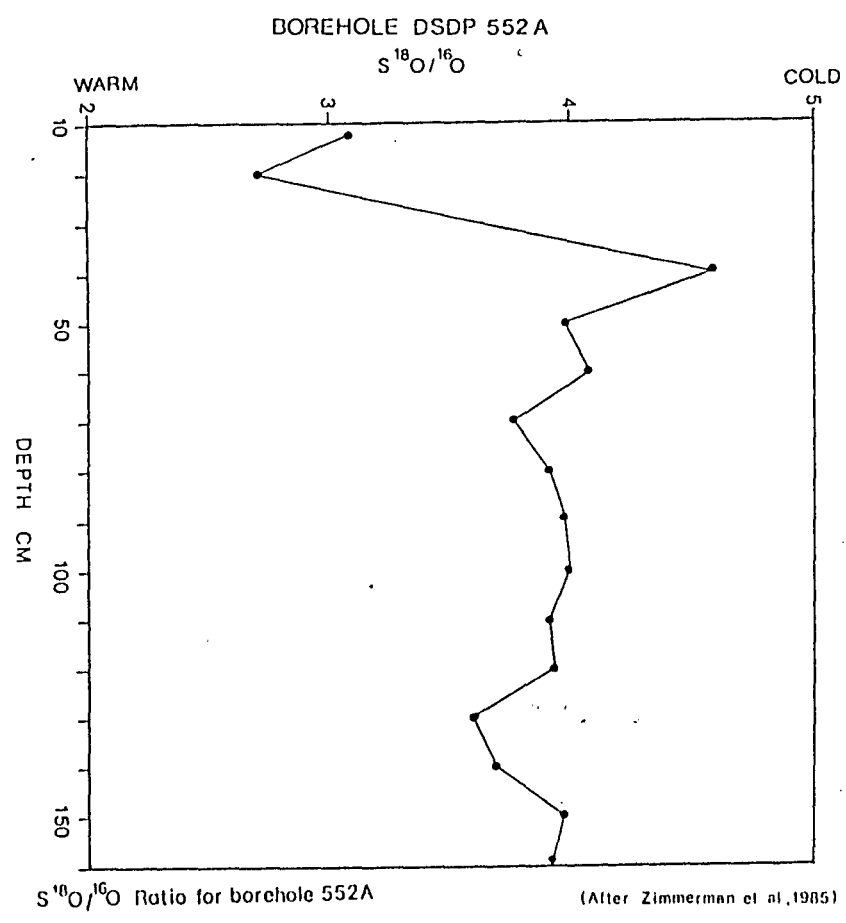


FIG. 17

- * Estimated 18 000 B.P.
- ▲ Estimated 11 000 B.P.

Examination of the sedimentological statistics reveals that several complicating factors exist. All curves (Appendix B) reflect the mixing of sediments from different environments and it is likely that the presence of several populations in one sample reflects the action of several different physical processes; wind, waves, ice-rafting, currents and gravitational processes.

Figure 12 displays frequency diagrams for Core 1862 in which polymodality is characteristic. The remainder of the cores exhibit similar polymodal characteristics.

Analysis of the granulometric statistics from samples representing the colder periods (identified by % of Arctic foraminifera species) (FIG.8) indicate that two groups of cores exist. Group-1 Cores, situated on the Pendragon Escarpment and in close proximity to each other (1867, 1868, 1869, 1871, 1872) (FIG.1) display polymodal characteristics throughout their lengths and a tendency towards a muddy character during the cold periods. However, overall mean and median grain-sizes were coarser and poorly sorted during the colder times due to the presence of ice-rafted detritus [Conolly and Ewing (1965)]. The sample statistics display negative skewness, i.e. they have a coarse tail of ice-rafted grains.

Group-2 cores, situated at various topographic positions throughout the study area (1861, 1862, 1866, S-1, S-3) (FIG.1), whilst also displaying polymodal characteristics, are generally coarser than the Group-1 cores. Sediment statistics are positively skewed in samples from the colder periods indicating the presence of a fine tail. Their topographic positions vary from flat plateaux to steep scarps (Core S-3) (FIG.1).

However, there are slight fining-upward trends during the colder periods. The median displays no major variations during the colder periods. In general Group-2 cores show a more passive response to glacial activity than Group-1 cores.

Bottom currents have been observed in the study area (CLIMAP (1976), Ruddiman and McIntyre (1981a, b), Zimmerman et al (1985), Loubere and Jakiel (1985)). Contourite deposits were identified in Cores 1861, 1862, 1867, 1868, 1869, 1871, 1872, S-1 and Core S-3 contained a large percentage of the benthic foraminifera Rupertia sp, a species capable of existing in strong currents [Boltovskoy (1973)]. Few or no foraminiferal fragments were encountered in any of the cores (0-10%), a factor suggesting winnowing, in that light fragments would be more likely to be removed by bottom current activity than whole forams. Visual analysis of the X-ray data (Appendix A) does not reveal any significant variation in contourite formation and presence (intensity/band width) during colder periods as opposed to the warmer periods. I therefore suggest that the current regime operating in the study area today has been active throughout the geologic time represented by the cores.

Belderson et al (1981) postulate a sea level some 100m lower than that at present during the last glacial maximum (20,000 B.P - 18,000 B.P). The coastline would therefore have been substantially closer to the study area, and the quantity of sediment debouched onto the seaward edges of the Fastnet and Western Approaches Basins greater (FIG.17). During this period strong tidal currents were actively sweeping sediment south-westwards [Belderson et al (1986)].

Terrigenous sediments deposited during glacial conditions are predominantly finer grained than those deposited during interglacials (Ruddiman and McIntyre (1980), Shackleton (1969), Ruddiman and McIntyre (1981a, b), Poag et al (1985), Pujol and Duprat (1985), Shackleton and Hall (1985). The relative abundance of terrigenous sediment increased during the glacial periods (FIG.10) and mean and median grain size appear to increase with glacial activity. However the presence of two or more modes complicates interpretation of all statistical measures and the samples analysed in this study have been shown to be polymodal, (FIG.12). The presence of relatively small quantities of coarse-grained ice-rafted detritus deposited during glacial conditions causes the mean and median to be less meaningful parameters in statistical analyses, due to the sediment acquiring polymodal characteristics.

In order to explain the contrasting sets of granulometric results between Group 1 and Group 2, I make the assumption, as previously stated, that the bottom-current regime operating in

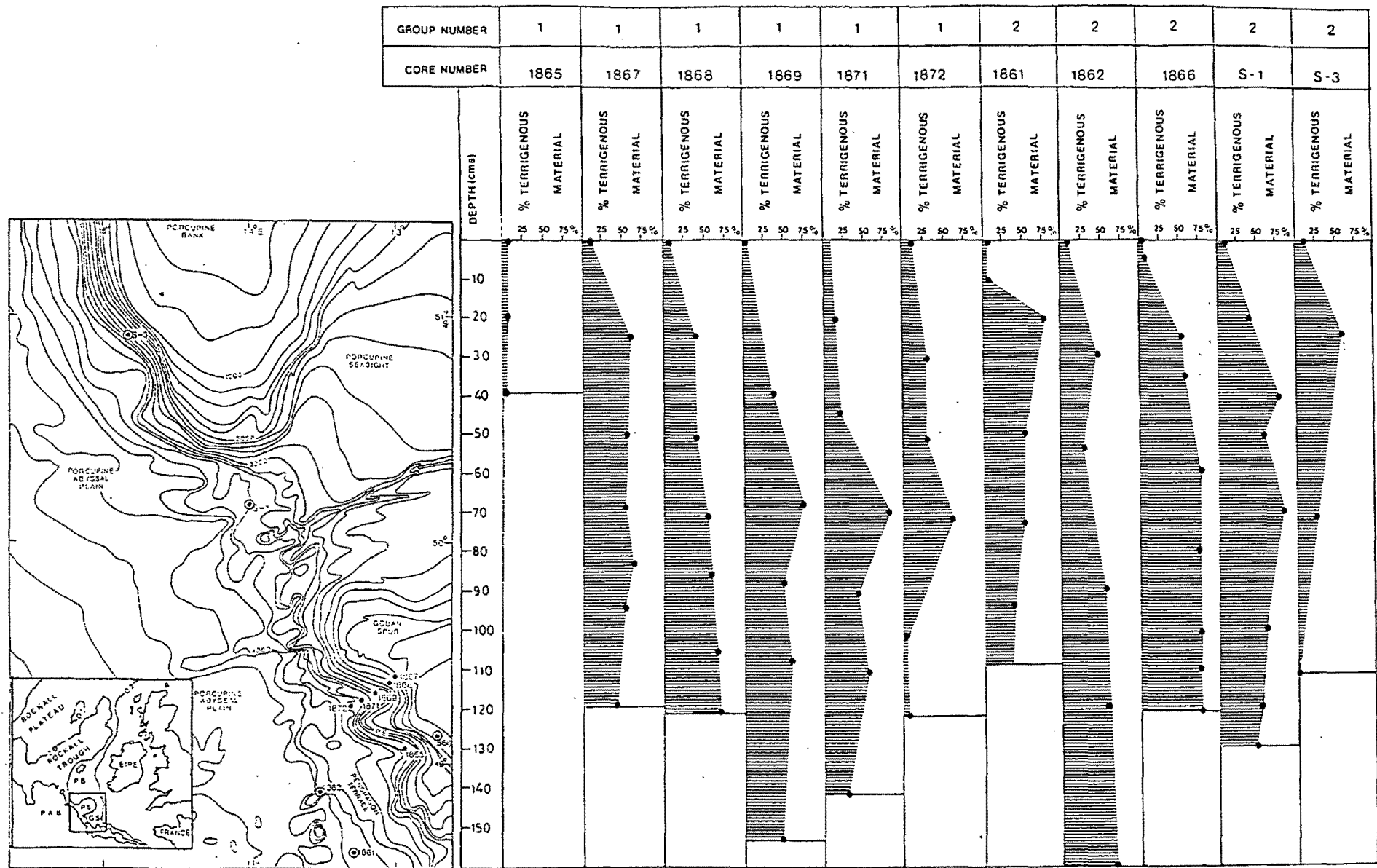


FIG.16 Upcore total % terrigenous material curves • Group 1 cores
 ● Group 2 cores

the study area, has remained reasonably constant during the time span represented by these cores.

The overall sediment package in Group-1 cores is muddier than that of the Group-2 cores (Group-1 Cores 1867 to 1872 and Group-2 Cores 1861 and 1862 in Appendix B).

The reason for these basic differences I suggest, is due to the proximity of the Group-1 cores to the Fastnet and Western Approaches Basins (FIG.19). I propose that a "shelf-spillover" mechanism is active in this area and that during the colder periods when the coastline was closer to the shelf break, quantities of fine sediment, the major sediment type being deposited at that time, cascaded over the Pendragon Escarpment in gravity flows thereby adding to the overall percentage of fines being deposited at the Group-1 core-sites on the Pendragon Escarpment (FIG.1).

I conclude therefore:

- i) that bottom current strength is and has been sufficient, throughout the timespan represented by these cores to promote winnowing of the sediment package. This is indicated by the lack of foramaminiferal fragments and by the presence of contourites. This resulted in an overall sediment package somewhat coarser than was originally deposited. This applies to both Group-1 and Group-2 cores.

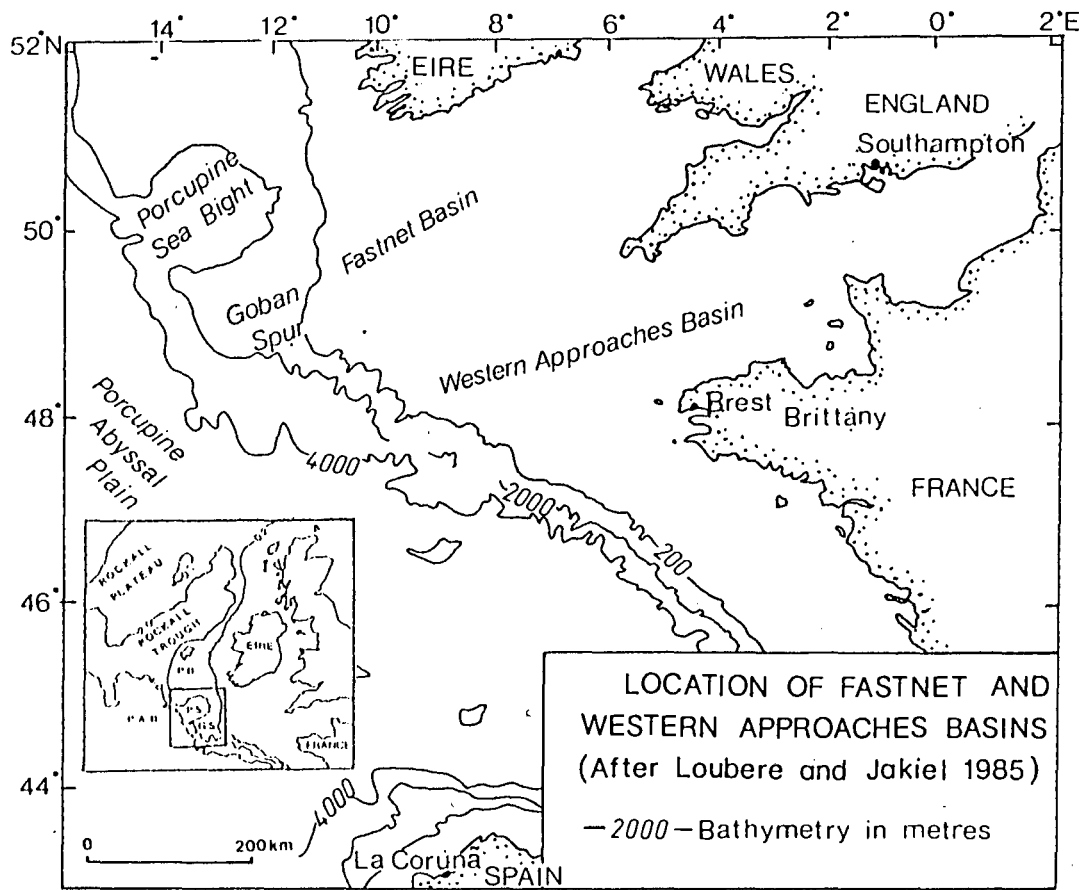


FIG. 17

- ii) The quantity of ice-rafted material deposited during the colder periods did not vary significantly from core to core, because all cores are well north of the postulated glacial position of the Polar Front.

- iii) Group-1 cores received increased quantities of fine sediment (muds) during colder periods from the adjacent Fastnet and Western Approaches Basins, a direct result of "shelf-spill over" during periods of lower sea level.

- iv) The sediment package deposited during the colder periods was statistically finer than that deposited during the interglacials.

Due to the presence of abundant ice-rafted debris throughout the cores accompanied with the fact that it is a good paleoclimatic indicator [Ericson et al (1967)] an analysis was conducted in order to attempt a correlation with the foraminiferal data. Connolly and Ewing (1965) note that cores taken North of 50°N, in pelagic sediment, contained abundant glacial debris, and that in many areas (near Labrador, Greenland and Iceland) there was so much glacial debris that variations in the amount and intensity of ice-rafting could not be measured. Ericson et al (1967) also noted abundant ice-rafted material in pelagic deep marine cores farther south (40-45°N).

A relationship appears to exist between the degree of frosting

and pitting of the quartz grains and increases in the quantity of ice-rafted debris. However this is rather tentative as frosting and pitting were also noted in samples containing only small amounts of glacial detritus. Angularity and colour did not vary significantly in any of the samples analysed.

As there are considerable fluctuations in the amount of the ice-rafted detritus deposited during these cold periods it should be possible to correlate the major cold and warm zones within each glacial/interglacial cycle with the increases/decreases of glacial detritus.

Ericson et al (1967) examined several North Atlantic cores and deduced that the distribution of ice-rafted detritus in deep sea cores in the North Atlantic could provide a powerful tool for delineating even minor fluctuations in the Pleistocene climate.

In order to confirm the hypothesis that changes in quantity of ice-rafted debris correlate with changes in the major cold and warm zones within each glacial/interglacial cycle, several samples were examined from Core 1869. The quantity of ice-rafted debris in the sand fraction was estimated by examination of the sand fraction under a binocular microscope. The results expressed semiquantitatively are plotted in Figure 19B. It can be seen from this figure that a major influx of glacial detritus occurs from between 70-100cm indicating I believe the 18,000 B.P. glacial maximum.

This 70-100cm influx correlates with increases exhibited by;

- a) % Planktonic foraminiferal Arctic species (FIG.8H).
- b) % *G. pachyderma* (FIG.9).
- c) % terrigenous material (FIG.18)

As I consider Core 1869 to be representative for this area, based on the sedimentological and foraminiferal evidence so far presented, I confirm the findings of Conolly and Ewing (1965) that changes in the quantity of ice-rafted debris correlate with climatic variations.

However the 11,000 B.P. glacial readvance is not so readily identifiable within this suite of cores. In order for the geological record to exhibit ice-rafted debris peaks that the glacial system must first be thoroughly established and not experiencing short-term oscillations.

As terrigenous components of hemipelagic sediments of the outer continental margin are assumed to be good palaeoclimatic indicators [Thiede (1977)], a mica analysis was conducted. Terrigenous components in the coarse fraction of the cores are relatively scarce and unfortunately none of the cores in this study yielded sufficient quantities of mica and quartz to generate upcore distribution curves. In fact in many samples there was no visible mica at all. However Core 12328-5 (FIG.20) obtained in a study of the North Atlantic off West Africa, by Thiede (1977) contained adequate quartz and mica to

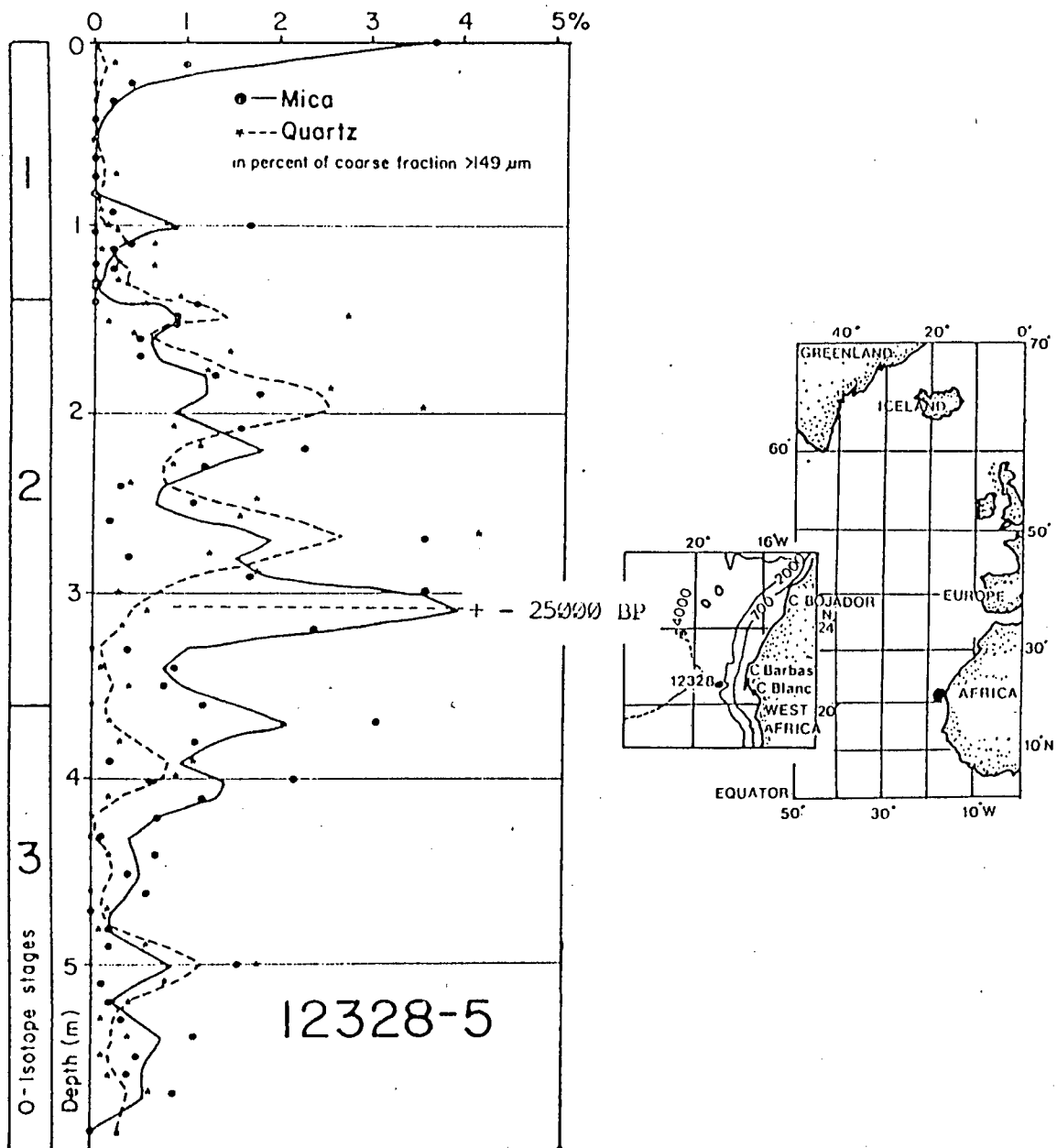


FIG 20: DISTRIBUTION OF QUARTZ AND MICA IN CORE 12328-5 IN % OF TOTAL COARSE FRACTION > 0,149 mm (After Thiede (1977))

generate an upcore plot. Thiede found that the frequency curves of the coarse terrigenous component in the core followed the curves of the oxygen isotope ratios.

Core 12328-5 has been compared with various upcore data obtained from this study, notably the oxygen-isotope data and foraminiferal data, specifically % G. pachyderma(s) and % Arctic species. These curves revealed several increases and decreases of the terrigenous input, and although the core 12328-5 site is far to the south of the study area, the fluctuations follow those of the $^{18}\text{O}/^{16}\text{O}$ ratios exhibited by these cores with a high abundance of mica present during the colder periods.

High input of mica into the sediments occurs at times of high oxygen isotope ratios, corresponding to glacial low sea levels and at times of rapid deglaciation. Increased quantities of mica are present in samples associated with these cores, however not all cores display significant increases at the colder intervals. Nevertheless increases in the mica content correlate with increases in the quantity of terrigenous material and ice-rafted detritus.

Similarly, increases in mica content correlate with increase in percentage Arctic forams and with decreases in the calcium carbonate content. Mica is therefore a useful tool in delineating cold episodes in the North Atlantic especially if there is sufficient abundance to produce upcore plots.

Semi-quantitative mica values for Core 1869 were plotted (FIG. 19A) and from the results it can be noted that the presence of mica in the sample correlates with increases in percentages of Arctic species. However the reason for the absence of mica between 90-120 cms is unclear, especially as the foraminiferal evidence indicates Arctic conditions. (See Appendix B for results).

During the sedimentological analysis it was noted that silt was present in the sand fraction. The majority of sediment samples from this study display percentages of coarse silt (16-62 μ m) and on occasions medium silt (8-16 μ m) (e.g. core 1866 at 25cm) in the sand fraction (>63 μ m) grain-size analysis results. These results, obtained utilizing settling techniques, highlight the observations of Flemming and Thum (1978) that during sieve analysis grain shape rather than grain density is differentiated. The silt grains are in this case assumed to be plate like or angular in nature enabling them to be retained on the finest (63 μ m) sieve. Similar findings were reported by Goodlad (1986) who noted in his study of the mid-Natal Valley (South Africa) that the overall retained silt-fraction percentage greatly decreased if the organics were removed from the sample prior to sieving. Due to sample size restrictions in this study it was not possible to carry out a similar analysis.

CONCLUSIONS

On the basis of the existing sample density the study has, on the whole, achieved a coherent and consistent description of sediment distribution, foraminiferal diversity and chemical composition within the suite of cores. As bioturbation has smoothed the geologic record and seemingly obliterated some short-term climatic oscillation there is no reason to believe that a closer sampling interval would have resulted in a different interpretation of the major trends outlined in this study. Indeed the results obtained correlate well with the work of other authors who have conducted similar analyses in the North Atlantic.

As no absolute dating has been carried out in this study, it has been necessary to correlate various upcore statistical parameters generated within these eleven cores with the work of other authors. For this reason I have attempted to compare my results with the work of Berggren (1972), CLIMAP (1976), Ruddiman and McIntyre (1981a, b) and Zimmerman et al (1985), whose analyses have acceptable radiometric control and sample spacing.

Termination of the latest (Würm) glaciation has been dated at approximately 11,000 B.P [Berggren (1972), CLIMAP (1976), Gates (1976), Duplessy et al (1981), Ruddiman and McIntyre (1981b), Zimmerman et al (1985)].

The sedimentation rate estimated by McIntyre et al (1972) for this part of the North Atlantic is between 3 to 5cms/1000 years, this would place the 11,000 B.P glacial readvance at between 33-35cm. The occurrence of cold-water fauna at 20cms to 25cms in cores 1861, 1865, 1867, and S-3 would necessitate a much slower rate of sedimentation if the cores are complete (± 2 cm/1000 years). Cores 1862, and S-1 exhibit cold-water peaks at 30cms and 40cms respectively, which correspond to cores analysed by Ericson et al (1967) in the North Atlantic. Cores 1866, 1868, 1869, 1871 and 1872 do not exhibit any pronounced 11,000 B.P peak.

The following reasons are suggested for these results:

- a) Erosion has occurred at all core sites and throughout the core lengths as indicated by the presence of contourites, partially reworked sediments and the foraminiferal fragment analysis. Each core displays varying degrees of erosion throughout its length. I draw this conclusion from the fact that all cores display the last major glacial maximum (20,000-18,000 B.P.) [Ruddiman and McIntyre (1981b)] at approximately the same depth (70cm), while the 11,000 B.P. (Würm) glacial readvance is represented at varying depths (20-40cm). This possibly implies therefore that following the last major glacial maximum (20,000-18,000 B.P.) bottom current conditions changed, resulting in differential degrees of erosion.

- b) Bioturbation smooths short-term climatic events on the geological record [Ruddiman and McIntyre (1981a, b)]. This resulted in the suppression of the 11,000 B.P. glacial readvance spike which was a shortlived event. The extent of this suppression varies from site to site, Cores 1866, 1868, 1871 displays severe spike suppression, whereas core 1861 displays only minimal suppression. This perhaps implies that the 'degree of suppression', is directly related to;
- i) increased benthic activity,
 - ii) increased benthic population. This implies that at sites of total suppression there was a more highly active and/or more abundant benthic fauna than at sites of limited or marginal suppression.
- c) The last maximum glacial (20,000-18,000 B.P.) was of considerably longer duration than the 11,000 B.P. (Würm) glacial readvance. Thus a stable geological and sedimentological depositional regime was established throughout the study area. Bottom-current activity appears to have been uniform throughout the core sites and bioturbation and sediment reworking had only a limited effect in smoothing the climatic record.

In conclusion therefore;

- a) Climatic results obtained from this study, indicate that the Polar Front (maximum glacial 20,000-18,000 B.P) was situated south of the study area for what appears to have been a substantial length of time, as indicated by the presence of the Arctic foraminiferal species Globigerina pachyderma (sinistral coiling). The high concentrations of Arctic foraminifera indicate that there was sufficient vertical convection to bring nutrients to the surface. However coccoliths were absent due to the presence of sea ice which greatly reduced the photic zone.

- b) All cores present a suppressed foraminiferal content as the ice sheet began to retreat. This correlates with Ruddiman and McIntyre's (1981a, b) 16,000-13,000 B.P period where they identified a similar trend. The barren period no doubt resulted from a suppression of nutrients, the direct result of a near-surface salinity stratification resulting from the large quantities of melt water entering the system before the front retreated to its present position.

- c) Towards the end of this period, productivity began to increase as the system adjusted and began to approach equilibrium.

- d) The 11,000-10,000 B.P glacial readvance [Ruddiman et al (1980), Duplessy et al (1981), Ruddiman and McIntyre (1984)] is noted in several cores and marks the final glacial pulse in the record as the Polar Front retreated to its present position.

REFERENCES

- Allen, J.R.L. 1985. Principles of Physical Sedimentology. George Allen and Unwin, London: 272pp.
- Bagnold, R.A. 1968. Deposition in the process of hydraulic transport. Sedimentology, 10: 45-56.
- Belderson, R.H., Kenyon, N.H. and Stride, A.H. 1981. Holocene sediments on the continental shelf west of the British Isles. Inst. Geol. Sci. Rep., 70/14: 157-170.
- Belderson, R.H., Pingree, R.D. and Griffiths, D.K. 1986. Low sea-level tidal origin of Celtic Sea sand banks - evidence from numerical modelling of M2 tidal streams. Marine Geology, 73: 99-108.
- Berger, W.H. 1976. Biogenous deep-sea sediments: production, preservation and interpretation. Chemical Oceanography, (2nd ed.) 5: 265-388. Academic Press, London.
- Berger, W.H., Killingley, J.S. and Vincent, E. 1985. Timing of deglaciation from an oxygen isotope curve for Atlantic deep-sea sediments. Nature, 314: 156-158.
- Berggren, W.A. 1972. Late Pliocene - Pleistocene Glaciation. Init. Repts. DSDP 12: 953-963. Washington (U.S. Govt. Print. Off.).
- Birch, G.F. 1981. The Karbonate Bombe: A precise, rapid and cheap method for determining calcium carbonate in sediments and rocks. Trans. Geol. Soc. S. Afr. 84: 199-203.

- Bjerkli, K. and Høltedahl, H. 1975. Pleistocene and Recent sediments of the Norwegian continental shelf (62°N-71°N), and the Norwegian channel area. Norg. Geol. Unders., 316: 241-252.
- Boltovskoy, E. 1973. Reconstruction of Post-Pliocene climatic changes by means of planktonic foraminifera Borea, 2: 55-68.
- Boltovskoy, E. 1974. Neogene planktonic foraminifera of the Indian Ocean. Init. Rept. DSDP 26: 675-741. Washington (U.S. Govt. Print. Off.).
- Boltovskoy, E. and Wright, R. 1978. Recent Foraminifera. The Hague, Dr W Junk. 515pp.
- Brenchley, P.J. and Williams, B.P.J. 1978. Sedimentology: Recent Developments and Applied Aspects. Blackwell Scientific Publications, London. 104pp.
- Broecker, W.S., Ewing, M. and Heezen, B.C. 1960. Evidence for an abrupt change in climate close to 11,000 years ago. Am. Jour. Sci., 258: 429-448.
- Broecker, W.S. and Van Donk, J. 1970. Insolation changes, ice volumes and the ^{18}O record in deep sea cores. Review Geophysics and Space Physics, 8: 169-198.
- Caralp, M.H., Pujol, C., Duprat, J., Labracherie, M., Vergnaud Grazzini, C. and Saliege, J.F. 1985. Quaternary Paleoceanography of the Northeastern Atlantic: Microfaunal and stable isotope evidence at sites 548 and 549. Init. Rept. DSDP 80: 817-822. Washington (U.S. Govt. Print. Off.).

- CLIMAP PROJECT MEMBERS 1976. The surface of the ice-age earth. Science, 191: 1131-1137.
- Coates, G.F. and Hulse, C.A. 1985. A comparison of four methods of size analysis of fine-grained sediments. New Zealand. J. Geol. and Geophys., 28: 369-380.
- Conolly, J.R. and Ewing, M. 1965. Pleistocene glacial-marine zones in North Atlantic deep-sea sediments. Nature, 208: 135-138.
- Cooper, L.H.N. 1967. The physical oceanography of the Celtic Sea. Oceanographic Marine Biology Annual Review, 5: 99-110.
- Craig, H. 1957. Isotopic standards for carbon and oxygen and correction factors. Geochim. Cosmochim. Acta. 12: 133-149.
- De Graciansky, P.C. and Bourbon, M. 1985. The Goban Spur of the North West Atlantic Margin during Late Cretaceous times. Init. Repts. DSDP 80: 863-884. Washington (U.S. Govt. Print. Off.).
- De Graciansky, P.C. and Poag, C.W. 1985. Geologic history of the Goban Spur, North West Europe Continental Margin. Init. Repts. DSDP 80: 1187-1218. Washington (U.S. Govt. Print. Off.).
- Delmas, R.J., Ascencio, J-M. and Legrand, M. 1980. Polar ice evidence that atmospheric CO₂ 20,000yr BP was 50% of Present. Nature, 284: 155-157.

- Dingle, R.V. and Scrutton, R.A. 1979. Sedimentary succession and tectonic history of a marginal plateau (Goban Spur, southwest of Ireland). Mar. Geol., 33: 45-69.
- Doeglas, D.J. 1968. Grain-size indices, classification and environment. Sedimentology, 10: 83-100.
- Duplessy, J.C., Delibrias, G., Turon, J.L., Pujol, C. and Duprat, J. 1981. Deglacial warming of the north eastern Atlantic ocean: Correlation with the paleoclimatic evolution of the European continent. Palaeography, Palaeoclimatology, Palaeoecology, 35: 121-144.
- Duplessy, J.P., Moyes, J. and Pujol, C. 1980. Deep water formation in the North Atlantic Ocean during the last ice age. Nature, 286: 479-482.
- Emery, K.O. and Uchupi, E. 1978. The Geology of the Atlantic Ocean. Springer-Verlag, New York: 1050pp.
- Ericson, D.B., Ewing, M., Wollen, G. and Heezen, B.C. 1967. Atlantic deep-sea sediment cores. Bull. Geol. Soc. Am. 72: 193-286.
- Flemming, B.W. and Thum, A.B. 1978. The settling tube - a hydraulic method of grain size analysis of sands. Kieler Meeresforschungen, 4: 82-95.
- Flint, R.F. 1971. Glacial and Quaternary Geology. John Wiley and Sons, London: 892pp.
- Frakes, L.A. 1979. Climates Throughout Geologic Time. Elsevier, Oxford: 310pp.

- Friedman, G.M. and Sanders, J.E. 1978. Principles of Sedimentology. John Wiley and Sons, New York: 792pp.
- Gates, W.L. 1976. Modelling the ice age climate. Science, 191: 1131-1144.
- Gibbs, R.J. 1972. The accuracy of particle-size analyses utilizing settling tubes. J. Sediment. Petrol., 42: 141-145.
- Grosswald, M.G. 1980. Late Weichselian ice sheet of Northern Eurasia. Quaternary Research, 13: 1-32.
- Holte Dahl, H., Haldorsen, S. and Vigran, J.O. 1974. Two sediment cores from the Norwegian continental shelf between Haltenbanken and Froyabanken (64°06'N, 7°39'E). Norg. Geol. Unders., 304: 1-20.
- Huddleston, P.F. 1985. Planktonic foraminiferal biostratigraphy, Deep Sea Drilling Project Leg 81. Init. Repts. DSDP 81: 429-438. Washington (U.S. Govt. Print. Off.).
- Jansen, E. and Erlenkeuser, H. 1985. Ocean circulation in the Norwegian Sea during the last deglaciation: isotopic evidence. Palaeogeography, Palaeoclimatology, Palaeoecology, 49: 189-206.
- Keigwin, Jr. L.D. 1985. Stable isotopic results on upper Miocene and lower Pliocene foraminifers from Hole 552A. Init. Rept. DSDP 81: 595-598. Washington (U.S. Govt. Print. Off.).
- Kiel, M.S. 1979. Indicators of continental climates in marine sediments: A discussion. Meteor Forsch.-Ergebnisse, 31: 49-51.

Kennett, J.P. and Srinivasan, M.S. 1983. Neogene Planktonic Foraminifera.

Hutchinson Ross Publishing Company, Pennsylvania. 265pp.

Long, O., Brent, A., Harland, R., Gregory, D.M., Graham, D.K. and Morton, A.C.

1986. Late Quaternary palaeontology, sedimentology and geochemistry of a vibrocore from the Witch Ground Basin, central North Sea. Marine Geology, 73: 109-123.

Loubere, P. 1981. Oceanographic parameters reflected in the seabed

distribution of planktonic foraminifera from the North Atlantic and Mediterranean Sea. J. Foram. Res., 11: 137-158.

Loubere, P. 1986. Late Pliocene variations in the carbon isotope values of

North Atlantic benthic foraminifera: Biotic control of the isotopic record. Mar. Geol., 76: 45-56.

Loubere, P. and Jakiel, R. 1985. A sedimentological, faunal, and isotopic

record of the middle-to-late Pliocene transition in the Northeastern Atlantic, Deep Sea Drilling Project Site 548. Init. Repts. DSDP 81: 473-485. Washington (U.S. Govt. Print. Off.).

McIntyre, A., Kipp, N.G., Be, A.W.H., Crowley, T., Kellogg, T., Gardner, J.V.,

Prell, W. and Ruddiman, W.F. 1976. Glacial North Atlantic 18,000 years ago: A CLIMAP reconstruction. Geological Society of America, 145: 43-76.

McIntyre, A., Ruddiman, W.F. and Jantzen, R. 1972. Southward penetrations of

the North Atlantic Polar front: Faunal and floral evidence of large scale surface water mass movements over the last 225,000 years. Deep-Sea Res., 19: 61-77.

- Mix, A.C. and Fairbanks, R.G. 1985. North Atlantic surface-ocean control of Pleistocene deep-ocean circulation. Earth and Planetary Sci. Lett., 75: 231-243.
- Molina-Cruz, A. and Thiede, J. 1977. The Glacial East Boundary Current along the Atlantic Eurafriean Continental Margin. Deep-Sea Research, 25: 337-356.
- Montadert, L., De Charpal, O., Roberts, D., Guennoc, P. and Sibuet, J. 1980. Northeast Atlantic passive continental margins : rifting and subsidence processes. Init. Repts. DSDP 47B and 48. Washington (U.S. Govt. Print. Off.).
- Morton, A.C. 1985. Coarse fraction of Plio-Pleistocene sediment from Deep Sea Drilling Project Hole 552A, Northeast Atlantic. Init. Repts. DSDP 81: 663-668. Washington (U.S. Govt. Print. Off.).
- Pautot, G., Renard, V., Auffret, G. and Pastouret, L. 1976. A granite cliff deep in the North Atlantic. Nature, 263: 669-672.
- Pastouret, L., Chamley, H., Delibrias, G., Duplessy, J.C. and Thiede, J. 1978. Late Quaternary climatic changes in western tropical Africa deduced from deep-sea sedimentation of the Niger delta. Oceanologica Acta, 1: 217-231.
- Poag, C.N., Reynolds, L.A., Mazzullo, J.M. and Keigwin, Jr. L.D. 1985. Foraminiferal, benthic and isotopic changes across four major unconformities at Deep Sea Drilling Project Site 548, Goban Spur. Init. Repts. DSDP 81: 539-556. Washington (U.S. Govt. Print. Off.).

- Pujol, C. and Duprat, J. 1985. Quaternary and Pliocene planktonic foraminifers of the North Eastern Atlantic (Goban Spur), Deep Sea Drilling Project Leg 80. Init. Repts. DSDP 80: 683-724. Washington (U.S. Govt. Print. Off.).
- Roberts, D.G., Masson, D.G., Montadert, L. and De Charpel, O. 1981. Continental margin from the Porcupine Sea Bight to the American Marginal Basin. Proc. Conf. Petrol. Geol. Cont. Shelf Northwest Europe: 455-473.
- Ruddiman, W.F., McIntyre, A., Niebler-Hunt, V. and Durazzi, J.T. 1980. Oceanic evidence for the mechanism of rapid northern Hemisphere Glaciation. Quaternary Research, 13: 33-64.
- Ruddiman, W.F. and McIntyre, A. 1981a. The mode and mechanism of the last deglaciation: Oceanic evidence. Quaternary Research, 16: 125-134.
- Ruddiman, W.F. and McIntyre, A. 1981b. The North Atlantic ocean during the last deglaciation. Palaeography, Palaeoclimatology, Palaeoecology, 35: 145-214.
- Ruddiman, W.F. and McIntyre, A. 1981c. Oceanic mechanisms for amplification of the 23,000-year ice-volume cycle. Science, 212: 617-627.
- Ruddiman, W.F. and McIntyre, A. 1984. Ice-age thermal response and climatic role of the surface Atlantic Ocean, 40° to 63°N. Geol. Soc. Am. Bull., 95: 381-396.

Saito, T., Thompson, P.R. and Breger, D. 1981. Systematic Index of Recent and Pleistocene Planktonic Foraminifera. University of Tokyo Press, Tokyo. 190pp.

Shackleton, N.J. 1969. The last interglacial in the marine and terrestrial records. Proc. Roy. Soc. Lond. B, 174: 135-154.

Shackleton, N.J. 1974. Attainment of isotopic equilibrium between ocean water and the benthic foraminifera genus Uvigerina : isotopic changes in the ocean during the Pleistocene : Colloq. Int. C.N.R.S. (Les Methodes Quantitatives D'etude des Valiation du Climat au Cours du Pleistocene). 219: 203-209.

Shackleton, N.J., Backman, J., Zimmerman, H., Kent, D.V., Hall, M.A., Roberts, D.G., Schnitker, D., Baldauf, J.G., Desprairies, A., Homrighausen, R., Huddlestun, P., Keene, J.B., Kaltenback, A.J., Krumsiek, K.A.O., Morton, A.C., Murray, J.W. and Westberg-Smith, J. 1984. Oxygen isotope calibration of the onset of ice-rafting and history of glaciation in the North Atlantic region. Nature, 307: 620-623.

Shackleton, N.J. and Hall, M.A. 1985. Oxygen and carbon isotope stratigraphy of Deep Sea Drilling Project Hole 552A: Plio-Pleistocene glacial history. Init. Rept. DSDP 81: 599-611. Washington (U.S. Govt. Print. Off.).

Shackleton, N.J. and Opdyke, N.O. 1973. Oxygen isotope and palaeomagnetic stratigraphy of Equatorial Pacific core V28-238 : Oxygen isotope temperatures and ice volumes on a 10^5 and 10^6 year scale. Quaternary Research, 3: 39-55.

- Shackleton, N.J. and Opdyke, N.D. 1975. Oxygen isotope and palaeomagnetic evidence for early northern hemisphere glaciation. Nature, 270: 216-219.
- Shackleton, N.J. and Vincent, E. 1977. Oxygen and carbon isotope studies in Recent foraminifera from the Southwest Indian Ocean. Marine Micropaleontology. 3: 1-13.
- Smythe, Jr. F.W., Ruddiman, W.F. and Lumsden, D.N. 1984. Ice-rafted evidence of long-term north Atlantic circulation. Marine Geology, 64: 131-141.
- Stowe, D.A.V. 1979. Distinguishing between fine-grained turbidites and contourites on the Nova Scotia Deep Water Margin. Sedimentology, 26: 371-387.
- Stowe, D.A.V. and Holbrook, J.A. 1985. Hatton Drift contourites, Northeast Atlantic, Deep Sea Drilling Project Leg 81. Init. Repts. DSDP 81: 695-701. Washington (U.S. Govt. Print. Off.).
- Stowe, D.A.V. and Lovell, J.P.B. 1979. Contourites, their recognition in Modern and Ancient sediments. Earth Sci. Rev., 14: 251-291.
- Thiede, J. 1977. Aspects of the variability of the glacial and interglacial North Atlantic eastern boundary current (last 150,000 years). Meteor Forsch.-Ergebnisse, 28: 1-36.
- Zahn, R., Markussen, B. and Thiede, J. 1985. Stable isotope data and depositional environments in the Late Quaternary Arctic Ocean. Nature, 314: 433-435.

Zimmerman, H.B. 1985. Lithostratigraphy and clay mineralogy of the western margin of the Rockall Plateau and the Hatton sediment drift. Init. Repts. DSDP 81: 683-694. Washington (U.S. Govt. Print. Off.).

Zimmerman, H.B., Shackleton, N.J., Backman, J., Kent, D.V., Baldauf, Kaltenback, A.J. and Morton, A.C. 1985. History of Plio-Pleistocene climate in the North Eastern Atlantic, Deep Sea Drilling Project Hole 552A. Init. Repts. DSDP 81: 861-876. Washington (U.S. Govt. Print. Off.).

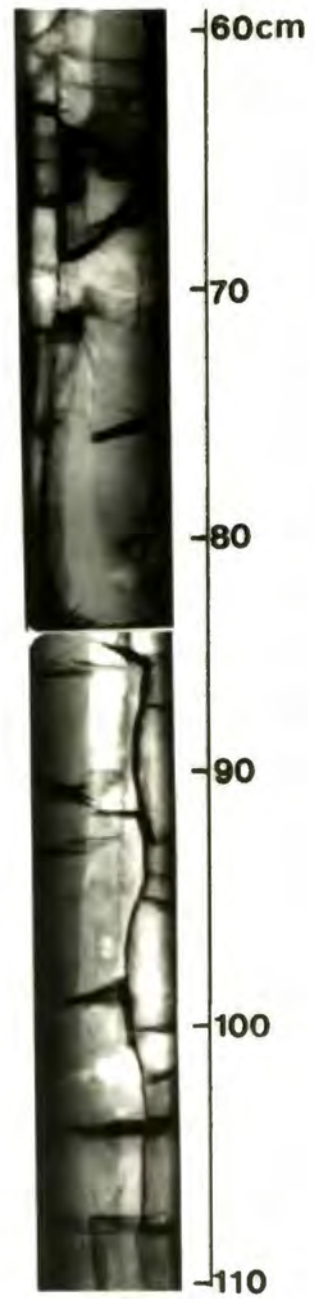
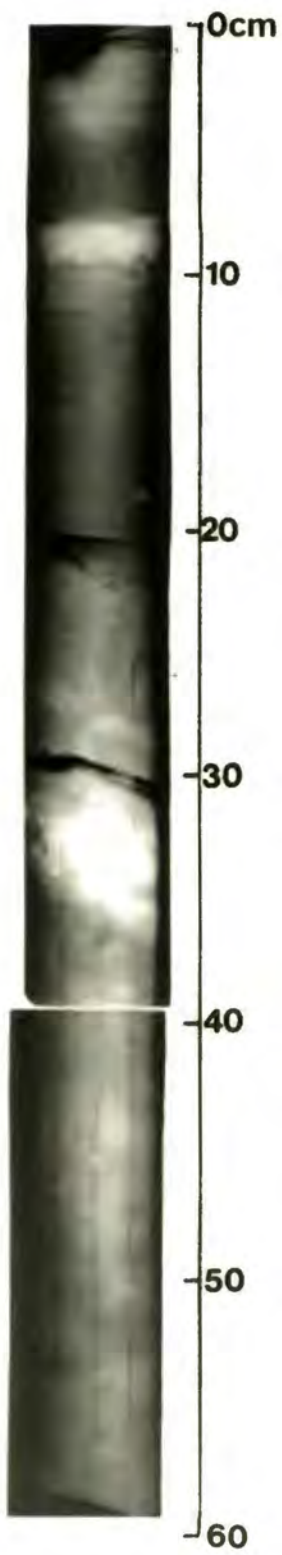
Additional reference

Fincham, M.J. 1987. Coccoliths and oxygen isotope observations from the sediment surface of the Southwest Indian Ocean. Bull. Jt Geol. Surv./ Univ. Cape Town Mar. Geosc. Unit, 19: 1-22.

APPENDIX A. X-RAY PHOTOGRAPHS FOR CORE 1861

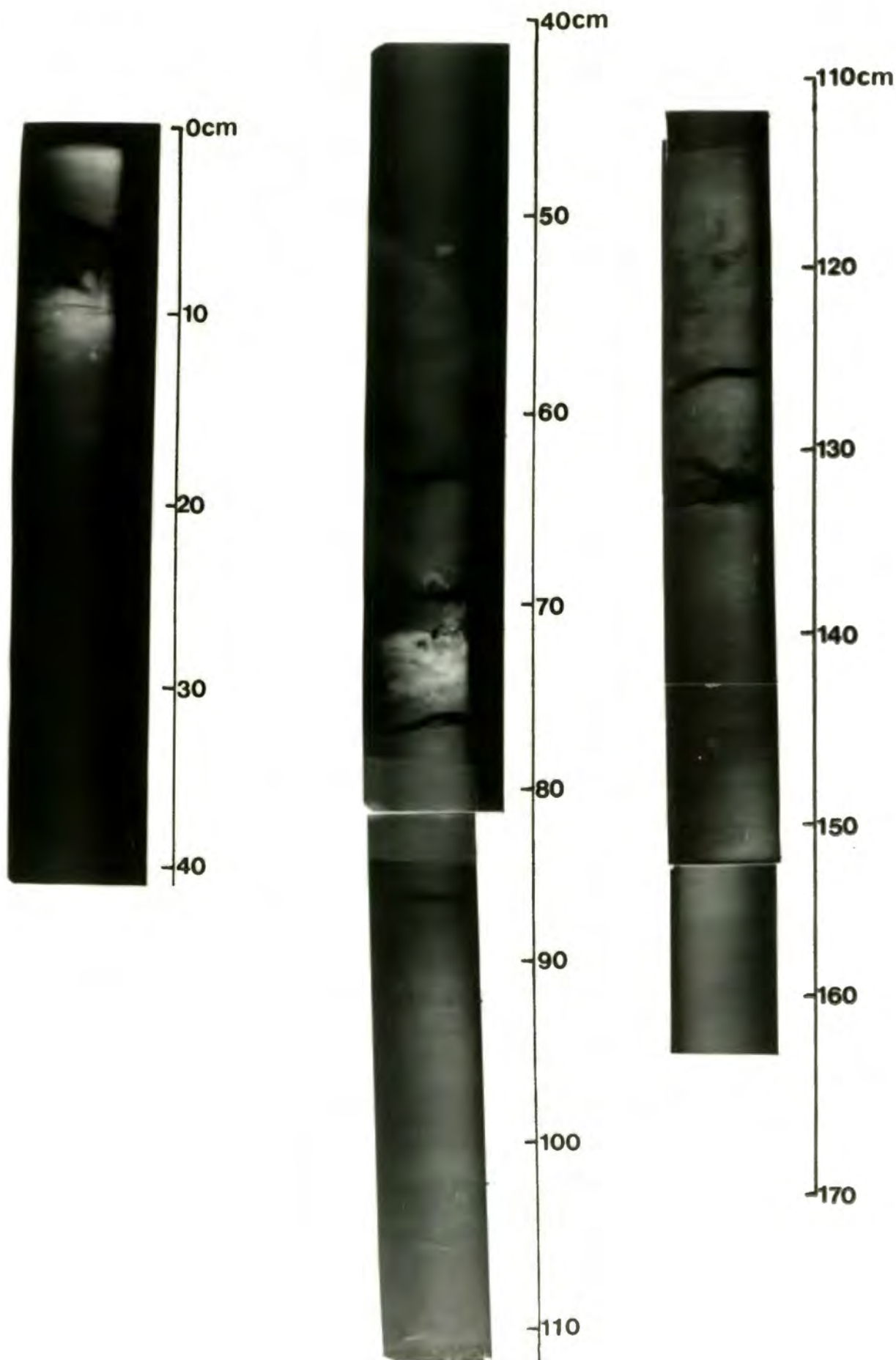
Core No 1861

Depth 4165 m



Core No 1862

Depth 2088 m

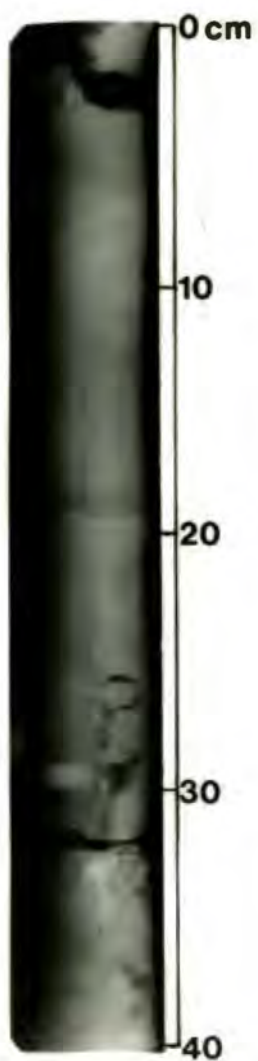


APPENDIX A. X-RAY PHOTOGRAPHS FOR CORE 1862

APPENDIX A. X-RAY PHOTOGRAPHS FOR CORE 1865

Core No 1865

Depth 2198 m



APPENDIX A. X-RAY PHOTOGRAPHS FOR CORE 1866

Core No 1866

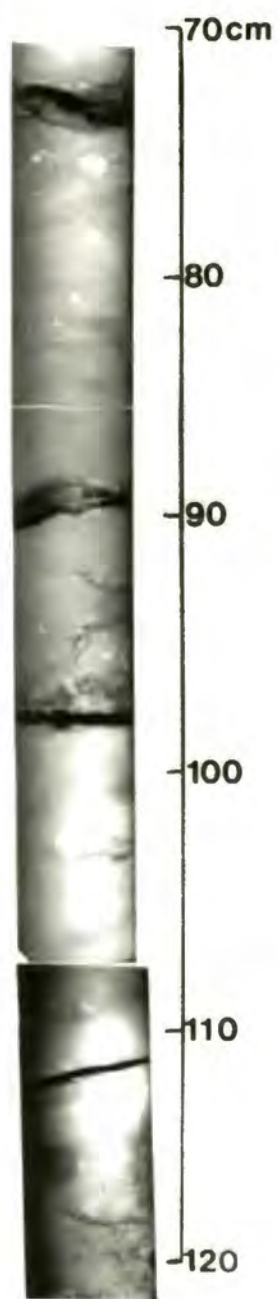
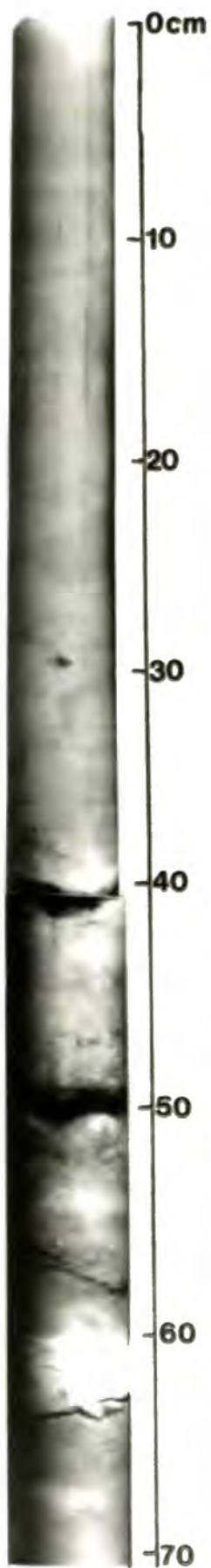
Depth 1361 m



APPENDIX A. X-RAY PHOTOGRAPHS FOR CORE 1867

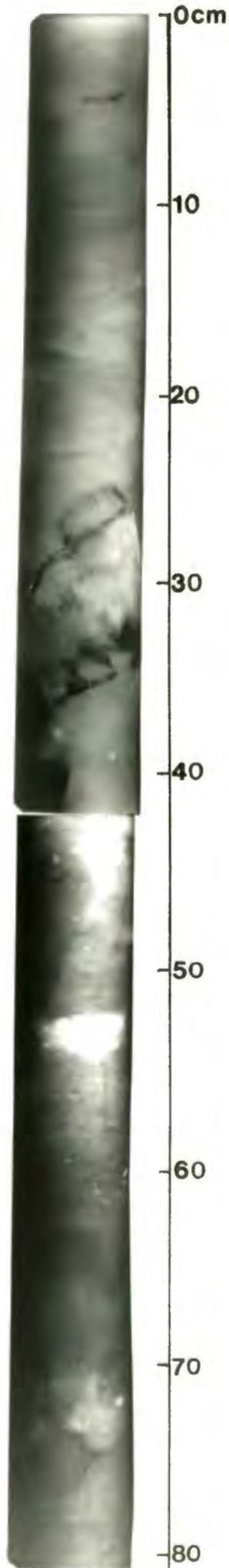
Core No 1867

Depth 1720 m



APPENDIX A. X-RAY PHOTOGRAPHS FOR CORE 1868

Core No 1868



Depth 4493 m

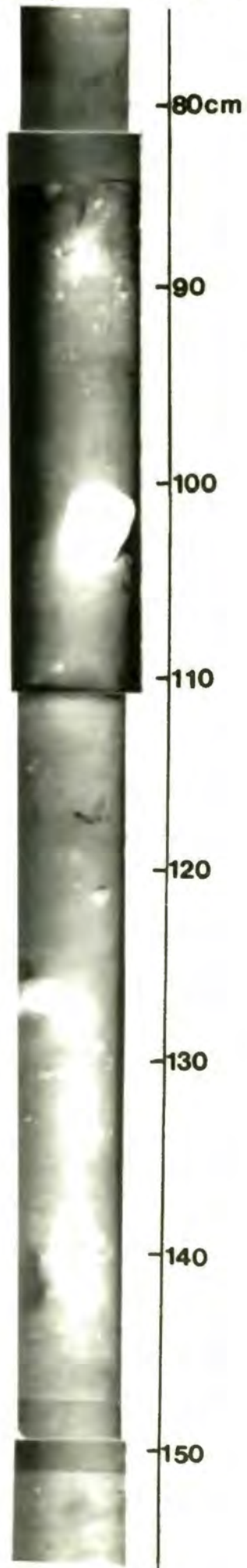


APPENDIX A. X-RAY PHOTOGRAPHS FOR CORE 1869

Core No 1869



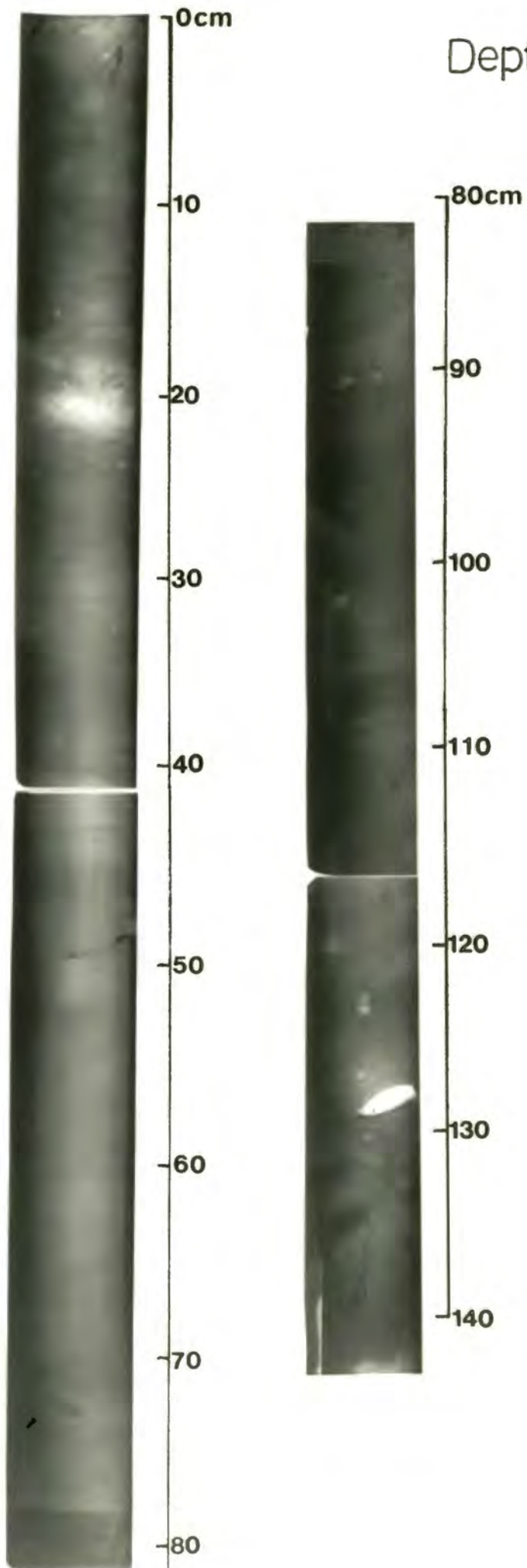
Depth 2187m



APPENDIX A. X-RAY PHOTOGRAPHS FOR CORE 1871

Core No 1871

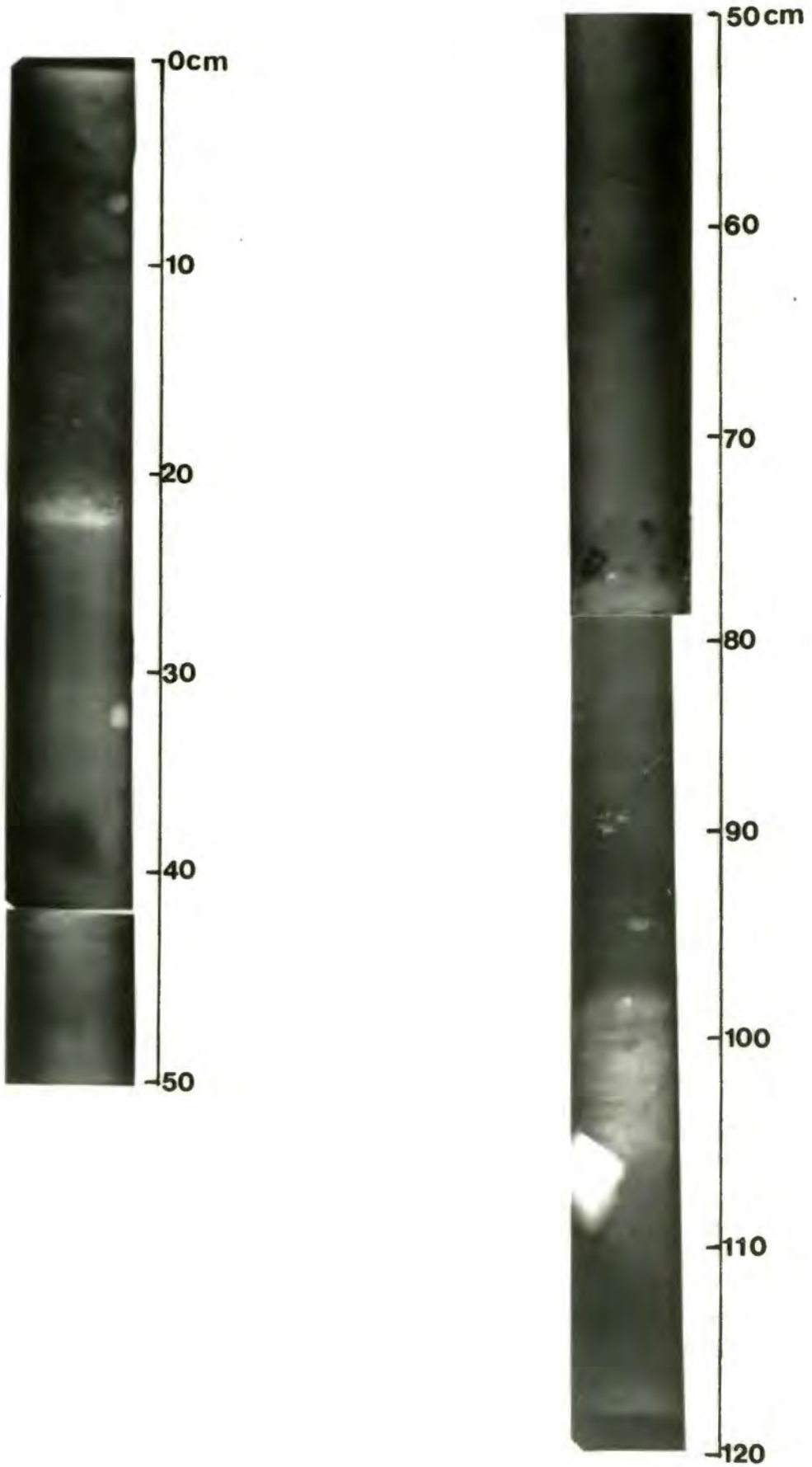
Depth 3238m



APPENDIX A. X-RAY PHOTOGRAPHS FOR CORE 1872

Core No 1872

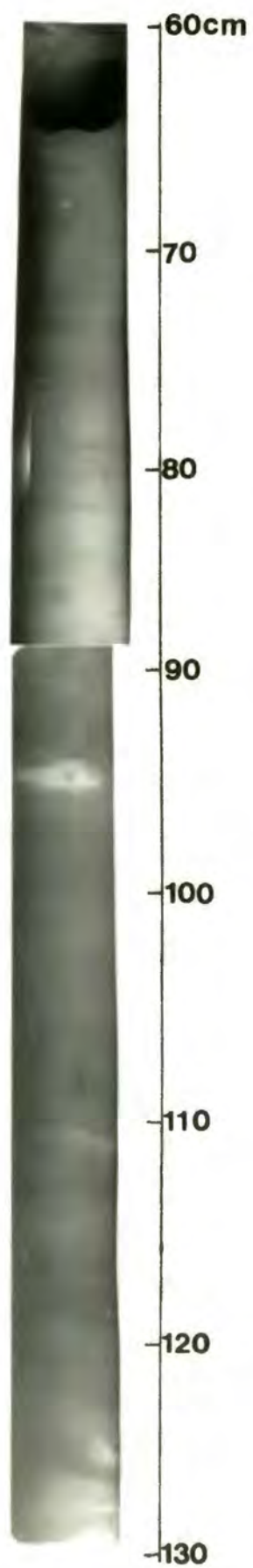
Depth 4200m



APPENDIX A. X-RAY PHOTOGRAPHS FOR CORE S-1

Core No S-1

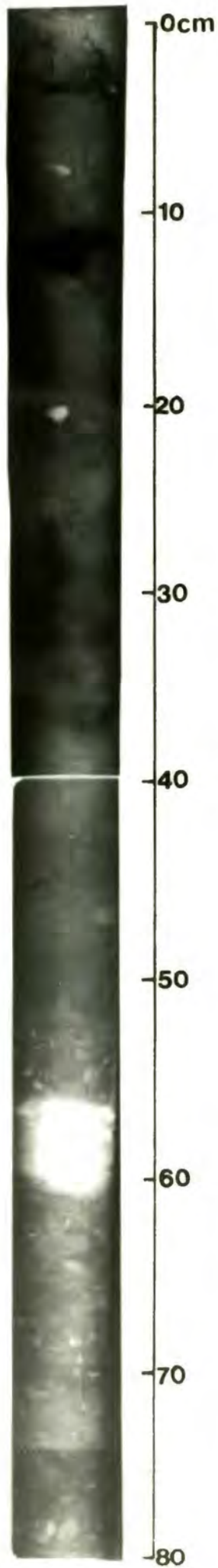
Depth 3500m



APPENDIX A. X-RAY PHOTOGRAPHS FOR CORE S-3

Core No S-3

Depth 2650m



CORE NUMBER/ SAMPLE NUMBER	PDB(18)	CORE NUMBER/ SAMPLE NUMBER	PDB(18)
1851/1	2.472	1868/1	NG
1861/2	4.786	1868/6	4.155
1861/11	4.746	1868/11	4.225
1861/16	4.887	1868/15	NG
1861/24	4.495	1868/19	NG
		1868/27	NG
1862/1	4.475		
1862/6	4.649	1869/5	4.712
1862/12	3.104	1869/8	4.559
1862/23	3.445	1869/14	4.017
1862/34	3.896	1869/18	5.487
		1869/23	4.896
1865/1	2.422	1869/28	3.646
1865/5	2.421	1869/31	NG
1865/9	1.090		
		1871/1	2.973
1866/1	NG	1871/5	3.450
1866/9	3.606	1871/10	3.614
1866/13	3.304	1871/19	4.155
1866/23	4.856	1871/24	4.330
1866/26	4.478	1871/29	4.187
1867/1	NG	1872/7	NG
1867/6	NG	1872/14	4.055
1867/15	4.468	1872/20	3.073
1867/18	4.569		
1867/25	4.137	S-3/1	2.010
		S-3/6	4.438
S-1/1	NG	S-3/11	3.503
S-1/5	2.622	S-3/19	NG
S-1/9	3.353	S-3/22	5.950
S-1/27	2.462		

APPENDIX C. OXYGEN-ISOTOPE DATA.